TRANSIT, RENDEZVOUS, & TAXI LAUNCHER

A proposal for a 2-vehicle autonomous human ascent from Mars

Submitted by:

George Blackwell
Jurist Chan
Sparsh Desai
Trey Farmer
Reid Fly
Aaron Hammond
Pessi Laensirinne
Elle Smith
Lonnie Webb

Faculty Advisor:

Dr. Álvaro Romero-Calvo

George Blackwell
AIAA#: 1423397

Jurist Chan
AIAA#: 1421085

Sparsh Desai
AIAA#: 1423367

Trey Farmer
AIAA#: 1421852

Reid Fly
AIAA#: 1423171

Aaron Hammond
AIAA#: 1423324

Pessi Laensirinne
AIAA#: 1423363

Elle Smith
AIAA#: 1097418

Lonnie Webb
AIAA#: 1421971

Dr. Álvaro Romero-Calvo
Faculty Advisor
AIAA#: 978289

Contents

A. Executive Summary

TRTL is designed to be the first mission to allow humans to ascend from the surface of another planet; namely, Mars. It responds to a Request for Proposal (RFP) by the American Institute of Aeronautics and Astronautics (AIAA) for two landers - one containing fuel and the other containing a Mars Ascent Vehicle (MAV) - to be autonomously prepared for a human arrival and launch 2 years after the landers touch down, carrying two astronauts and 50 kg of samples to a Deep Space Transit (DST) in a 5-sol orbit. Assuming the two landers are about 1 km from each other, fuel must be transferred autonomously from one lander to the MAV. Additionally, the payload mass for both landers cannot exceed 25 metric tons nor can they exceed a diameter of 8.4 meters in their folded configurations.

Probability of mission success and by extension, astronaut safety, were the primary considerations in the mission design. High-level mission architecture trades were conducted to maximize simplicity and reliability. While initial designs ranged from a large fuel shuttle to kilometer long hoses, all forms of fuel transfer appeared to be risky or mass inefficient. Instead, TRTL opts to utilize only a single lander supporting a Mars Ascent Vehicle (MAV). On its own, it cannot reach the 5-sol orbit of the DST, but an Orbital Taxi (OT) waiting in a lower orbit will dock with the MAV capsule to boost it to the higher orbit. This reduces the landed mass on Mars, avoids hazardous trips across Martian terrain to transfer fuel, and takes advantage of the well-practiced procedure of in-space docking to accomplish the mission.

TRTL's mission begins on Earth, where the MAV and OT launch aboard two separate SLS rockets. In order to meet the AO requirements of arriving on Mars by 2038 and being ready for a launch in July of 2040, both rockets will launch within a launch window spanning August 1st, 2037 to September 20, 2037. The large window gives room for launch issues due to weather or maintenance issues, but if the entire window is missed, the next one will come 26 months later.

Upon arrival, the Orbital Taxi inserts itself into a 250 km circular orbit, awaiting rendezvous with the MAV. The MAV and lander assembly enter into Mars' atmosphere using a hypersonic inflatable aerodynamic decelerator (HIAD) design, an inflatable heat shield that slows the vehicle and protects it from heating during descent. HIAD's ability to inflate allows it to fit within the SLS's 8.4 meter fairing while also expanding to 16 meters during entry and descent. The MAV will target Amazonis Planitia as its landing site. Among other locations, it appears to have the best balance of safety, elevation, latitude, and scientific value while not being a site already visited by past missions.

The MAV is designed to act not only as an ascent vehicle, but also an emergency getaway vehicle and refuge. Should any issues occur during their surface mission, the crew can retreat to the MAV for safety, with enough stored supplies to allow for missing up to 2 launch windows. Thus, the ECLSS is sized to support the crew for 10 sols on the Martian surface and up to 1 sol during ascent and transit to the DST, with a 50% margin of consumables for safety. For this short duration mission, a high-heritage, open loop system is used. Waste collection during ascent and transit to the DST is comprised of the Off Nominal Waste Management System (ONWMS) developed for the Orion Crew Survival Systems (OCSS). This system is built into the ascent suit. The MAV's food management system accounts for the low number of

food items with a high enough shelf life to be launched with the MAV by allowing the crew to supplement the supplies with food brought with their roving habitat and any successful plant experiments. Additional logistics such as body wipes and disposable clothing are also brought to accommodate for long duration contingency scenarios.

The crew's health and safety is critical for mission success. Thus, ascent suit, ingress method, and interior configuration trades, all pay particular attention to mitigation of risks such as radiation from the nuclear reactor, exposure to Martian dust, and ineffective interfacing between the crew and MAV systems. Additional analysis is also completed to ensure that the final combination of systems is capable of recovering from the most likely and salient contingency scenarios. With all of this taken into account, the MAV crew will wear IVA suits for ascent with access to extra long umbilical chords. An inflatable tunnel acts as the ingress method form the roving habitat, allowing the crew to don their IVA suits within the habitat prior to ingress. The capsule size and internal configuration are validated by a task analysis, ensuring the crew will have adequate volume to effectively execute each of their mission tasks.

The MAV features a main human capsule module that is situated near the Martian ground, surrounded by four spherical propellant tanks, placed along the sides. The tanks are attached to the capsule by means of two sets of two Titanium-64 struts, placed on the top and bottom of each propellant tank. The struts were made to be as short as possible, to minimize bending moment of inertia and minimize the bending loads on the structure. Aluminum 2021 was selected for the tanks in order to best accommodate the selected cryogenic fuel, as the material is extremely resistant to crack corrosion at cryogenic temperatures. The main capsule is comprised of Aluminum-2024 T3 for maneuverability and manufacturing since there are no driving loads or subsystem demands. Lastly, composite overwrapped pressure vessels (COPVs) are chosen for the pressurant tanks to minimize mass. The top of the MAV vehicle incorporates a docking port for connecting with the OT and DST. Structural requirements include structural quality control such as non-destructive and structural testing.

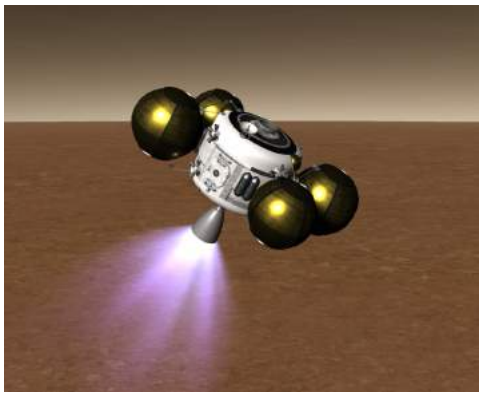

Fig. 1 MAV during ascent.

MAV attitude and determination control systems (ADCS) were made capable of dealing with the primary attitude determination driving requirements. The first of two requirements is a pointing budget of 0.001° for the communications failure contingency of properly pointing the high gain antenna to handle communications from the surface of Mars back to ground stations on Earth. The other driving factor is the stability control for Mars entry and on ascent, which needs an accuracy of 1° pointing budget. The MAV ADCS is fitted with 16 200N RCS thrusters, 4 Custom single-gimbal control moment gyros for fine attitude control, 2 star trackers for low frequency state estimation updates, 2 inertial measurement units (IMUs) for Kalman filtered attitude propagation, and 16 sun sensors for coarse attitude acquisition and contingency. Vehicle propellant sloshing concerns were accounted for through an additional determined six degrees

of gimbal range on the main propulsion system engine to counteract any undesired moments. The propellant feed system monitors the level of propellant within the tanks to prevent uneven mass distributions. Baffles were also put in the tanks to reduce sloshing. Finally, the MAV RCS and ADCS systems are distributed such that the capsule alone maintains full control for docking procedures.

The single lander design with the MAV is made possible by landing only the methane needed for launch, as well as only needing to reach a 250 km orbit on landed mass alone. A total of 12662.19 kg LOX would then be produced by means of the in situ resource utilization (ISRU) propellant generation system on the lander. Nominal ISRU propellant generation will produce all of the necessary fuel in 14 months, however, a fully redundant ISRU system is included, and sub-optimal conditions will still complete fuel production in 24 months, just before launch preparations in 2040. The MAV main propulsion system (MPS), which is a methalox ox-rich staged combustion cycle, will provide a thrust of 315 kN to accomplish mission critical 3860 m/s ΔV during ascent. On liftoff, the MAV will carry a total 16,179.47 kg of methane and LOX propellant, amounting to a total vehicle mass of 21,224.86 kg. The RCS/OMS fuel type is MON25/MMH, selected for its coherence and robustness, and an included 340 kg of fuel is carried for the ADCS systems. A common COPV was also implemented to supply Helium to both the RCS system and MPS in order to prevent engine pump captivation.

The ISRU propellant generation apparatus is the driving factor in power systems design, requiring far more power than all other subsystems. The 10 kW nuclear fission reactor, as included in the mission by AIAA RFP, will only be able to supply 58% of the needed power to produce all of the required LOX. Four 8 m diameter Ultraflex solar arrays supply the rest of the needed energy, as they are the most mass efficient option. The gimbaled solar arrays are equipped with an electromagnetic dust shield to prevent any buildup of Martian dust. These solar arrays generate excess power to charge batteries which supply the ISRU throughout the Martian night. During launch and taxi rendezvous, the MAV relies on stored battery energy which includes enough charge for contingencies.

Storing the ISRU produced cryogenic LOX propellant on surface of Mars is of utmost concern, as solar radiation and Mars' atmospheric climate will drive tank temperatures well above the maximum allowable of 90 K. In order to best maintain cryogenic temperatures for the MAV tanks, a vacuum jacketed multi-layer-insulation (MLI) thermodynamic vent system with vapor cooled shielding and refrigerators is used. The low conductivity of aluminized mylar and fiberglass paper spacers allow for the vacuumization of the exterior layers of MLI, thus providing the best effective defense measures against Martian convection. The multitude of layers within the MLI, paired with low absorptivity of aluminized mylar, allows for redundancy and protection from solar radiation as well. The main capsule on the MAV is equipped with a similar system, however, there are no vapor cooled shielding or refrigeration, and instead cartridge heaters with copper belts are put inside the MAV, allowing adequate temperature heating for the crew within the cold Martian atmosphere.

Once human arrival stage begins, provided the MAV has successfully passed all system checks, the crew proceeds

to touchdown on Mars surface and begin their surface operations along with sample retrieval. The awaiting MAV is accessible to the crew at any point during surface operations and acts as safe "turtle shell" refuge to protect and support the crew during any emergencies. By July of 2040, the crew prepare launch sequence and begin the journey back to the Deep Space Transit (DST) vehicle awaiting in Mars 5-sol orbit. During ascent, the MAV detaches from the lander and propels with its now filled LOX and liquid methane tanks to the 250 km orbit of the Taxi in order to rendezvous for a needed boost. The Taxi has been patiently awaiting the MAV for 2 years now, and is necessary for mission completion as the MAV does not have all of the necessary fuel to propel itself the full length to the DST.

The Orbital Taxi structural design is purely to accommodate the hypergolic fuel during the 2 year orbit and incorporate means of dealing with maximum driving load situations. The driving load is during boost to DST, however, this determined pressure equivalent bending load (PEQ) due to acceleration of the vehicle is minimal such that material selection of Aluminum 2024-T3 is employed on the Taxi body for ease of welding manufacturing. The Taxi body is for simplicity in the packaging of the fuel. For separating the fuel and oxidizer tanks, while minimizing structural mass, a common dome is used in the main tank.

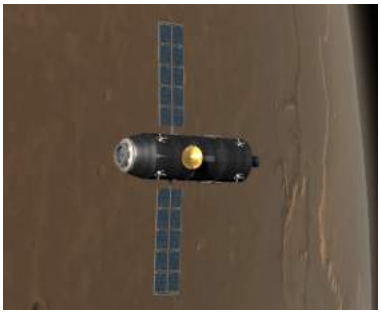

Fig. 2 Taxi in orbit.

The docking section is located on the primary axis of the vehicle for ease of attitude control and stabilization of the spacecraft. For sake of redundancy, a stiffening structure was placed inside the tank to avoid any potential failure modes caused by local buckling on the thin walled pressure vessel.

A total 8916 kg of propellant mass is required for the Taxi to perform mission duties and carry the MAV to DST. The Taxi main propulsion system engine cycle is constructed as an ox-rich staged combustion cycle. Main propulsion system propellant type for the Taxi is MON25 and MMH, as the Taxi does not require high specific impulses and cryogenic risks of boil-off, leakage, and thermal management can be avoided. The Taxi RCS/OMS systems also utilize MON25 and MMH to achieve simplicity in the overall propulsion design. Four extra ullage thrusters will be dedicated to the general system to make certain that the main propellant is fully covering the main propulsion tank drains before starting the main engine. This engine design maximizes simplicity and reliability considering the 2 year waiting period.

To maintain the Taxi for the 2 year duration in orbit, establish communications link to Earth ground station, and provide means to docking mechanisms, an attitude control and determination system of both momentum dumping RCS thrusters and fine tuning reaction wheels are utilized. Specifically, 4 pods of 4 200N RCS and 4 reaction wheels to achieve the 0.001° pointing requirement. Then for redundancy measures: 2 Star trackers for low-frequency state estimation updates, 2 IMUs for kalman filtered attitude propagation, and 16 sun sensors for coarse attitude acquisition as contingency are implemented.

Preservation of OT fuel integrity and electronic hardware throughout mission Taxi orbit durations warrant reliable

thermal management systems. The Taxi is arranged to incorporate passive control methods of Kapton exterior and Aluminized Mylar MLI, along with interior metal aluminum spacecraft coating to promote overall vehicular heat preservation. Then active control Teflon radiators are built in either sides of the Taxi. These radiators are coupled with heat pipes to sufficiently transport waste heat to the correct locations for ejection away from the spacecraft.

Two gallium arsenide triple junction solar arrays are used to meet OT power demands. Excess solar power will be stored in the Taxi's 115 kg Panasonic lithium-ion battery pack. The battery pack is sized to sustain all systems for 5 sols in the worst case that the solar arrays become non-functional after docking with the MAV.

The communications systems for TRTL are designed to provide a reliable and redundant communications link with ground control. The primary communications link consists of a low gain link between the MAV and the OT, which relays the data to the Deep Space Network (DSN) via a high gain antenna. This architecture minimizes mass on the MAV and eliminates a potentially high drag, high gain antenna. In the event of a failure in this primary communications link, a small diameter high gain antenna on the MAV can communicate directly with the DSN using a reduced datarate emergency mode. The mission architecture also allows for larger mass margins, which supports the inclusion of fully redundant internal communications components to reduce probability of such a failure. This communications strategy should, overall, provide a reliable and functional link for the ISRU phase of the mission and for crew communication during the ascent and rendezvous phases of the mission.

After successful MAV launch, the capsule sheds the tanks and engine, and the mission proceeds with the MAV and Taxi docking together. Then, the Taxi propels the pair towards 5-sol orbit in order to reach the DST, undergo one more final docking sequence, and complete the mission.

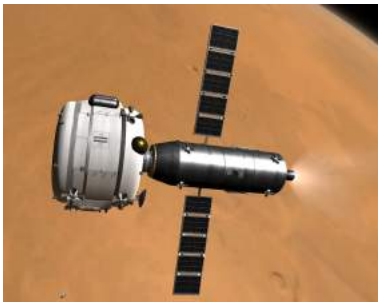

Fig. 3 MAV and Taxi docked configuration.

Mission costs allowances were up to $4 billion. The final TRTL mission plan includes an estimated total project cost of $3.942 billion USD. An additional 10% of reserves have been included as part of the overall cost as margin for unexpected expenses. The entire timeline for the TRTL mission, including development, manufacturing, testing, and operation is estimated to be 187 months.

TRTL reduces complexity from the original suggested mission architecture and adds in components of extensibility for future missions. **TRTL's proposal incorporates the use of a 16 metric ton lander, 68% less than the two sets of 25 tonnes allowed by the AIAA competition**. TRTL also establishes simplicity in the avoidance of an autonomous fuel transport method and the risks associated with navigating over Martian surfaces. Then, a legacy backed mechanism of rendezvous and docking is incorporated. Finally, extensibility means of leaving the the ISRU system on Mars and having a refuel-able Taxi establishes a presence on Mars and provides great potential for future missions to Mars.

B. Introduction

Mars has been a topic of interest for the space industry - specifically NASA - for decades, beginning with the very first Martian flyby of Mariner 4 in 1964 [1]. Since then, expeditions to Mars have become more and more ambitious, escalating to orbiters, rovers, and most recently, a small helicopter: Ingenuity. With each robot sent, NASA expands its knowledge of the Martian environment, collecting more and more data about its atmosphere, geology, and history. This spirit of innovation and exploration drives towards an inevitable manned Martian mission, which remains a serious challenge due to numerous complications linked to launching off of Mars' surface and providing a safe environment for humans. These problems include landing exceedingly heavy masses through a thin atmosphere, launching with no ground support equipment, and communication delays and blackouts.

A Request for Proposal (RFP) provided by the American Institute of Aeronautics and Astronautics (AIAA) requests a mission design of the transport of two humans and 50 kg of samples from the surface of Mars to an awaiting Deep Space Transit (DST) in a 5-sol orbit, accomplished by two landers. In a packed configuration, both landers must fit in an 8.4 m diameter payload fairing, land payloads not to exceed 25 metric tons, and launch no later than 2037 with an arrival to Mars no later than July of 2038. One lander contains an unfueled MAV, while the other lander contains the needed fuel. With the landers assumed to be 1 km apart, a concept must be designed to autonomously transport fuel from one lander to the other and prepare the MAV for human ascent by July 1st, 2040.

Since TRTL would be part of the first manned mission to Mars, safety was the top priority when considering different mission architectures. Preliminary analysis showed that while a two-lander system with a 1 km fuel transport was possible, it would not be a very practical choice. Instead, we opted to have only one lander. This lander would not be able to reach the 5-sol orbit on its own, so the second vehicle would be an orbital taxi that, once docked with the MAV, boosts it to the 5-sol orbit. There are several advantages to such a design. First, transporting fuel across the surface of Mars is a dangerous and untested process. Historically, Martian rovers move very slowly and machines on Mars are frequently coated in dust, not only covering solar panels but degrading mechanical components as well. Any fuel transport robot would also likely need to make the 1 km trip hundreds of times through harsh terrain. Overall, transporting fuel appeared to significantly increase the chances of a mission failure before humans ever arrived. Second, Perseverance, weighing in at around 1 metric ton, is the heaviest payload landed on Mars [2]. Landing one 25 metric ton payload already introduces a new set of potential failure modes; landing two doubles the chance of failure. In contrast, rendezvous and docking with another vehicle has been thoroughly developed and tested. The first successful orbital rendezvous occurred 57 years ago with the docking of Gemini VIII to the spacecraft Agena [3]. Additionally, with the ISS alone, over 162 docking maneuvers have been performed [4]. A rendezvous in space is a safe and proven procedure, and for a mission where human lives are at stake, it is the most logical choice.

C. Mission Overview

C.1. Mission Requirements

Below is a table of high-level mission requirements derived from the AIAA RFP. Requirements for each subsystem can be found within their respective sections.

Table 1 Overall System Requirements

Req. ID	Requirement Description
TRTL-RFP-1	The MAV shall launch from the surface of Mars and travel to Mars 5-sol parking orbit.
TRTL-RFP-2	Each lander payload shall not exceed the payload capacity of 25,000 kg per lander.
TRTL-RFP-3	Lander payload shall fit within the lander 8.4m diameter fairing.
TRTL-RFP-4	One of the landers shall carry a 10 kW surface fission power unit with a minimum mass of 5,000 kg.
TRTL-RFP-5	The system Landers shall depart from Earth no later than 2037 and arrive at Mars no later than July of 2038.
TRTL-RFP-6	The MAV shall be fueled and ready to support humans for ascent by July 1, 2040.
TRTL-RFP-7	The mission cost, not including the landers or launch vehicles, shall not exceed 4 billion USD in 2022.
TRTL-RFP-8	The MAV shall support 2 humans from Mars surface to Mars 5-sol parking orbit.
TRTL-RFP-9	The MAV shall have the capacity to return 50 kg of Mars samples to DST.

As mentioned previously, the use of two landers and an autonomous fuel transfer system were additional requirements by the AIAA; however, upon contacting Dr. Patrick Chai in late February, we were given permission to deviate from these requirements as long as justification and proper engineering analyses were provided.

C.2. Concept of Operations

TRTL begins its mission in August of 2037 with the MAV and orbital taxi launching on two separate SLS rockets. 6 to 7 months after launch, both vehicles arrive at Mars. The orbital taxi inserts itself into a 250 km circular orbit while the MAV, attached to a lander, enters Mars' atmosphere and descends to the surface using the lander's engines. For the majority of the mission, the orbital taxi will stay in its circular orbit, waiting for the MAV to launch and dock with it.

Once the MAV touches down (with its oxidizer tanks empty but fuel tanks full of liquid methane), it begins producing liquid oxygen (LOX) from the atmospheric carbon dioxide through a solid oxide electrolysis process. At nominal solar power, the LOX tanks will be full before the humans leave Earth, about 14.4 months after LOX production begins. However, a full 2 years are allotted for ISRU, which assumes 60% of the nominal solar power amount. In this case, the LOX tanks will be full when the humans arrive. A fully redundant ISRU unit is also included in case the primary unit fails.

When the humans are ready to leave, they board the MAV, which separates from the lander at launch. Extra hardware

including some batteries, solar panels, and the ISRU units remain on the lander. Their launch window is dictated by the DST's 5-sol orbit. Roughly 1 hour after launch, the MAV docks with the orbital taxi and drops its engine and fuel tanks to shed unnecessary mass. The taxi then ignites its engines, pushing itself and the MAV command module from the 250 km circular orbit to the higher 5-sol orbit of the DST. Around 6 hours after launch, the taxi and MAV command module rendezvous and dock with the DST. The mission is complete once the humans are onboard the DST.

A visualization of the entire mission operation is shown on the next page.

CONCEPT OF OPERATIONS

1. LAUNCH | August 2037
The orbital taxi and MAV launch aboard two SLS rockets.

2. ARRIVAL | March 2038
The orbital taxi inserts itself into a 250km orbit while the MAV touches down on Mars with the aid of a lander. The taxi remains in orbit until rendezvous.

3. LOX PRODUCTION W/ ISRU | 2038-2040
The MAV, with liquid CH4 already stored onboard, begins producing LOX from the atmosphere.

4. HUMAN ARRIVAL | April-July 2040
Humans arrive on Mars to perform their mission. The MAV is already fueled and ready to launch.

5. TAXI RENDEZVOUS | T+1 hr
The MAV separates from the lander and ascends from the surface, docking with the orbital taxi and jettisoning its engine and tanks in the process.

6. DST RENDEZVOUS | T+6 hrs
The orbital taxi kicks itself and command module of the MAV to a 5-sol orbit to dock with the Deep Space Transport.

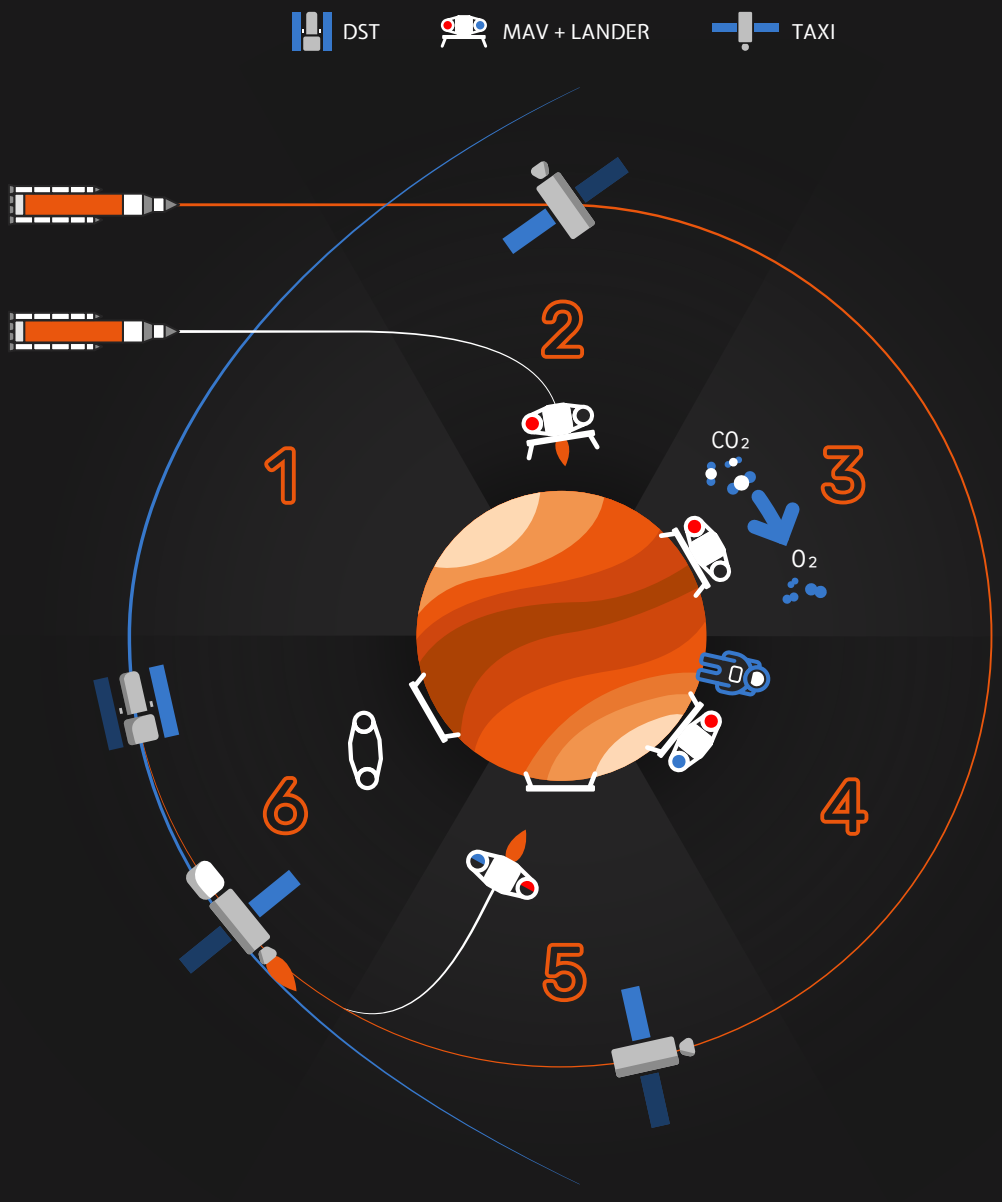

D. Vehicle Overview & Trades

Our team considered all vehicle level architectures and left no stone unturned before choosing our final architecture. We also weighed options of vehicle architectures that did not utilize the two lander, Mars based remote refueling process that was stated in the Request for Proposal. One of the first vehicle trades that was made was staging of the rocket system. We considered whether a multi-stage system was necessary since a singe stage to orbit (SSTO) rocket would reduce system complexity and increase robustness by removing stage separation and integration necessities brought by a multi-stage rocket system. In order to see if an SSTO was possible a simple calculation with the ideal rocket equation is done. The ideal rocket equation enables the calculation of the ΔV from the vehicle propellant mass fraction,

$$\Delta V = I_{\text{sp}}\, g_0\, ln\left(\frac{m_{\text{w}}}{m_{\text{d}}}\right), \tag{1}$$

a rearranged form of the equation is

$$\frac{m_{\text{w}}}{m_{\text{d}}} = e^{\frac{\Delta V}{I_{\text{sp}} g_0}}, \tag{2}$$

where ΔV, I_{sp}, g_0, m_{w}, and m_{d} are the change in velocity, the specific impulse of the engine, the gravitational acceleration on Mars, the vehicle wet mass, and dry mass respectively. For a first-order estimation, the required ΔV can be taken from literature and this value is 5600 m/s. This corresponds to a mass ratio of 5.1 which means that the rocket must be 80% propellant mass assuming an engine Isp is 350 s. From using literature to generate some vehicle mass estimates it is seen that 28 metric tonnes of propellant would be required for a 6 tonne vehicle. This makes an SSTO an unattractive option considering when including the additional system mass such as the fueling system that would be required and the 5 tonne nuclear fission unit this puts the SSTO design very close to the total 50 tonne landing limit with two 25 tonne payload landers. This early analysis shows us that TSTO (two stage to orbit) vehicles are likely to be the final solution. A high-level list of the system architectures we considered can be seen in Table 2.

The factors we considered when trading these many different architectures were reliability, robustness, expected cost, safety, tech readiness level (TRL), reuse capability, and expected mass. Reliability and robustness is seen as a category directly relating to minimizing risk and maximizing the likelihood of mission success. In this regard, being able to remove a remote refueling process brings a large risk reduction; while NASA has operated robotic systems on the surface of Mars for years many rover systems, which are much lighter than a theoretical fuel transport rover, have been plagued with problems maneuvering the surface of Mars due to the harsh Martian environment [5]. All of the architectures that include a refueling process involve some sort of rover, however, some of these architectures would provide more resilience to potential anomalies than others. The one-time transport of a large tanker full of propellant as opposed to a smaller lander doing multiple trips or a small rover laying out a hose is seen as an inferior architecture, since this would require an ambitious feat of moving an over 15 tonne vehicle through the soft Martian soil. The size

Table 2 Overall Mission Vehicle Trades

Method	Landers Required	Rocket Type	MAV initial fuel amount	MAV initial oxidizer amount	Needs fuel transport?	Uses OT Rendezvous?	Uses ISRU?	Additional Notes
1	2	TSTO	Partially fueled	Partially fueled	Y	N	N	Large transport system to move the entire tanker over to MAV for refueling.
2	2	TSTO	Partially fueled	Partially fueled	Y	N	N	Small tank rover system to transfer the propellant in batches, taking multiple trips.
3	2	TSTO	Partially fueled	Partially fueled	Y	N	N	Autonomous rover to connect a hose between tanker and MAV for propellant transfer.
4	1	SSTO	Fully fueled	Fully fueled	N	Y	N	Launches to lower orbit to rendezvous with OT for boost to DST orbit.
5	1	TSTO	None	None	N	N	Y	Propellant generation for LOX and liquid methane.
6	1	TSTO	Fully Fueled	None	N	N	Y	Propellant generation for only LOX.
7	1	SSTO	Fully fueled	None	N	N	Y	Propellant generation for only LOX.

of the rover for both the hose layout and multi-trip refueling tanker would be quite similar, however, the hose layout reduces the number of trips to only 1 which would enable fuel transport simplicity. The hose system does bring another challenge of maintaining proper thermal conditioning within the hose as the surrounding Martian environment changes, but for a non-cryogenic fuel, this problem can likely be solved with a heating coil system. There are 3 systems that discard both an entire lander and most robotics, which brings a large reliability boost the two Oxygen ISRU systems and the fully fueled SSTO to an orbital rendezvous system (note the ISRU propellant generation of methane requires the excavation of the Martian surface with rovers).

Regardless of the chosen method, this mission will rely on low TRL technology to some degree. Rover technology has been tested quite extensively on the surface of Mars, lots of data has been collected along with many discovered problems that have been worked through. ISRU technology also is a very low TRL technology in particular, fuel generation that includes excavation of the Martian surface to retrieve water for usage in a Sabatier reactor with atmospheric CO2 to generate both oxygen and methane. While the Sabatier process is a common industrial process here on Earth the extraction of the gaseous water required for the process from the ice in the Marian soil is a completely untested engineering field and drilling operations on the surface of Mars have proven to be exceptionally difficult. Any of the options relying on an orbital rendezvous for a boost to a higher orbit should be seen as a well-tested and developed technology with hundreds of operations completed in LEO and a handful of successful orbital rendezvous during the Apollo program around the moon.

The reason we considered reuse capability is because of the high-priority NASA goal to build an established

presence on the surface of Mars, specifically Strategic Goal 2 within the 2022 NASA Strategic Plan [6]. Of the refueling processes, only the architecture with the small rover tanker that makes multiple trips presents capability for re-use in that if it is still functional at the end of this operation, it can help out in a future mission. Any of the ISRU mission architectures also provide a potential reuse opportunity, in assisting future missions by potentially producing their required propellants. Also, ISRU is vital long term for building an established presence on Mars and proving the technology would be pivotal for NASA's Mars missions.

As far as cost and safety it is difficult to analyze these factors within the early design phase. For cost it is acknowledged that ISRU development will be a multi-billion dollar project itself, nevertheless, ISRU is a project that is already planned to be developed in parallel with this mission development and has already started with the recent demonstration of MOXIE on the Perseverance rover. A great cost reduction would be found in the deletion of a second lander and the fuel transport robotics systems. In terms of safety for the astronauts, many of these systems can be designed to the same safety level considering the rocket itself is largely same across all designs. However, some architectures present more capacity for additional leeway due to the minimum design linked with higher mass margins. Specifically the LOX-only ISRU SSTO and the storable fuel refueling options.

After considering all of the above it was apparent to us that deleting one lander, if possible, proves to be advantageous in that it decreases cost, increases reliability and robustness, and has the potential to leverage a better mix of high and low TRL technologies. Given this, we next computed some literature based first-order mass estimates [7] for the different single lander options and the results are in Table 3.

Table 3 Lander System Mass Estimates

System	Landed Mass (Metric tons)	Takeoff Mass (Metric tons)
Ox ISRU, 2 stage	26.52	45.05
Ox ISRU, 1 stage	16.20	31.40
Both ISRU, 2 stage	27.68	39.05
No ISRU, 1 stage	24.650	24.95

From this, we were able to make our overall architecture choice of the Oxygen ISRU SSTO which launches to a rendezvous with an orbital taxi to kick the MAV and crew out to the DST orbit. The decision from here was heavily influenced by the landing mass estimates, the chosen method's mass came out to almost 9 tonnes below the 25 tonne lander maximum. While all of this was an estimate and it is likely the other 3 designs could be configured to be below the 25 tonne limit, this estimate provides a clear picture that our chosen architecture contains by far the most mass margin and thus the most room to add safety redundancies and make this mission design a better performing and safer mission for the crew.

E. Mission and Trajectory Analysis

The overall mission trajectory and operations were chosen with a philosophy of driving to simplification and robustness in order to maximize the likelihood of mission success and minimize unnecessary risks taken. On a high level, the baseline mission is to safely send humans to the surface of mars, and safely have them return back to Earth. Under the given assumptions of the problem space, the scope of this team's mission design directly encompassed only the mission elements from initial Mars orbit injection until final MAV liftoff and DST rendezvous, but the entirety of the overall mission was always taken into consideration for converging to a trajectory and operations design that would be realistic, compatible with available technology and resources, and highly reliable.

E.1. Trajectory Requirements

As specified by the AIAA competition rules, the vehicle is required to transport the two humans and sample cargo into a 5-sol orbit around Mars in order to dock with the DST to be transported home. The specific orbit parameters were not detailed in the requirements. This is as far as the requirements specify relevant to the mission's trajectory analysis.

E.2. Trajectory Trades

As mentioned in the Vehicle Overview & Requirements Section D (Vehicle Level Trades), the overall vehicles were chosen with the philosophy of leaving no stone of possible solutions unturned. In exploring these solutions, the trade showed that it would be most robust to have one lander that landed the MAV and filled its oxygen side of propellants utilizing ISRU. The second vehicle would remain in a lower orbit around Mars, which the launched MAV would rendezvous with before transferring to the 5-sol orbit and rendezvousing with the DST. This second vehicle is hence called the Orbital Taxi (OT). With the general mission format outlined, there were some specific trades to be studied from a trajectory point of view: the launch and arrival windows, OT orbit type and altitude, and DST rendezvous transfer.

The first trajectory trade was to look at the potential launch and arrival windows. The requirements of the competition stated that our system(s) must arrive on Mars by 2038 and be there for roughly two years, before the humans arrive in another vehicle in 2040. From this general time frame, a porkchop plot was generated [8] for departure ΔV on a trajectory from Earth to Mars. This plot is depicted in Figure 4, and shows the contours for various ΔV values with respect to launch date and time of flight. Given the unprecedented importance of this mission, the team wanted to maximize the launch window date, while keeping the required ΔV as low as possible. By fixing the time of flight (ToF) to 210 days, this allowed the team to operate within the widest range of the light-blue section, which essentially gives the lowest required departure ΔV for a rather wide launch window of 7 weeks. Specifically, this meant a launch window from 1 Aug, 2037 to 20 Sep, 2037, with a required ΔV of between 4.11 km/s and 4.62 km/s. It is vital that this window is as large as possible, because if launched missed due to insufficient time to solve unforeseen issues, the next potential

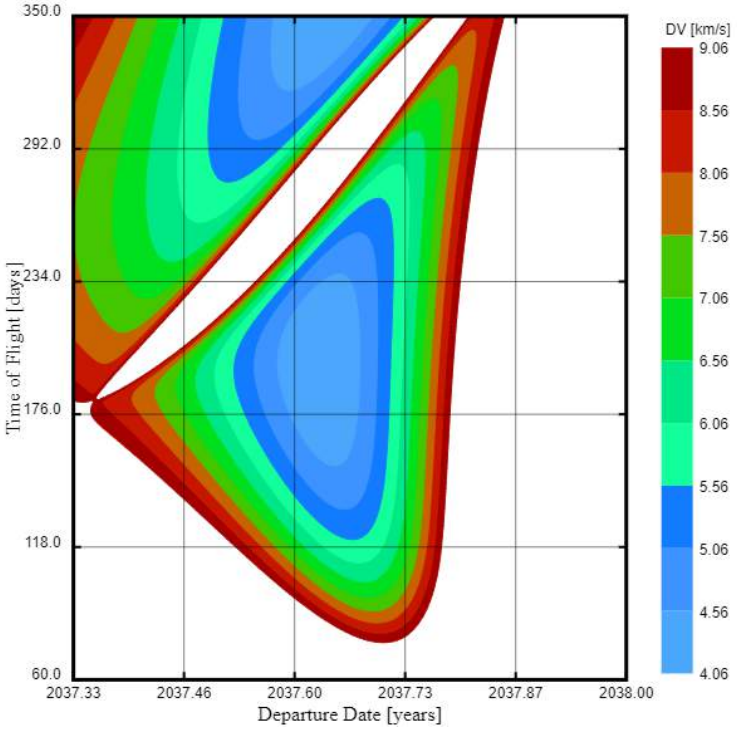

Fig. 4 Departure ΔV porkchop plot

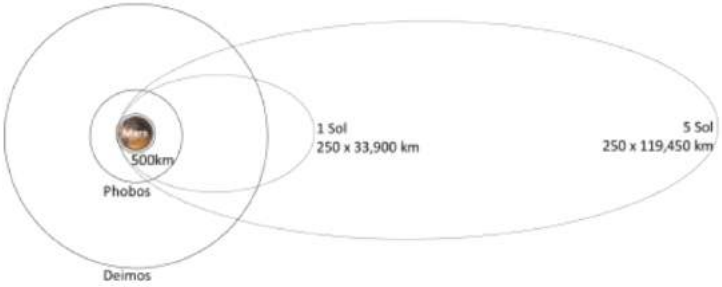

Fig. 5 Mars orbit options, including NASA chosen 5-sol parameters for DST

window would be 26 months later, when Mars and Earth line up for optimal transfer again [9]. This delay would result in a failure to meet the timeline requirements of the mission stated earlier.

The next trade relevant to mission trajectory was regarding the orbit type and altitude of the OT, which is a trade that is coupled with the potential DST orbit that would be chosen. Initially, it seemed that most papers that included Mars orbit trajectories had a 500 km circular orbit, but it was unclear as to why that specific altitude was so consistently chosen [10] [11]. With some deeper digging, it was found that there was already a NASA-chosen orbit apogee and perigee as a prime candidate for a 5-sol orbit for future Mars missions [11]. Hence, this 250 km x 119450 km highly elliptical orbit was chosen to be set as a requirement for the DST, as seen in Figure 5. It is worth noting that the 5-sol orbit given requirement from the competition was vague and did not specify a particular orbit, hence this is set as a

requirement from this team in order to close in on mission operations and orbits. The orbit 250 km x 119450 km specified is in fact roughly 5.43-sol, not exactly 5-sol.

With the DST orbit now fixed, the trade remained of whether to have the OT remain in the well-speculated 500 km circular orbit that so many other papers mentioned, or to do something else. With a 500km circular parking orbit, the OT would have to perform two burns, in a Hohmann transfer. For a more time-efficient transfer, it would perform a retrograde, then prograde burn to the DST orbit. For a more fuel-efficient transfer in minimizing ΔV, it would have to perform a prograde burn, then retrograde. The last option would be to simply have the OT already in a 250 km orbit, allowing it to perform only one prograde burn to transfer into the 250 km x 119450 km DST orbit. The ΔV of each burn was calculated using a simple rearranged energy equation, calculating the velocity of each separate orbit and finding the difference between orbit and transfer orbit velocities to get the required ΔV assuming an instantaneous impulse burn, and utilizing standardized NASA provided values for constants specific to the bodies involved in this problem [12].

$$v_i = \sqrt{2\mu_M \left(\frac{1}{r_1} - \frac{1}{r_1 + r_2}\right)} \tag{3}$$

$$\Delta V_i = v_2 - v_1 \tag{4}$$

$$\Delta V_{\text{tot}} = |\Delta V_1| + |\Delta V_2| \tag{5}$$

Here, v_i is the velocity at a given point in a given orbit i, μ_M is the gravitational constant for Mars, r_i is the distance from the center of the planet to the orbiting body at a given point in a given orbit i, and ΔV is the difference in velocity required to change the vehicle's orbit. With the utilization of these equations and NASA's Mars to calculate the total ΔV (ΔV_{tot}) needed for each case, it was sensible to compare each quantitatively, as seen in Table 4. From this table, it is evident that although the 500 km orbit is most fuel efficient with the lowest ΔV, it is unrealistic and not optimal due to the amount of time that it would require the humans to remain inside the MAV capsule. This would significantly drive up ECLSS requirements, and increase the ECLSS system mass, hence increasing the overall MAV mass. Instead, the next best option is to have the OT remain in a 250 km circular parking orbit, since this requires the next lowest ΔV, and also theoretically would have the lowest time of flight to minimize the amount of time the humans have to spend in the MAV.

One last trade that was considered was putting the orbital taxi in a sun-synchronous orbit, in order to minimize

Table 4 Trade results for transferring from various OT orbits to DST

Transfer Type to DST	ΔV_1 (km/s)	ΔV_2 (km/s)	ΔV_{total} (km/s)	Time of Flight (hr)
500 km (Fuel-Efficient)	1.3007	-0.0046	1.3053	67.27
500 km (Time-Efficient)	-0.0554	1.5164	1.5718	00.98
250 km (Single Burn)		1.3492	1.3492	0

thermal cycling on the OT body, as well as maximizing the solar energy harnessed from the sun using solar panels. This would only be a consideration if the thermal control system did not close, or in the case that there was insufficient power supply over the mission duration. Since nether of these issues arose, the sun-synchronous orbit was not pursued, since the out-of-plane maneuver to rendezvous with the DST would be costly to the available ΔV, and would likely end up increasing system mass through the requirement of having to carry more propellant.

E.3. Entry, Descent, and Landing Trades

The considered EDL methods for this mission come from NASA recommendation and documentation. A trade was initiated between the Co-Optimization Blunt-body Re-entry Analysis (COBRA) and Hypersonic Inflatable Aerodynamic Decelerator (HIAD). COBRA is a mid lift-to-drag (L/D) vehicle with major dimensions of 19.8 m long and an 8.8m diameter [13]. The angle of attack for COBRA EDL is 55°, and the engines ignite at 3.2 km altitude above Mars surface. For mission criteria, the main concern with COBRA is that it is unable to fit within SLS's 8.4 m payload fairing.

The method that TRTL selected for its landing system is HIAD, a deployable Low L/D vehicle. With a payload of under 17,000 kg the HIAD's rigid heat shield has a diameter of 8.3 m [13]. This smaller diameter will allow HIAD to fit in SLS 8.4 m payload fairing. Before entering the Martian atmosphere, HIAD inflates its outer heatshield to a diameter of 16m to drastically reduce vehicular entry speed. The angle of attack is -17°. HAID the pitches to 0 degrees and engines are ignited. Although inflatable heat shield technology is new TRTL believes that it is a more proven technology then a mid L/D vehicle.

The selection of a landing site for a Mars mission is crucial to the success of the mission. In general, a site must be safe for landing, experience adequate sunlight to power solar panels, and offer some sort of scientific value. With the case of TRTL, a landing site may already be determined based on the mission the two astronauts perform. Nevertheless, several locations of interest were compared under the assumption that no site was already chosen.

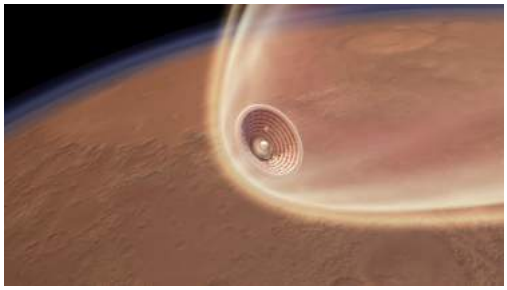

Fig. 6 MAV during descent.

In choosing candidate sites, locations already explored by previous missions were avoided so that new areas could be explored by the astronauts. The first, Amazonis Planitia, was chosen for its proximity to the equator and to the site of a recent meteoroid impact, one of the largest witnessed in the solar system [14]. The second, Arcadia Planitia, was chosen for its potential for both methane and oxygen ISRU, as being close to the north polar cap would give a lander access to subsurface ice. The third, Elysium Planitia, was the landing site of the InSight lander and was the safest location of the choices listed here due to the vast, flat landscape [15]. The final potential landing site was Holden Crater, a location also relatively close to the equator and containing "some of the most ancient rocks on Mars" [16].

The elevation and latitudes of all four sites were inputted into the TOPSIS table and each site was given a 1-5 ranking of safety and scientific value, with 1 being the least safe or least scientifically valuable and 5 being the most safe or most scientifically valuable. Elysium Planitia was given the highest safety rating because a previous spacecraft has already landed there and it was cited by NASA to have been selected primarily because of its safety; however, it was given a scientific value rating of 1 due to the lack of significant items of interest on the surface. InSight landed there because it is only monitoring seismic activity, so any surface features are of no value to it. Arcadia Planitia and Holden Crater were given the highest ratings of 5 for scientific value. Arcadia Planitia would provide ideal conditions for testing ISRU equipment; however, because the site is located so far from the equator and little is known about the area, it was given the lowest safety score of all the sites. The initial TOPSIS table can be seen below.

Table 5 Input TOPSIS table for four candidate landing sites based on elevation, latitude, safety, and scientific value

	Elevation	Latitude	Safety	Scientific Value
Weights ->	0.3	0.15	0.35	0.2
Target ->	Min	Min	Max	Max
Amazonis Planitia	-3.76	24.8	4	4
Arcadia Planitia	-3.1	39.8	3	5
Elysium Planitia	-3	4.5	5	1
Holden Crater	-2	26	4	5

The TOPSIS analysis calculated a final value for each site within a range of 0 to 1 to reflect its closeness to the ideal values. Amazonis Planitia ended up as the first choice, being a good balance of the four characteristics and having the lowest elevation. This location was selected to be our planned landing site for our MAV and lander.

Table 6 Closeness values and final TOPSIS analysis results for four candidate landing sites

	Closeness	Ranking
Amazonis Planitia	0.63	1
Elysium Planitia	0.57	2
Holden Crater	0.50	3
Arcadia Planitia	0.45	4

E.4. Finalized Mission Operations

With all aspects of the overall trajectory and mission finalized, a time stackup and ΔV budget breakdown can be made highlighting the critical points of the mission design. They are as follows:

- Aug 2037 - Mar 2038: Earth departure and transit on SLS Block II
- Mar 2038 – Apr 2038: Arrival

Table 7 Mission phase duration stackup and ΔV budget

Mission Phase	[Nominal] Duration	[Nominal] Required ΔV (km/s)	[With-Margin] Duration	[With-Margin] Required ΔV (km/s)
Launch Burn	106 s	2.23	200 s	2.75
Cruise to 250 km	13 m	-	20 m	-
Circularizing Burn	46 s	1.36	90 s	1.65
Dock with OT	1 hr	0.003 [RCS]	2 hr	0.01 [RCS]
System Checkouts	1 hr	-	2 hr	-
OT to 5-sol Burn	90 s	1.35	180 s	1.70
Shed OT & Maneuver	1 hr	0.005 [RCS]	2 hr	0.01 [RCS]
Dock with DST	1 hr	0.003 [RCS]	2 hr	0.01 [RCS]
System Checkouts	2 hr	-	4 hr	-
DST Boarding Prep	30 m	-	1 hr	-
TOTAL (Launch to DST Boarding)	6 hr 45 m	3.86 + 1.35	13 hr 30 m	4.70 + 1.70

- 2038 - 2040: Fill MAV LOX tanks using ISRU system
- April-July 2040: Humans arrive. Pack samples, board MAV, and prepare for launch
- T+00 hr: Launch from Martian surface
- T+01 hr: Rendezvous and dock with OT
- T+02 hr: Complete OT checkouts
- T+04 hr: Rendezvous and dock with DST
- T+06 hr: Complete DST checkouts

With all critical operations in mind, the breakdown of total required ΔV can be stacked up along with time duration after launching from the Martian surface, as shown in Table 7.

The solar radiation pressure (SRP), as expanded upon in the ADCS section, will be very minimal for this flight. The information for SRP values was derived from the Mariner 9 Mars orbiter mission, and scaled based on the first order estimates of the Orbital Taxi surface area and mass [9]. Hence, there is some ΔV allocated for that purpose in the RCS system. With the maximum error stackup on RCS and worst-case SRP scenario, the vehicle still maintains a sun aspect angle of +/- 4.6 degrees. However, there is no sunlight on the solar panels while the spacecraft is within the shadow of Mars, which is roughly 41% within Mars's penumbra.

F. Mars Ascent Vehicle

F.1. Environmental Control and Life Support Systems

The AIAA RFP requires the ascent vehicle to support a crew of two humans during ascent from the surface of Mars to docking with the DST. Nominal ascent time of flight is 6 hours. Adding in contingencies, this transit time is about 16 hours. Additionally, should an issue occur within the roving habitat's ECLSS system during any portion of the crew's surface mission, the MAV can act as an alternative habitat, sheltering the crew until the next launch window. With a launch window to the Taxi every 5 days, and allowing for up to two missed launch opportunities, the full duration for this contingency is about 11 days. To account for check outs and docking contingency scenarios, the system must also support 4 pressurizations. Adding in a margin of 50% for safety, the ECLSS equipment and consumables were sized for up to 16 days usage and 6 pressurizations. Sizing was done using NASA's ALSSAT software, modified to reflect the design of our mission. In particular, this required specifying the MAV's manned mission duration, unmanned mission duration, mission location, crew size, capsule size; updating the number of redundant unites for particular systems; and removing multiple pieces of consumable processing and regeneration hardware to reflect the MAV's open loop ECLSS system.

Table 8 ECLSS Requirements

Req. ID	Requirement Description
TRTL-ECLSS-01	The MAV shall support two humans during liftoff from Mars to rendezvous with DST.

F.1.1. Open Versus Closed Loop

Given the short mission duration, the material savings from any degree of closed loop system does not outweigh the mass, and complexity costs of the necessary equipment. Thus, an open loop system consisting of high-heritage technologies was selected to reduce mass and development costs while still ensuring high reliability.

F.1.2. Air Management System Trades

The Apollo crew lived for 2 weeks in an atmosphere of 100% O_2 at 5 psia. This composition required a lengthy prebreathe procedure prior to EVAs and raised concerns of flammability. Since then, a number of different atmospheric compositions have been used, each with their own pros and cons in regards to structural loads, leakage, convective cooling capacity, EVA prebreathe requirements, flammability, and toxicity. For the MAV, particular attention was given to the prebreathe requirements and likelihood of decompression sickness. Ascent is one of the highest risk portions of the crew's overall mission. Should an emergency occur, the expedience of a prebreathe procedure and likelihood of

decompression sickness could be the deciding factor whether the crew survives. The recently developed Exploration Atmosphere enables an expedient 15 minute prebreathe procedure and decreases the likelihood of decompression sickness for the crew, as well as decreases the flammability of the atmosphere and reduces leakage [17]. To ensure internal atmospheric quality given the short mission duration, lightweight and nonrenewable systems should be used for the atmospheric monitoring and control systems.

F.1.3. Waste Management System Trades

The waste management will support the crew for up to 10 sols on the Martian surface and up to 1 sol during the ascent portion of the mission. Four options were considered for this system: the Universal Waste Management System (UWMS), the Off Nominal Waste Management System (ONWMS), Maximum Absorbency Garments (MAG), and fecal bags. The UWMS was developed for unsuited crew in microgravity and 0g environments. This unit is designed for use in closed loop systems and includes processing equipment unnecessary for the MAV's short mission duration [18]. The ONWMS is currently in development for microgravity and 0g environments as a part of the Orion Crew Survival Systems. It is built into the IVA suit, removing the need for crew to doff their suits, and is rated for use up to 6 days [19]. MAGs are simple, lightweight, designed for all gravity environments, and are already worn within EVA and IVA suits as standard procedure. However, MAGs are only rated for 8 hours, and ascent can take upwards of 17 hours [20]. Fecal bags, such as those used in the Apollo program, comprise of simple bag with an adhesive ring which allows the crew member to affix the collection device to themselves and then seal the bag after use [21]. In the event the crew must take refuge in the MAV while it is still on the surface, this system would be the most accessible and easiest for the crew to use for multiple days in the 1/3 g environment.

F.1.4. Food Management System Trades

Any food sent with the MAV will have to be stored for up to 3 years before consumption. However, the current food system used on the ISS is rated for a shelf-life of only 18 months. Advances in low oxygen and moisture content packaging systems can be expected in the future, but these are not guaranteed to improve the system well enough to double shelf-life. A study on changes in acceptability of the ISS thermostabilized food items over a course of 5 years was done to assess the ability of using the ISS's system for long duration space missions. As shown in Table 7, of the 65 NASA thermostabilized items, only 27 remained 'acceptable' after 3 years [22].

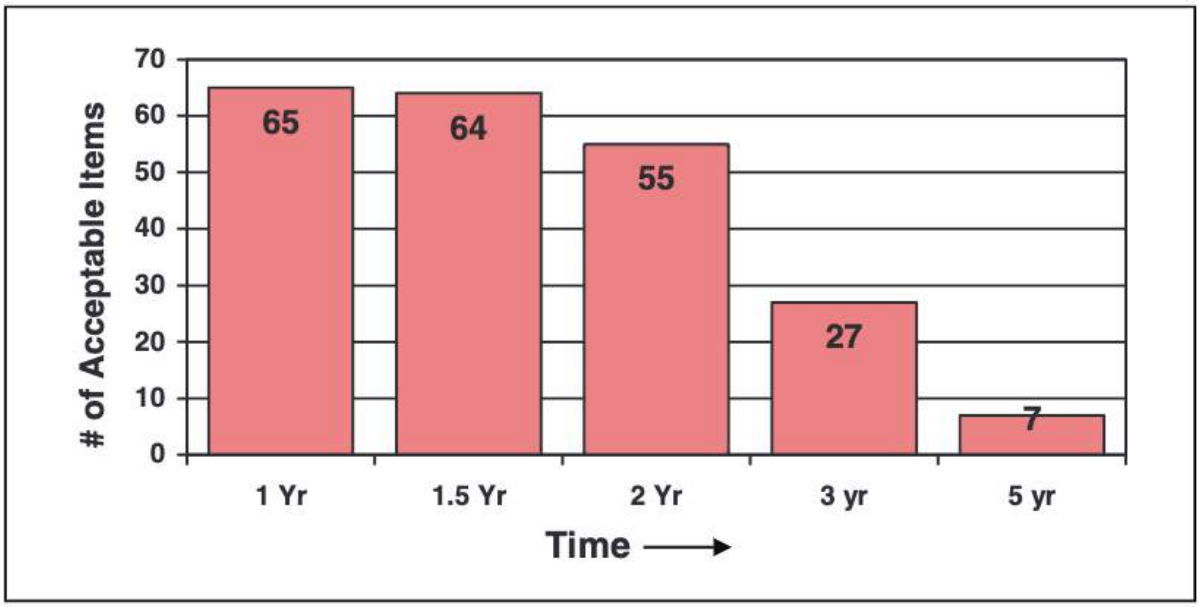

Fig. 7 Number of thermostabilized space foods as shelf life extends to 5 years.

Similar trends are expected with rehydratable, and natural form food items. Given the MAV's short mission duration, a system could be developed using only the 27 thermostabilized items, supplemented with the similarly acceptable rehydratable items, but the overall acceptability of the menu is likely to decrease due to individual preferences and the limited variety of the menu, especially if multiple items are also included in the menu during the crew's surface mission. Alternatively, food brought with the crew would require a shelf-life of at most 12 months, well within current capabilities, and could easily be transferred to the capsule with the crew. These items could be used to supplement the MAV's menu, adding variety and increasing acceptability. Lastly, plant growth experiments are expected during the surface mission, and could supplement the menu with fresh greens, a highly regarded perk for crew nutrition supplementation. The exact ratio of food brought with the MAV versus with the crew will need to be determined by coordinators in accordance with crew preferences, advances in food storage technology, and the affordability of adding additional mass to the roving habitat. However, the amount stored on the MAV should not drop below the amount required to sustain the crew for a 6-day contingency in which an expedited loading process does not allow for the loading of additional food items.

F.1.5. Final Configuration

The MAV capsule will take advantage of NASA's predefined 'exploration atmosphere,' a 56.4 kPa atmospheric composition made up of 34% O_2 and 66% N_2, held at 'shirt-sleeve' temperature, which is between 291-297° K [23]. The full amount of O_2 and N_2 needed for this composition will be brought from Earth and stored in tanks until the ECLSS system is activated. Lithium hydroxide canisters, activated charcoal with a catalytic oxidizer bed, and HEPA filters were chosen to act, respectively, as the CO_2 removal, trace contaminant control, and bacterial filtration systems.

A fire detection and suppression system will also be on board for the crew's safety. The water system is comprised of two tanks, one for potable water, the other for waste water, and is sized to include both the crew's drinking and hygiene water. The MAV's food management system will comprise of 3 main pieces: food brought with and stored on the MAV, food brought with the crew and initially stored in the roving habitat, and potentially fresh greens from any plant growth experiments. The waste collection is a fully stored system without processing. It comprises of the ONWMS for the ascent portion of the mission and fecal bags. The fecal bags are primarily available to support the crew during any contingencies which force them to take refuge within the MAV while still on the surface. To also accommodate for these contingencies, additional logistics added for the astronauts' comfort include body wipes and disposable clothing.

Table 9 ECLSS system mass, volume, and power budget.

System	Mass (kg)	Volume (m^3)	Power (W)
Air Management Subsystem	338.04	1.00	174.00
Water Management Subsystem	141.21	0.26	8.86
Solid Waste Management Subsystem	3.55	0.10	0
Thermal Control Subsystem	195.81	0.55	563.49
Food Subsystem	90.41	0.25	10.00
Human Accommodations	26.24	0.09	0
TOTAL ECLSS System	673.43	1.89	756.17

F.2. Human Factors

The crew's health and safety is critical for mission success, as emphasized by the AIAA RFP-9 requirement previously mentioned. These considerations significantly affect the methods used to evaluate challenges such as: ascent suit selection, crew ingress method, and ensuring that pressurized volume of the capsule is large enough to accommodate all crew functions.

F.2.1. EVA Versus IVA Suit Trades

F.2.1.1 Ascent Suit

As an ascent suit, both EVA and IVA suits have been used. EVA suits are best suited for short ascent missions in which the suit can independently support the crew, removing the need for an ECLSS system and pressurized cabin. EVA suit technology is rated for 8 hours, with more advanced, current concepts capable of supporting the crew for upwards of 12 hours. Beyond this duration, however, a pressurized cabin and separate ECLSS system is required, and the main advantage of EVA ascent suits is lost. IVA suits, although requiring a pressurized cabin, are significantly smaller, lighter, and more ergonomic. Task volumes associated with IVA suits are more than half the size, loosening constraints on MAV capsule size. The suits themselves also weigh significantly less, reducing overall MAV mass. As for ergonomics, IVA suits offer much greater maneuverability and visibility, improving the human to system interface and reducing the risk of accidents.

F.2.1.2 Contingency Scenarios

During ascent, the main contingency for the crew is a failed docking with the DST. Docking can fail in three ways. In the first, the MAV manages to hard dock, but the hatch jams. This scenario is solved by including a dock jamming kit onboard the MAV. The second is when the MAV manages to soft dock, but not hard dock. In this scenario, the MAV depressurizes and the crew ingresses to the DST wearing either an EVA or IVA suit. The third occurs when the MAV fails to both soft and hard dock. The recoverability of this scenario heavily depends on how far apart the vehicles are. If the vehicles are anywhere between a few inches to a few feet of each other, the DST crew can perform an EVA to tie the vehicles together. The MAV would then depressurize and its crew would transfer to the DST. If the vehicles are only a few inches apart, the crew could accomplish this with their regular IVA suits, having up to a minute or two of time off either vehicle's suit loop during the transfer. For any transfer longer than this amount of time, the MAV needs to be equipped with contingency O_2 and extra long umbilical chords. Depending on the situation, the DST crew could also perform an additional EVA to deliver EVA suits to the MAV crew. This would require an additional repressurization cycle, as well as space in the MAV for donning EVA suits, though. Alternatively, EVA suits could be brought aboard the MAV.

F.2.2. Ingress Method Trades

The main concepts considered for the ingress method were airlocks, suitlocks, double bladder airlocks, suitports, and inflatable tunnels. Prioritizing both planetary protection and the crew's safety from toxic Martian dust hazards, any concept which brings the suits into the vehicle would require not only an additional airlock but also an additional dust mitigation system. The second airlock is necessary to separate the contaminated suits from the internal cabin. The dust mitigation system, such as an Electrodynamic Dust Shield enabled brushing system, along with a lengthy cleaning procedure would be necessary to reduce the amount of Martian dust brought into the vehicle. These additional systems add a significant amount of mass and volume to the overall vehicle and still do not ensure complete dust removal. For these reasons, airlocks, suitports, and double bladder airlocks were all ruled out early in the design process. The remaining two methods are described in detail below.

F.2.2.1 Suitports

Suitports are advantageous because they ensure that EVA suits stay outside of the main cabin without increasing the capsule's pressurized volume. This ingress method is already planned to be used on the roving habitat as well, resulting in ingress commonality between the vehicles, reducing the MAV's development costs, and potentially reducing the crew's cognitive load. Additionally, if the suits are kept attached to the suitports after ingress, they could be used in failed docking contingency scenarios. However in order to take advantage of this benefit, the suitports would also require protection for the suits during ascent [24]. IVA suits and the necessary volume to don them would also still be required onboard, as the IVA suits would act as the necessary counterpressure garments to protect the crew during ascent. Keeping the suits attached would also affect the MOI of the vehicle, introducing additional complexities for propulsion and ADCS subsystems. Additional assets also cannot be passed through the suitports, meaning that either an additional external holding cell or an additional ingress method would be needed for the required 50 kg of samples. The MAV capsule is also 2.53 m above the ground and would require some system to help the crew traverse that height. Ladders are a simple solution, but have been found unergonomic in the EVA suits, requiring a second crew member's aid and raising concerns of injury from the crew slipping on the metal rungs [25]. Alternative options include a deployable ramp such as the Deployable Extravehicular Activity Platform for planetary surfaces, shown in Figure 8 [26].

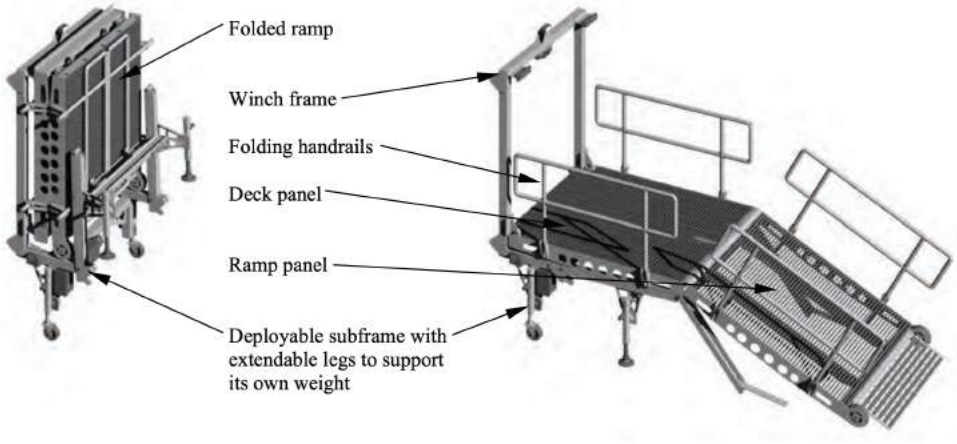

Fig. 8 DEVAP in stowed (left) and deployed (right) configurations.

Lastly, suitports have poor extensability to and reusability for future missions. The NASA Mars Roadmap projects crew size to immediately double after the initial surface mission. The 2 suitport system, used to support a crew of 2, could not accommodate a crew size of 4 without a prohibitive increase in risk. In this configuration, the crew loses the ability to retreat back to the roving habitat after initially ingressing the MAV. As shown in Figure 9, after the first 2 crew members ingress the MAV, their suits would need to be dropped on the Martian surface to allow the second 2 crew members to ingress. This renders the first 2 EVA suits unusable, effectively trapping half of the crew within the MAV, should any issues occur during pre-ascent checkouts. To circumvent this issue, either a major redesign is required for the suitport systems used, or any ascent vehicle must be equipped with one suitport per crew member.

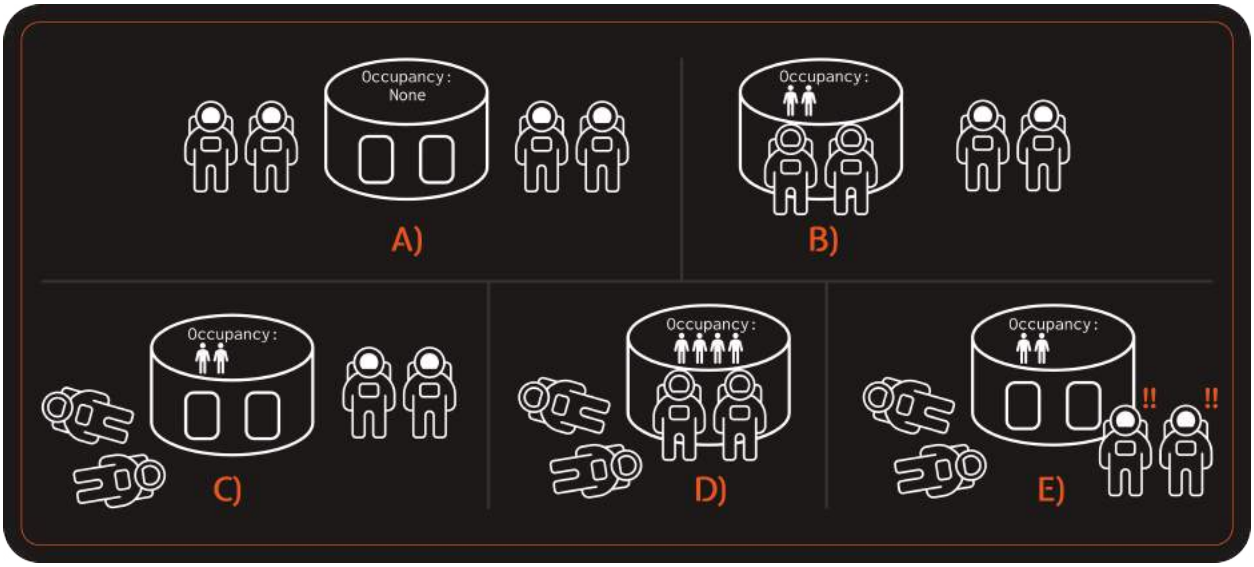

Fig. 9 Loss of MAV emergency egress capability with 2 suitports and a crew size of 4.

F.2.2.2 Inflatable Tunnel

Inflatable tunnel concepts leverage many of the benefits of suitports without the same issues, by relying on the crew having already ingressed into another habitat, using that habitat's suitports. By doing so, this concept benefits from all the same planetary protection and crew health benefits of suitports as well as allows for the crew to don their IVA suits in the roving habitat before transferring to the MAV in the same suits. Donning suits requires the largest task volume and, thus, allowing the crew to don these suits prior to ingressing the MAV not only increases the crew's comfort, but it also loosens constraints on the MAV capsule's interior configuration and pressurized volume. Due to their greater mobility, IVA suits also afford the use of either an internal ladder or handrails along a sloped ramp section for the crew to reach the MAV hatch height. This is advantageous, as both of these systems add little to no mass to an inflatable tunnel, unlike the deployable ramp necessary for suitports. For the same reasons as for suitports, the sloped ramp concept is preferable.

Lastly, an inflatable tunnel has the best future mission extensability, as it requires no scaling to accommodate larger crew sizes and preserves the greatest amount of reusable equipment on the surface of Mars. The crew's EVA suits are left attached to the roving habitat, and the tunnel detaches from the MAV immediately prior to ascent, protected by a dust cover on one end and attached to the roving habitat on the other. Regardless of crew size, and without any design modifications, an inflatable tunnel preserves the crew's ability to retreat to the roving habitat until the very last moment before ascent.

F.2.3. Interior Capsule Configuration Trades

F.2.3.1 Preliminary Sizing

Preliminary sizing for the MAV's capsule was completed using the Sherwood-Capps Dual Curve and Fraser's Impairment Curves. Many models exist for estimating the appropriate pressurized volume for manned space vehicles based on historic data, but these two models in particular are most applicable to the MAV's overall mission and goals. Given the MAV's short mission duration and objectives, the Sherwood-Capps Dual Curve was used because it specifically derives separate models of pressurized volume per crew member for both capsules and space stations. Using the capsule specific model, the MAV's pressurized volume came out to be 9.7 m^3[27]. As shown in Figure 10, 4.85 m^3 per crew member sits below the Fraser's No Impairment curve for a 11 day mission. Thus, the MAV's minimum pressurized volume per crew member was increased to 7 m^3, totalling in 14 m^3 of pressurized volume.

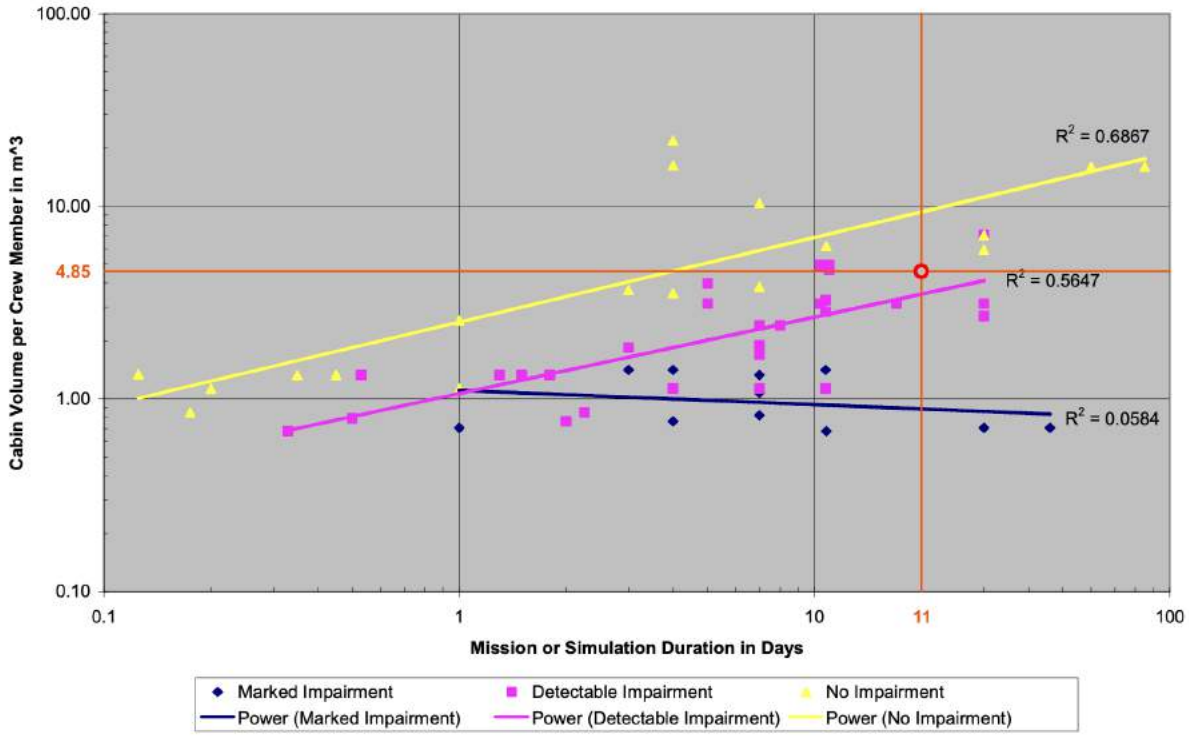

Fig. 10 Fraser Impairment Curves.

F.2.3.2 Habitability and Task-Based Analysis

A preliminary ECLSS packaging and task-based analysis was completed to validate that a capsule size of approximately 14 m^3 can be configured to accommodate the crew and enable them to complete their mission tasks effectively. An example task breakdown was completed to inform the analysis. Each of the tasks within the breakdown corresponds to a task volume as defined in NASA's Human Integration Design Handbook. An iterative design process was employed to develop an example interior configuration. This configuration is shown in Figure 11.

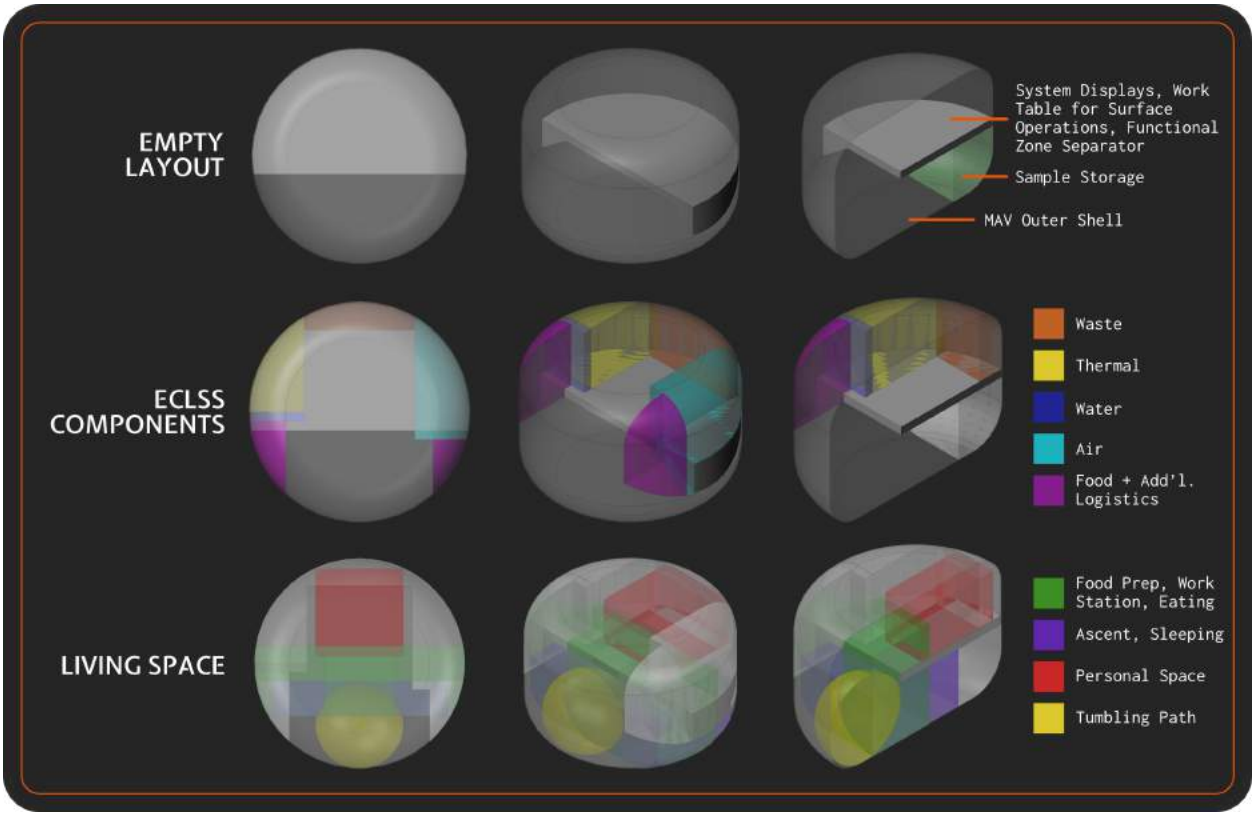

Fig. 11 Example interior capsule configuration, including ECLSS packaging and task analysis volumes.

F.2.3.3 Acceleration Analysis

A high level acceleration analysis was completed to evaluate whether the ascent seats could be tilted high enough to reduce the capsule diameter without dangerously increasing the risk of incapacitating the crew. In order to reduce the capsule's diameter, simple trigonometry shows that the ascent volumes must be tilted at least 80°. In accordance with NASA STD 3001 Volume 2, the loads due to acceleration are evaluated separately on each axis using trigonometry. These loads are evaluated between the angles of 0 and 55 °. The results, as well as the limits as outlined by NASA STD 3001 Volume 2, are displayed in Figure 12. For simplicity and safety, the loads applied due to acceleration were simplified to a single load of 4 Mars g's (14.88 m/s^2 over the span of 300 seconds, and a margin of 20% was added. These results show that the ascent seats cannot, in fact, be tilted enough to reduce the capsule diameter without endangering the crew. For this reason, the capsule diameter is constrained to 1.5m.

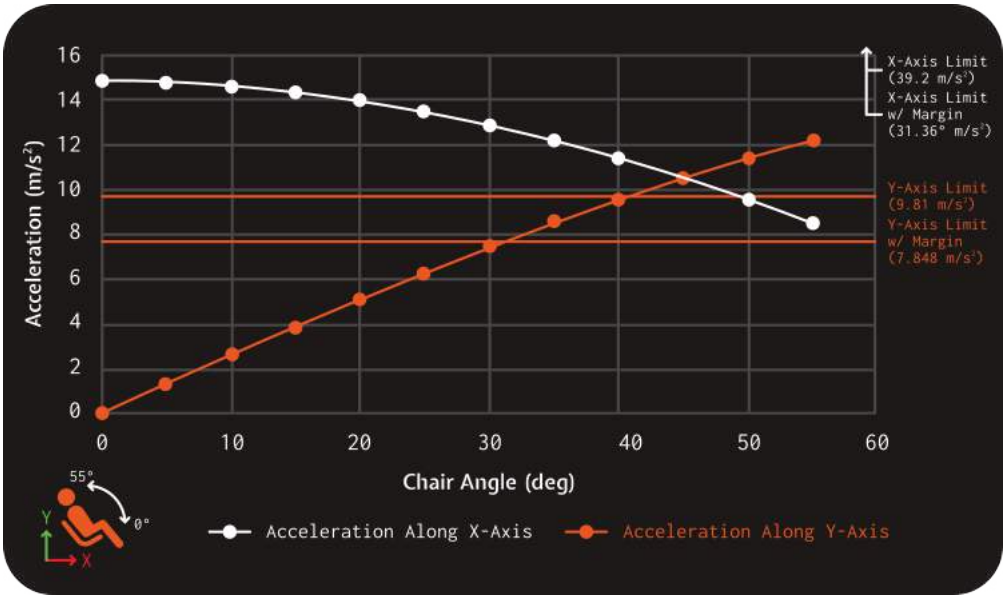

Fig. 12 Applied loads due to acceleration in the x and y axes as a function of ascent seat tilt, compared to NASA STD 3001 Volume 2 acceleration limits.

F.2.4. Final Configuration

The MAV crew will ascend in the OCSS IVA suits, with access to extra long umbilical chords to accommodate failed docking contingencies. The MAV features an inflatable tunnel ingress system as developed for the The National Aeronautics and Space Administration's Evolvable Mars Campaign. The tunnel, shown in Figure 13, has a fabric layup construction and features a sloped middle section with interior handrails. Immediately prior to ascent, the tunnel detaches from the MAV with pyrotechnics and a dust cap to protect it from the Mars surface until its next use. The MAV capsule's pressurized volume is 14.14 m^3 with a 3 m circular diameter and 2 m height.

Fig. 13 Tunnel ingress method developed as a part of the National Aeronautics and Space Administration's Evolvable Mars Campaign.

F.3. Structures

Table 10 below depicts the derived structural requirements from the RFP overall mission requirements.

Table 10 Structural Requirements

Req. ID	Requirement Description
TRTL-STR-01	All structural margins shall be positive.
TRTL-STR-02	Equivalent plastic strain in a material shall not exceed 5%.
TRTL-STR-03	Metal design allowable shall come from Metallic Materials Properties Development and Standardization (MMPDS) 11^{th} edition A basis values.
TRTL-STR-04	All materials used shall come from NASA stress corrosion and cracking tables I and II.
TRTL-STR-05	All fasteners used shall be NAS standard.

The structural design of the mission was driven by maneuverability of the parts and materials used in the mission, minimizing vehicle mass, and minimally compacting constrained packaging. Material compatibility for the space and Martian environment was another critical factor among other considerations that influenced the structural design. Therefore, a requirement was put in place that all materials used must come from NASA's stress corrosion and cracking Tables I and II [28]. Reference to the NASA tables was of utmost importance, as most plastics not included within PEEK have major out gassing concerns in the space environment, making them an unfeasible choice in material selection. Additionally, design Factors of Safety (FOS) were put in place according to the standards typically used in the aerospace industry, the Table 11 below shows the required safety factors used in the vehicle design.

Table 11 Design Factors of Safety

Case	FOS
Yield Strength	1.10
Ultimate Strength	1.40
Environmental	2.00
Geometric	1.50

Finally, the manufacturing verification of the parts was in large focus when choosing the structural requirements for the vehicles. For example, as cracking was a concern due to manufacturing deficits and thermal expansion, X-ray and blue light scanning requirements were implemented for all welds and vehicle components. All primary MAV structural members were also required to undergo load and vibration testing [29].

F.3.1. Load Cases

For preliminary analysis of the MAV, the two main loads considered were acceleration load due to vehicle thrust and the radial load due to angular velocity of the vehicle. Additionally, the hoop stress due to tank and capsule pressure loads were considered. Every one of these loads were analysed at each flight regime. The driving load cases ended up

being the takeoff from the Martian surface due to the maximum vehicle mass and pressure [30]. Tables 12 below are a depiction of the expected takeoff loads and vehicle geometry.

Table 12 MAV Loads and Geometry

Property	Value	Unit
MAV Thrust	316.73	kN
MAV Acceleration	18.6	m/s^2
Max Rotational Velocity	10	deg/s
Fuel Tank pressure	3.5	Bar
Ox Tank Pressure	3.5	Bar
Total Ox Tank Mass	6354.28	kg
Tot Fuel Tank Mass	1777.6916	kg
Ox Dist from Center	2.5	m
Fuel Dist from Center	2.35	m
Load X OX	118310.61	N
Load Radial OX	120.97655	N
Load X Fuel	33096.877	N
Load Radial Fuel	31.814054	N
Capsule Length	2	m
Diameter	3	m
Top Ring Diameter	0.68	m
Angle A OX	0.27	rad
Angle A Fuel	0.77	rad
Angle B OX	0.68	rad
Angle B fuel	0.79	rad

The resulting moments of inertia (MOI) about the axes given in Figure 14 of the MAV are: I_x = 100574.75 kg· m^2, I_y = 81125.27 kg· m^2, I_z = 21331.36 kg· m^2. These MOIs for attitude control system requirements were calculated from computationally-aided-design (CAD) software as well as using parallel axis theorem of simplified body shapes.

F.3.2. Structural Trades

F.3.2.1 Material Selection

Material selection for the body of the MAV is critical, as the material must be able to withstand the driving load case as well as all other loads throughout the entirety of the mission. Aluminum 2021 was chosen for the primary tank material due to its high ultimate strength to mass ratio, weldability and ease of machining, as well as crack corrosion resistance at cryogenic temperatures [31]. Since the required tank thickness from the hoop only load case (3.5 barD tank pressure) would make the machining and welding of the tanks impossible, a thickness of 3 mm was enforced. This thickness allows machining of the tanks with a ball end mill, using sand as the supporting structure. Additionally, TMAG welding can be used to join the two tank hemispheres together. Other tank materials considered were Aluminum 2024, 7075, 6061, stainless 304L, titanium-64, and composite over wrapped pressure vessels (COPVs). Table 13 below

is a comparison of the metallic alloys considered for the main MAV propellant tanks [31].

Table 13 Metals Considered for Tank Material

	Ultimate Strength (Mpa)	Elongation (%)	Density (kg/m^3)	Thickness_FT (mm)
Al 2021-T62	476.00	3.00	2840.00	0.52
Al 2021-T81	455.00	3.00	2849.00	0.55
AL 2024 T3	440.00	10.00	2780.00	0.56
AL 7075 T6	572.00	9.00	2810.00	0.43
Al 6061 T6	289.00	9.00	2700.00	0.86
Stainless 304L 50% RA	1080.00	50.00	8000.00	0.23
Ti6Al-4V	900.00	10.00	4430.00	0.28

Table 14 Tank Metal and Manufacturing Trades

Thickness_OT (mm)	Mass_FT (kg)	Mass_OT (kg)	Total Mass (kg)	Notes
0.57	19.05	23.18	84.47	Good overall
0.60	20.00	24.33	88.65	Not as strong as Al 2021-T62
0.62	20.18	24.55	89.45	
0.48	15.69	19.09	69.56	Difficult to machine, not weldable
0.95	29.83	36.29	132.23	Weak but good availability
0.25	23.66	28.79	104.91	Rolled,welded endcaps
0.30	15.72	19.13	69.71	Expensive but good properties

For the large main propellant tanks and the RCS thruster tanks on the MAV, AL 2021-T62 was the best option for manufacturability and structural properties. However, COPVs were chosen for the pressurant tanks due to mass reduction capabilities. As this size COPVs are commonly used in the aerospace industry, the testing and validation can be outsourced to achieve the most reliable design.

Similar material trades were done for the main capsule body as well as the truss structure holding the propellant tanks. The main capsule body of the vehicle was chosen to be Al-2024 T3 since the loads on the structure were not driving the vehicle mass. The pressure and thrust loads on the main vehicle body were minuscule such that maneuverability and easiness of welding drove the design [31].

The main truss of the MAV was chosen to be Titanium-64. Since the size of the truss was driven simply by the strength to weight ratio, titanium proved to be the best option. The chosen design only weighs about 50 kg per truss unit, making the overall truss mass of the MAV approximately 192 kg. Furthermore, the low conductivity of Titanium-64 makes it an appealing selection for thermal management in reducing heat loads between MAV components. Metal matrix composites were considered for the truss structure but were finally not chosen due to their high cost, lead time, and importance in manufacturing validation.

F.3.2.2 MAV Packaging

The driving requirements for the packaging of the MAV were supporting the large propellant tanks as well as facilitating an effortless and safe access for the crew and samples to enter and exit the vehicle. Due to demands from ECLSS, the human capsule module of the MAV had to be placed adjacent to the Martian surface. The propellant tanks could now be put either on top of the capsule or along its sides. Since having a large amount of propellant on top of the capsule would produce a novel and unproven design, which would increase overall structural mass, the propellant tanks were positioned on the sides of the main capsule. Baffles were placed inside the tanks to reduce sloshing and the propellant feed system was designed to monitor the propellant level during Mars ascent to avoid uneven mass distribution. Additionally, the ADCS system was designed to have the performance to counteract any torques due to sloshing or uneven mass distribution. Placing the propellant tanks on the side of the vehicle also allows for the placement of a docking port on the top of the vehicle, which is used for docking with the Orbital Taxi during Phase 5: Taxi rendezvous. The tanks were placed as close to the capsule body as possible to minimize bending moment of inertia around the primary axis of the vehicle and the bending loads on the structure.

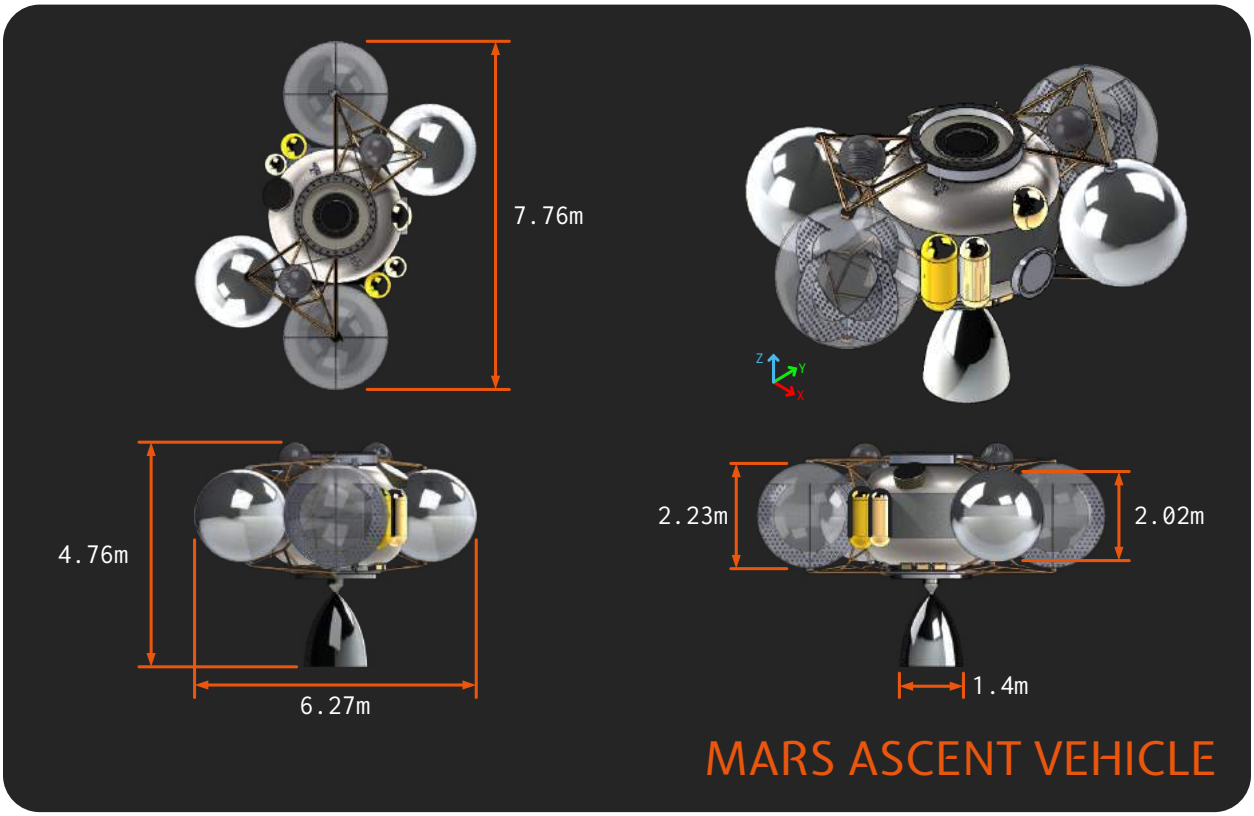

Fig. 14 Overall MAV CAD and Dimensions.

F.3.3. MAV Structure Driving Stress Analysis

The highest stresses on the MAV structure are seen on the titanium truss during the takeoff from Mars. The large propellant mass supported by the titanium truss places large bending loads on the primary structure of the vehicle. The titanium truss was analysed as a pinned truss achieving predictable loads as the bending moment does not transfer through these pinned connections. Also, the pinned truss allows the vehicle structure to be fully minimally constrained, diminishing the residual and thermal stresses on the structure. Table 15 below indicates the MAV truss masses calculated from the material strength.

Table 15 MAV Driving Loads and Material Strengths

Beam	Load (N)	Ultimate Strength (MPa)	Area (m^2)	Length (m)	Volume (m)	Mass/beam (kg)
A OX	225554.69	900	0.000350863	1.77	0.000621027	22.35698121
B OX	175956.94	900	0.000273711	1.85	0.000506365	18.22913879
A Fuel	46451.424	900	7.22578E-05	1.66	0.000119948	4.318124412
B Fuel	33799.239	900	5.25766E-05	1.68	8.83287E-05	3.17983241

F.3.4. MAV Structural Mass Budget

Below, within Table 16, is the structural mass budget for the MAV. The masses result from the required component size due to loads and manufacturability. The docking system used is based on the NASA Docking System [32].

Table 16 Mass Breakdown for MAV Structure (Dry Mass)

Component	**Mass (kg)**
Fuel Tanks	38
OX Tanks	46
Capsule Mass	1069
RCS tanks	55
COPVS	20
Truss	192
Docking System	320
Total Mass	1740

F.4. Propulsion

The architecture of the propulsion system was designed with robustness, reliability, and performance as the paramount design criteria, and this lead to a high level propulsion system design for both the MAV and Orbital Taxi that is ready to fulfill and exceed the propulsion system requirements.

The propulsion system requirements pertain to ensuring other subsystems can provide the necessary support for the propulsion system. For example, making sure the thermal system can keep the propellants at their proper temperatures, the communications system must be capable of transmitting all of the propulsion telemetry, the structures must be capable of handling the loads imposed by the engines, and the power system must provide the required power for all propulsion components. The requirements also pertain to the performance of the propulsion system such as ensuring the engines provide enough thrust, all systems must stay functional after the long duration on Mars or in Martian environment, and including sufficient redundancy to ensure mission success. Table 17 portrays all of the subsystem requirements for enabling mission success.

Table 17 MAV Propulsion Requirements

Req. ID	Requirement Description
TRTL-PS-01	The MAV engines shall be throttle-able to 40% of their nominal thrust.
TRTL-PS-02	All propulsion components shall be nominally operable after the yearlong interplanetary journey and up to 5-year stay on the Martian surface.
TRTL-PS-03	The MAV engines shall be capable of changing propellant mixture ratio between 3.5 and 3.7, as determined by the vehicle computer.
TRTL-PS-04	The first stage engines shall communicate chamber pressure to the vehicle computer.
TRTL-PS-05	MPS computer shall sample required sensors at 50 Hz.
TRTL-PS-06	The MAV total main engine thrust shall meet 4 times the vehicle weight at liftoff.
TRTL-PS-07	The MAV MPS shall achieve a Delta V of 3860 m/s.

F.4.1. MAV Main Propulsion System Trades

As was previously discussed in the vehicle level trades discussion, the decision was made to go with an ISRU based propellant generation system which limits the oxidizer to LOX (Liquid Oxygen) since that can be derived from the Martian CO2 atmosphere. The fuel then could be any rocket fuel with the most common and tested with liquid oxygen being RP-1 (refined kerosene), liquid hydrogen, ethanol, and liquid methane.

Table 18 Propellant trade table

Propellant	Density (kg/m3)	MR	Isp (s)	Temp Range (K)	ISRU capable?
RP-1	813	2.6	340	240-600	N
CH4	422	3.6	380	<120	Y
H2	70	6	450	<20	Y

From looking at the propellant trade table [33], there are four main conclusions to draw: how much mass and

volume of each propellant would be required, how efficient is an engine with this propellant, does the temperature range impose a large thermal control constraint, and can this propellant be made on mars? When considering the mass of each propellant required it is seen that Hydrogen requires the least landed propellant mass, however, the density is so low that the tanks would be larger than the oxygen tanks, making them heavier. When looking at the Isp Hydrogen provides the largest potential efficiency, which would decrease the overall vehicle mass. The temperature range favors RP-1 since it is not cryogenic, which brings challenges keeping the fluid liquid protected against the solar radiation. However, methane is not nearly as cold as hydrogen, which is one of the coldest propellant liquids. In terms of the ISRU capabilities, RP-1 is the only option not manufacturable on the surface of Mars, but it is worth noting that CH4 is easier to produce due to the Sabatier reaction producing both oxygen and methane, as well as the liquefaction process takes less energy. One more important note is that the propellant will have to be transported from Earth to Mars and cryogenic liquids in space for a long term is a completely new area of development. Nonetheless, liquid hydrogen is especially difficult due to how small of a molecule it is, enabling ease of diffusion through the walls of a tank. Overall, the trades favor methane when considering everything with a strong emphasis on the potential for future production on Mars since that was the reason ISRU was selected in the first place. It is logical to use a propellant that could be produced on Mars in the future.

Next, the engine cycle had to be chosen. Note that only turbomachinery-based feedsystems were considered, since this system needs far too much impulse to use a pressure-fed system efficiently [33]. Within turbomachinery-based engine cycles, there are closed and open cycles- of which, closed is more efficient and many new engines in the past decade have successfully been designed to be closed cycle. Therefore, we decided to choose an ox-rich staged combustion cycle. Oxygen rich was chosen in order to avoid the added complexities of a full-flow staged combustion cycle and since the oxidizer will not have to run through regenerative cooling channels as the fuel does. While oxygen rich does bring material burning problems, the preburner can be run at lower temperatures than a fuel preburner, since there is a much higher mass flow. New companies like Ursa-Major Space Technologies are currently developing Methane-Oxygen ox-rich staged combustion engines and could be contracted for the development of the MAV MPS engines[34].

Fig. 15 Ursa Major's Arroway. A Heavy Launch LOX/Methane engine in development.

F.4.2. MAV RCS/OMS

The MAV RCS/OMS system selection was heavily influenced by the later selected Taxi RCS/OMS system, in order to maintain closeness for facilitation of development and manufacturing. Therefore, the propellant was chosen to be the MON25/MMH for reasons of development ease and coherence with the Taxi RCS/OMS. The MAV RCS system will be pressure-fed like most other RCS systems in order to achieve the fastest possible response

to commands (a driving requirement for RCS thrusters from ADCS subsystem). The tanks for the RCS were chosen to be titanium bladder tanks since these thrusters are meant to operate mainly in the microgravity region.

F.4.3. MAV Propulsion System Sizing and Design

F.4.3.1 MAV Main propulsion system sizing

The ΔV required for mission operation is 3860 m/s the MAV. This information is then used along with the known dry mass from the total mass accumulation of all other systems to calculate the required propellant mass with the ideal rocket Equation (1). Then a volume from this propellant mass is calculated based on the density of the propellant, multiplied by an ullage factor of 1.05 [33] to get the total tank volume. Which, since the propellant tanks are included in structural mass, is then used to re-calculate the structures mass. This process is iterated until the propellant mass stops changing within some tolerance. From this total vehicle mass, a thrust was calculated assuming a vehicle thrust to weight ratio (TWR) of 4, a number obtained from a paper that ran a more in-depth sizing code for a similarly designed MAV, but taking into account more load cases on the structural design. This documentation found a thrust to weight of 4 to correspond to the minimum vehicle mass [11]. Since our MAV has a similar configuration with four tanks mounted radially around the capsule and will have the same general flight path, the optimum TWR was selected to be the same.

With this engine thrust and knowledge of the engine parameters, the exhaust throat and exit areas of the engines can be computed. The MAV engine parameters are as follows: a mixture ratio of 3.6, a chamber pressure of 100 bara, a chamber temperature of 3500 K, a specific heat ratio of 1.2, and an expansion ratio of 100. The engine parameters were found from sources for a reasonably designed engine meant to operate on the surface of Mars for the MAV and in space for the Taxi [7, 33]. Isentropic flow equations were utilized to also assist in determination of the throat and exit areas of the engines. A contraction ratio of 5 was assumed to obtain the combustion chamber area. The final parameters were found to be an exit diameter of 1.44 m, along with a Isp of 355 s, a $\dot{m}$ of 101 kg/s, and a thrust of 315 kN. The MAV MPS system still needs a supply of pressurant to keep the propellant tanks at a sufficient pressure such that the engine pumps do not cavitate. The RCS and OMS system also needs a supply of pressurant, so we sized a common COPV to supply Helium to both the RCS system and MPS. In order to size this the desired pressure in the tanks for the MPS and RCS is known, 3.5 bara for MPS and 25 bara for RCS since it is pressure fed. The volume of each tank is known and the amount of moles of Helium required to fill up the entire volume of each tank with some leftover depletion pressure in the volume of the COPV is calculated with the ideal gas law [33],

$$n = \frac{PV}{RT}, \tag{6}$$

where n, P, V, and T indicate the number of moles, pressure, volume, and temperature respectively for each tank and R is the helium gas constant. The required number of moles for each tank is added together and additional moles are added

for pneumatics by multiplying by 1.1 and a constant leak rate of .001 mol/Hr is multiplied by the total mission duration. This leads to a final number of moles required which is then used in combination with the COPV pressure (600 bara) to calculate a total COPV volume of 155 L for the taxi and 360 L for the MAV. In the system we add 2 entirely redundant COPVs of this size and pressure in case one experiences an anomaly for failure somewhere along the mission duration.

The P&ID for the MAV MPS is shown within Figure 16 and contains many of the likely required valves, but of course, is still an early stage concept and excludes certain systems like sensors, ignition, and pneumatics.

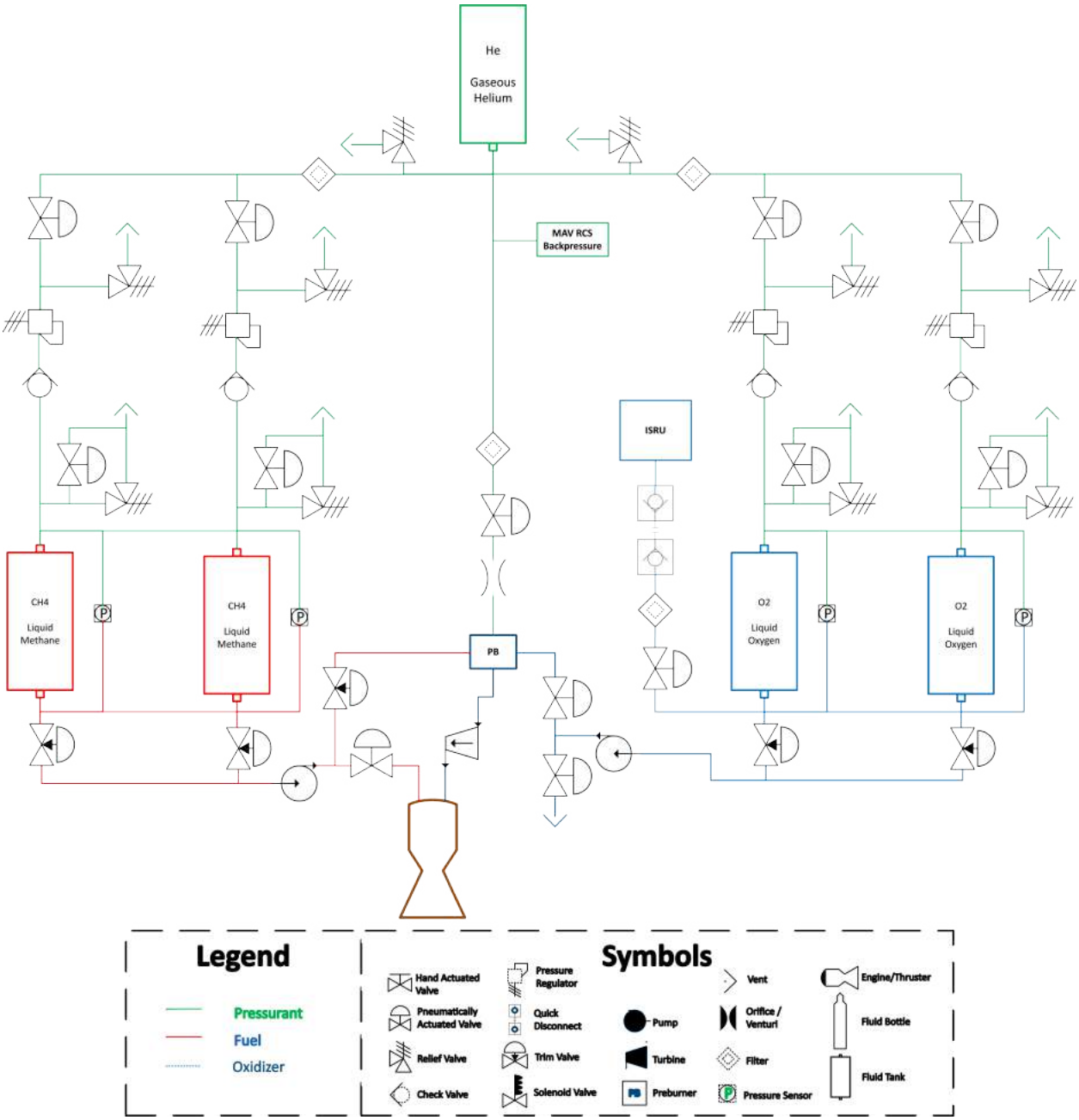

Fig. 16 MAV MPS P&ID

Some of the key features of this P&ID are the redundant pressurant legs that connect each of the pairs of respective tanks. Every component in the pressurant supply flow path will be sized for 2 times the necessary flow rate for a single tank, such that if a regulator or valve in the pressurant section of one tank fails, it can still supply the necessary flow rate to keep both tanks at 3.5 barA. There is similar redundancy in the main propellant flow path in that there is a line connecting the two main propellant flow lines for each propellant before the pre-valve. This is a backup mechanism so that both tanks will still be able to drain through the non-faulty pre-valve, in case one of the pre-valves fails. Note, the oxygen rich preburner flows all of the oxygen, as well as a small portion of the fuel, through for providing energy to drive the turbine which operates the fuel and ox pumps. There exists a throttling valve in line with the fuel leg that goes to the preburner, this notable part will act as the main engine throttle valve. Also, note that the engine's pumps are spun up by pressurant gas flown through a spin start system. Another eminent addition is the throttling pre-valves and differential pressure sensors on every tank. These will be used to level sense every tank and closed loop control to make sure all tanks deplete evenly.

In order to calculate the mass of the propulsion system an empirical model from documentation [35] was used:

$$m_{\text{MPS}} = [K_{ph} + K_n(\epsilon_1 - 1) + K_{pf} + K_{ga} I_{sp}] N_{eng} \dot{m}, \tag{7}$$

where m_{MPS}, K_{ph}, K_n, ϵ_1, K_{pf}, and K_{ga} are the MPS mass, powerhead constant, nozzle constant, expansion ratio, feed system constant, and gimbal actuators constant respectively. This mass equation contains all MPS relevant mass including the feed system components.

F.4.3.2 MAV RCS and OMS sizing

For sizing the RCS system we leaned heavily on past missions sizing like Orion, Dragon, Apollo LEM, and Soyuz. From looking through these past missions 16 RCS thrusters in 4 pairs of 4 seems to be a common design, so this was chosen. Only 3 linearly independent thrusters are required to navigate a spacecraft through 3D space, however, possessing extra thrusters allows for more efficient maneuvers as well as an additional level of redundancy, should one fail. The RCS system is chosen to be an adapted version of the Orion capsule's system, which consists of 220 N thrusters that run off of MON and MMH [36]. In addition to the 16 RCS thrusters, the MAV capsule will have 4x 490 N OMS thrusters for correcting any erroneous orbital insertions. A representation of the RCS system P&ID can be found in Figure 17.

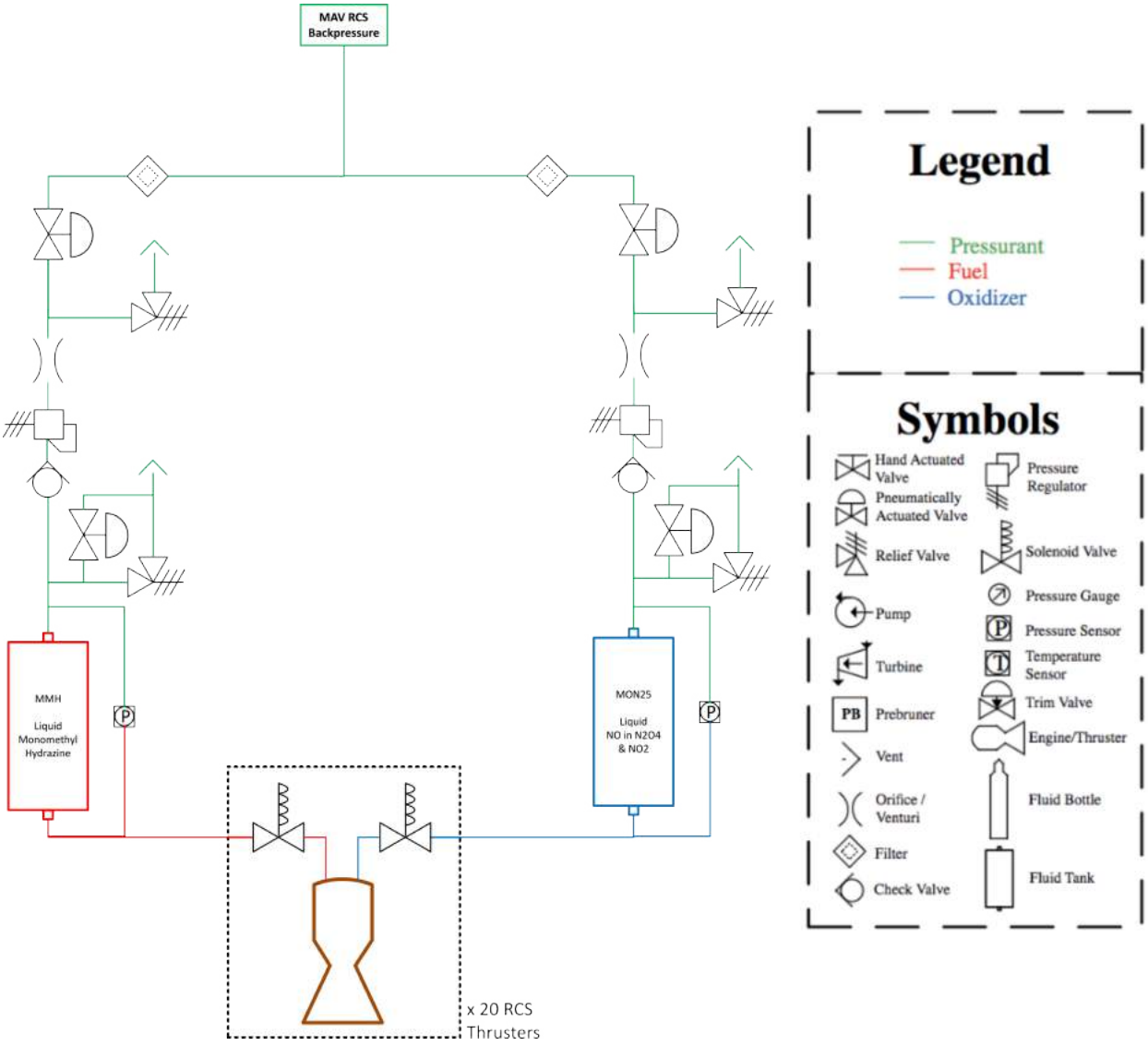

Fig. 17 MAV RCS P&ID

In order to estimate the mass of the RCS system,

$$m_{\text{rcs}} = \frac{n_{\text{rcs}} T_{\text{rcs}}}{R_{\text{thruster}}}, \tag{8}$$

was utilized [35], where m_{rcs}, n_{rcs}, T_{rcs}, and R_{thruster} are the RCS mass, number of thrusters, thrust of each thruster, and thrust to weight of each thruster respectively.

As for the common pressurant COPV, the following equation is used for mass estimation [35]:

$$m_{\text{COPV}} = 1.5(0.1153 V_{\text{COPV}} + 3), \tag{9}$$

where m_{COPV} and V_{COPV} are COPV mass and volume respectively.

The total mass of the MAV propulsion system is 666.6 kg, with MPS mass being 465 kg, the pressurant gas mass being 31.1 kg, the COPV mass being 67.5 kg, and the PCS/OMS mass being 103 kg.

F.5. Communications

The communications subsystem is designed to facilitate the stated overarching mission goal of safely delivering two humans and 50 kg of samples from the surface of Mars to the DST. The requirements necessary for the communications subsystem to meet this goal are given in Table 19.

Table 19 Overall System Requirements

Req. ID	Requirement Description
TRTL-COM-1	The MAV shall maintain uplink and downlink with ground control during the stated mission duration.
TRTL-COM-2	The MAV backup communications shall support the full emergency data budget of 16.66 kbps.

The first decision to be made about communications for TRTL is the general architecture. The MAV and Orbital Taxi must be able to communicate with each other to relay telemetry for rendezvous. They must also be able to communicate with ground control for receiving commands and relaying telemetry, as well as maintaining communication with astronauts while they are onboard.

For each link in the chosen architecture, the primary design drivers are system mass and power requirements, antenna volume, datarate, and pointing requirements. Trades between these drivers were decided by using the link budget equation, which is a generalized formula for determining the signal to noise ratio at the receiving antenna. This method was used because it allows the effect of these design decisions to be quantified and compared.

F.5.1. The Data Budget

The primary requirement for the communications system is the ability to transfer a specified datarate during specified communication windows. A preliminary data budget is constructed by estimating the amount of data each subsystem will need based on telemetry and sensors that will be needed for subsystem operation as well as miscellaneous data requirements such as video feed. The data budget includes all data requirements even if they will not always be necessary so that the maximum data throughput can be used for communications system sizing. The minimum datarate necessary for mission completion has also been estimated and included as the backup data budget, which will be necessary for contingency measures as discussed later. The transmitted datarate from ground control has been estimated in a similar fashion, and is expected to be relatively low due to most processes being automated during the TRTL phase of the mission. The complete data budget and backup communications data budget are given in Figure 20 and Figure 21, respectively. Therefore, the required datarate for the primary communications link is 132 kbps and required datarate for the backup communications link is 17 kbps. The transmitted data budget is given in Figure 22 and requires 14 kbps.

Table 20 Total data budget for the OT. Note that the OT budget includes all data from the MAV because it serves as a communications relay.

System	Sensor Name	Qty	Polling Rate (Hz)	Data per Sample (bits)	Bits Per Second
PROP	Pressure	30	50	32	48000
	Temperature	30	50	32	48000
	Misc	20	10	32	6400
	ISRU	20	10	32	6400
ADCS	Star Tracker	2	50	192	19200
	IMU	5	50	32	8000
ECLSS	Pressure	5	5	32	800
	Temperature	5	5	32	800
	Misc Habitat	20	5	32	3200
Power	Solar	20	1	32	640
	Battery	20	1	32	640
TCS	Temperature	40	2	32	2560
MISC	1080p Video Feed	1			6755.6
Margin					0.4
Compression Factor					0.625
Total (kbps)					132.471

Table 21 Backup data budget. Note this includes only the MAV.

System	Sensor Name	Qty	Polling Rate (Hz)	Data per Sample (bits)	Bits Per Second
PROP	Pressure	15	5	32	2400
	Temperature	15	5	32	2400
	ISRU	5	1	32	160
ADCS	Star Tracker	1	10	192	1920
	IMU	5	50	32	8000
ECLSS	Pressure	5	1	32	160
	Temperature	5	1	32	160
Power	Solar	20	1	32	640
	Battery	20	1	32	640
TCS	Temperature	40	2	32	2560
Margin					0.4
Compression Factor					0.625
Total (kbps)					16.660

Table 22 Data transmission budget.

Sensor Name	Qty	Polling Rate (Hz)	Data per Sample (bits)	bps
Telecommand	20	25	32	16000
Margin				0.4
Compression				0.625
Transmit Datarate (kbps)				14

F.5.2. The Link Budget

The primary method of analysis for sizing the communications system is the calculation of the link budget for every link in both directions. The link budget accounts for the power being transmitted through the system and the noise present in the link, resulting in the signal to noise ratio (SNR) for the link. A required SNR can be determined and compared to the link's available SNR. The SNR for a link is calculated as

$$\frac{E_b}{N_0} = \frac{P_{\text{in}}\eta_{\text{comm}}G_{\text{trans}}L_sL_aL_\theta G_{\text{rec}}}{kT_sB}, \tag{10}$$

where $\frac{E_b}{N_0}$ is the SNR, P_{in} is the power supplied, η_{comm} is the amplifier efficiency, G_{trans} is the transmitting antenna gain, L_s are losses due to free space, L_a are atmospheric losses, L_θ are pointing losses, G_{rec} is the receiving antenna gain, k is the Boltzmann Constant, T_s is the system noise temperature, and B is the bandwidth. All the gains and losses in the link budget are converted from decibel to linear values. The following sections detail assumptions and values used for each of the terms.

F.5.2.1 Communications Efficiency

Communications efficiency is estimated based on existing hardware. Solid state amplifiers are used for power outputs up to 10 W, with an efficiency of 3% at 10 W input power. Travelling wave tube amplifiers (TWTA) are generally preferred for higher power outputs, with an efficiency of roughly 60% for power outputs above 100 W [37].

F.5.2.2 Transmitting Gain

Transmitting antenna gain is dependent on the type of antenna used. The peak gain for a parabolic antenna is calculated as

$$G = 17.8 + 20\log(D) + 20\log(f) \tag{11}$$

where G is the peak gain in dBi, D is the diameter in m, and f is the frequency in GHz [37]. The gain for a half wave dipole antenna is always 1.64 dBi. These are the two antenna designs chosen for TRTL; the peak gain for other antenna designs can be similarly calculated. For links transmitting from the Deep Space Network (DSN), the gain is referenced from documentation as shown in Table 23.

Table 23 Specifications for DSN Antennas [38]

Antenna	Freq. Band	Gain (dBi)	Noise Temp. (K)	G/T (dB)	HPBW (deg)
34-m BWG	S	56.8	36.8	41.1	0.23
	X	68.0	33.0	52.9	0.063
	Ka	78.5	31.0	63.6	0.017
34-m HEF	S	56.0	38.0	40.2	0.23
	X	68.1	19.8	55.1	0.063
	Ka	NA	NA	NA	NA
70-m	S	63.4	22.0	50.0	0.11
	X	74.4	20.6	61.3	0.031
	Ka	NA	NA	NA	**NA**

F.5.2.3 Space Losses

Space losses are calculated based on the frequency of the signal and the distance travelled. The maximum distance used for Mars to Earth communications is 2.5 AU, which is the maximum distance between the planets when the sun is not blocking the signal. For links to a planet's surface, the slant range at 30° elevation is used for maximum distance to account for situations where the orbiting craft is not directly above the ground craft. Space losses are calculated as

$$L_{\text{s,dB}} = 20\log(D) + 20\log(f) - 147.55, \tag{12}$$

where D is the distance in m and f is the frequency in Hz.

F.5.2.4 Atmospheric Losses

Atmospheric losses for Mars and Earth are referenced from Table 24 and Figure 18, respectively. For Mars, the total vertical losses are 0.5 dB for the UHF link on the MAV and 1.15 dB for the X-Band backup link on the MAV. For Earth, the total vertical losses for X-Band are 0.05 dB for a sea level ground station. Increased travel time through the atmosphere due to slant range is accounted for as

$$L_{\text{a, slant}} = \frac{L_{\text{a, vertical}}}{\sin\beta}, \tag{13}$$

where β is the elevation angle.

Table 24 Radio Wave Attenuation Around Mars for Various Frequency Bands [39]

	VHF (100–500 MHz)	S-Band (2–4 GHz)	X-Band (10–12 GHz)	Ka-Band (30–38 GHz)
Ionosphere (absorption & scintillation)	0.5 dB	0.15 dB	0.1 dB	0.05 dB
Troposphere (scattering)	0	0	0	negligible
Gaseous	0	0 dB	0 dB	0 dB
Cloud	0	0	0.05 dB	0.1 dB
Rain	0	0	0	0
Fog	0	0	0	0.1 dB
Aerosol (haze)	0	0	0	0.1 dB
Dust*	0.1 dB	0.3 dB	1.0 dB	3.0 dB
Total Vertical Losses	0.5 dB	0.45 dB	1.15 dB	3.35 dB

* Worst case

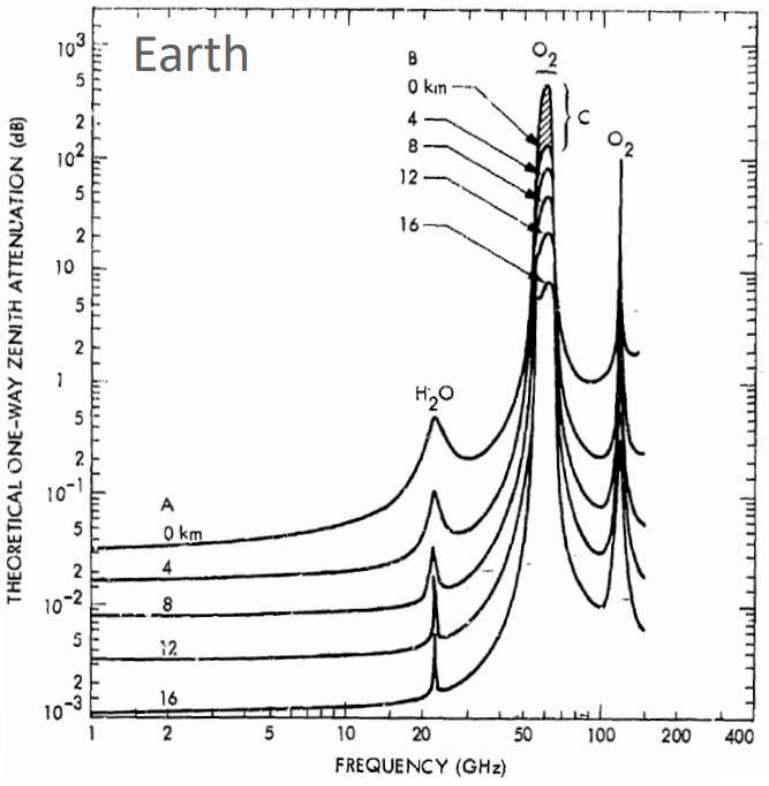

Fig. 18 Radio Wave Attenuation Around Earth for Various Frequencies [40]

F.5.2.5 Pointing Losses

Pointing losses for a parabolic antenna are dependent on pointing error and antenna half-power beamwidth. The half-power beamwidth is calculated as

$$\delta = \frac{21}{fD}, \tag{14}$$

where f is the frequency in GHz and D is the diameter. The pointing loss in decibels is calculated as

$$L_{\theta,dB} = 12\left(\frac{\theta}{\delta}\right), \tag{15}$$

where θ is the pointing error [37]. For half-wave dipole antennas, the radiation pattern shown in Figure 19 is used to determine losses due to pointing accuracy. To allow for relaxed pointing requirements during ascent and EDL, the pointing loss corresponding to a 30° offset from peak gain, which is 2 dB, is used for the MAV to Taxi link. The pointing losses incurred on the system will drive pointing requirements. To meet the high pointing requirements of the high gain parabolic antennas, a high precision gimballing system is used.

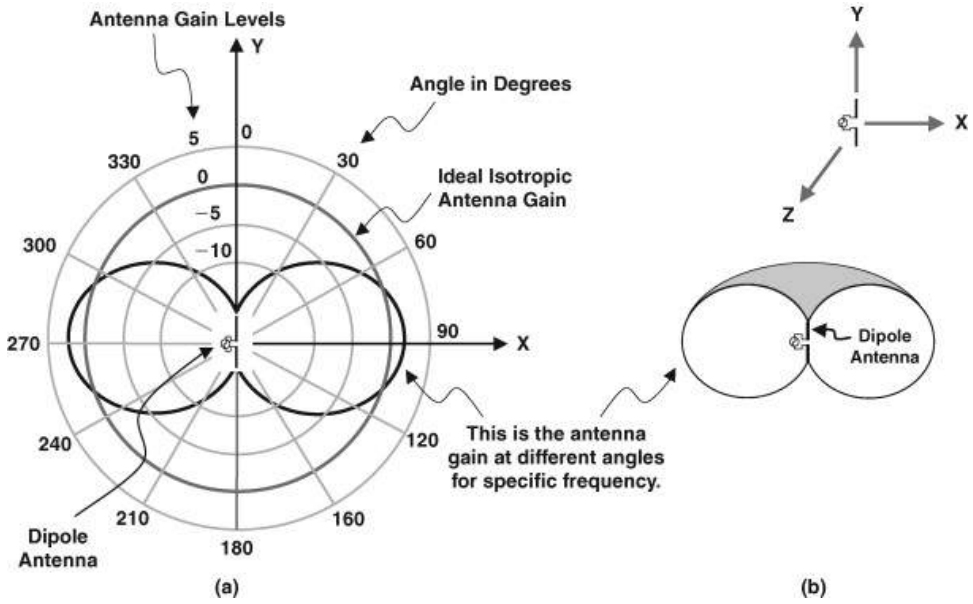

Fig. 19 Radiation Pattern for Half Wave Dipole [41]

F.5.2.6 Receiving Gain

For spacecraft to ground control links, the receiving gain can be referenced from the receiving facility documentation. This value is typically used in the link budget as $\frac{G}{T_s}$. The specifications for the 70 meter DSN dish used by the communications system are given in Table 23. For uplinks to spacecraft, the receiving gain is calculated as described in Section F.5.2.2. The system noise temperature for these systems is estimated to be 289 K based on typical

communications systems as shown in Table 25.

Table 25 Typical System Noise Temperature in Satellite Communications Links in Clear Weather [37]

Noise Temperature	Frequency (GHz)					
	Downlink			Crosslink	Uplink	
	0.2	2-12	20	60	0.2-20	40
Antenna Noise (K)	150	25	100	20	290	290
Line Loss (dB)	0.5	0.5	0.5	0.5	0.5	0.5
Line Loss Noise (K)	35	35	35	35	35	35
Receiver Noise Figure (dB)	0.5	1.0	3.0	5.0	3.0	4.0
Receiver Noise (K)	36	75	289	627	289	438
System Noise (K)	221	135	424	682	614	763
System Noise (dB-K)	23.4	21.3	26.3	28.3	27.9	28.8

F.5.2.7 Bandwidth

As a first order approximation, it is assumed that data rate is equal to the bandwidth of the link. Therefore, the bandwidth for each link is selected based on the data budget in Table 20 or Table 21.

F.5.2.8 Required Signal to Noise Ratio

The required signal to noise ratio is based on the modulation scheme used and desired bit error rate (BER). For these links, binary phase-shift keying (BPSK) was chosen for sizing calculations due to its good use of the signal spectrum and low BER. A BER of 10^{-7} is used for all sizing as this is standard for telecommand signals and is the largest BER that will be required. The required signal to noise ratio is determined to be roughly 10.5 dB for a bit error rate of 10^{-7} as shown in Figure 20. A link margin of 3 dB for low frequencies and 5 dB for X-Band frequencies is applied, as well as an implementation loss of 2 dB, such that the designed signal to noise ratio is

$$\left(\frac{E_b}{N_0}\right)_{\text{design}} = \text{Margin} + I + 10.5. \tag{16}$$

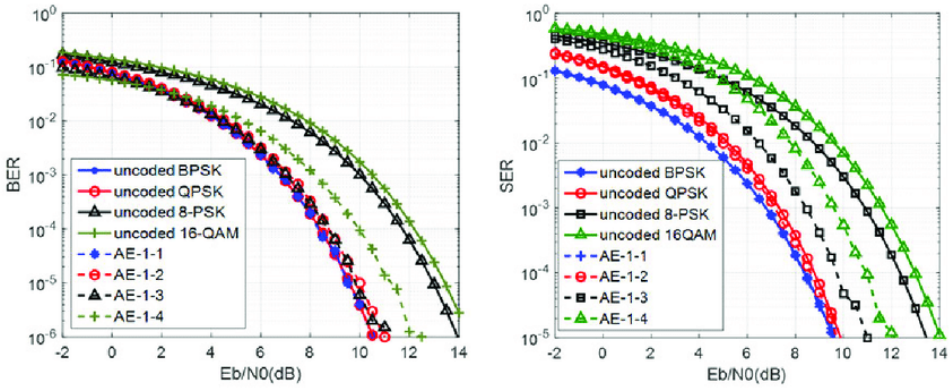

Fig. 20 Required Signal to Noise Ratio Based on Bit Error Rate and Modulation Scheme [42]

F.5.3. Trades

The trades section outlines some additional trades not explicitly outlined in the previous sections.

F.5.3.1 Overall Architecture

We decided to design our communications system such that the orbital taxi serves as a relay between the MAV and ground control for the primary communications link. This architecture is beneficial because it will allow for slightly wider communications windows and it will minimize mass and drag on the MAV by allowing for a smaller antenna with lower power requirements. The main concern with this architecture is the possibility of any communications system failing resulting in a total communications failure. Therefore, a small backup antenna which can use high power to transmit a lower datarate directly to ground control was also added to the design. This architecture is shown in Figure 21. In designing each antenna, the primary trades to make are the communication band, the antenna type and size, the bandwidth, pointing requirement, and the power requirement. The selected combination of design criteria must result in a link budget that closes, and each choice will affect the SNR at the receiving antenna as described in Section F.5.2.

F.5.3.2 Band Selection

Higher frequency bands are typically preferred for high datarate links as they allow for higher bandwidth communications. An important consideration when choosing the frequency band is the attenuation of that frequency due to atmospheric effects. X-Band and Ka-Band links were considered for the long distance, high datarate connections from the taxi to ground control and from the MAV to ground control. Both bands perform similarly for this use case when compared via the link budget, however X-Band is already in use by satellites in orbit around Mars, and attenuates less in the Martian atmosphere. Therefore, X-Band was chosen for the links from the taxi to ground, MAV to ground, and the taxi to other satellites. For the link between the MAV and taxi, the primary consideration is attenuation due to

the atmosphere. A 440 MHz link was chosen due to its low attenuation compared to X and Ka-Band, as well as its past use on the perseverance mission. Using frequencies that have been proven on previous missions means reliable, tested hardware with field performance data can be used to maximize chances for mission success.

F.5.3.3 Antenna Selection and Sizing

The antenna type primarily affects the antenna gain, pointing requirements, and mass. For the MAV to taxi link, the primary considerations are low pointing requirements for maintaining communications during EDL and ascent, as well as low mass. For this link, high gain is not as important due to the relatively short distance and losses. A half-wave dipole was chosen for this purpose as it satisfies these design criteria and is an extremely simple and reliable design. For this analysis, we assume this design has a peak gain of 1.64 dBi and maximum mass of 0.4 kg. For the long distance links to ground control, the most important factor is a high gain because the signal experiences extremely high losses when travelling from Mars to Earth. A parabolic high gain antenna is typically necessary achieving these long distance links and has been chosen for both vehicles due to the need for high gain. The peak gain for a parabolic antenna is calculated using Equation 11. The mass of the dish is also approximated as

$$m_{\text{par}} = 0.4 + 4.5(\pi D^2/4), \tag{17}$$

where D is the antenna diameter in meters. This mass value is important for use in trades between antenna size and transmission power, as well as for mass budgeting [43].

F.5.3.4 Command and Data Handling

The onboard computer system is sized based on past missions with similar mission requirements. The TRTL mission does not require any novel computer technologies, so it is highly beneficial to use reliable systems that have been proven on past missions. The computer chosen for this mission is the BAE RAD 750 which was proven in the Mars 2020 Rover mission. This system has a processor speed of 200 MHz, 2 GB memory, and 256 MB of RAM which can handle the data processing requirements imposed by the data budget and processes such as automated launch and docking. Both the orbital taxi and MAV will have two independent and redundant computer systems with radiation hardening. Each unit consumes 6 W when active and weighs an estimated 5 kg.

F.5.4. Final Configuration

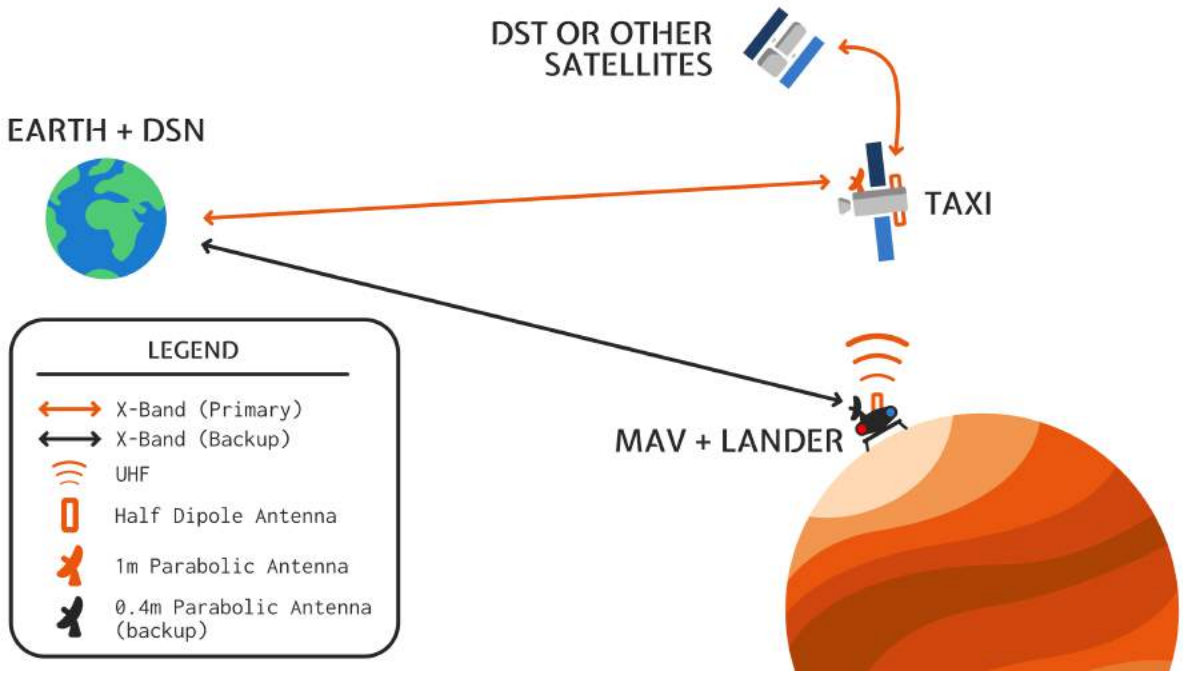

Fig. 21 Final communications architecture.

The final selected configuration is a an OT communications relay architecture. The primary link is the path starting at the MAV, relayed through the OT, and reaching the DSN and vice versa. The Orbital Taxi uses a high gain parabolic X Band antenna to communicate with the DSN, and both the MAV and OT use a low gain half wave dipole antenna for communication with each other. A small high gain antenna is included on the MAV capsule to allow a low data rate connection directly to the DSN if the primary link fails.

Due to an estimated average communications delay of twenty minutes, all time sensitive operations will be fully automated. Since TRTL does not include a fuel transfer phase, this includes ascent, rendezvous, docking, and burns. The technology for automation of each of these processes has been thoroughly developed on Earth and low Earth orbit. Additionally, astronauts will be locally present for each of these steps, and procedures will be developed for astronauts to take over in the event of any automation failures. This should allow for minimal impact of communications delay on mission operations. During these phases, communications with ground control will still be available, however they will be subject to the communications delay.

F.5.4.1 Complete Link Budget and Sizing

The link budget outlines the relevant selected parameters for the final link configuration. Most notable for overall craft design are the transmit power requirements and the bandwidth.

Table 26 Key link budget parameters for the backup link between MAV and the DSN.

Parameter	MAV to DSN 70 m	DSN 70 m to MAV
Max Distance (km)	3.74E+08	3.74E+08
Transmit Power (W)	1000.00	21440.00
Max Pointing Error (deg)	0.1	0.01
Central Frequency (GHz)	8.45	8.45
Bandwidth (kHz)	16.66	14.00
DSN Channel	37	37
Transmitting Antenna Gain (dB)	28.38	74.40
Antenna Diameter (m)	0.40	70.00
Antenna Mass (kg)	0.97	
Receiving Antenna G/T (dB)	61.30	0.10
Design Signal to Noise Ratio (dB)	17.50	17.50
Available Signal to Noise Ratio (dB)	18.71	17.68

Table 27 Key Link Budget Parameters for the Link Between MAV and OT.

Parameter	MAV to Taxi	Taxi to MAV
Max Distance (km)	474	474
Transmit Power (W)	0.40	0.40
Max Pointing Error (deg)	45	45
Central Frequency (GHz)	0.40	0.40
Bandwidth (kHz)	132.47	132.47
Transmitting Antenna Gain (dB)	1.64	1.64
Antenna Mass (kg)	0.40	0.4
Receiving Antenna G/T (dB)	0.01	0.01
Design Signal to Noise Ratio (dB)	15.50	15.50
Available Signal to Noise Ratio (dB)	16.09	16.09

F.5.4.2 Mass Estimate

Mass estimates for the antennas are as described in Section F.5.3.3. Mass estimates for all other components are based on typical systems of similar design [37]. While the individual components of a finalized system may not be identical, these should provide a representative mass estimate. All electronic components except for the antennas have also been doubled for redundancy. The complete mass budget is given in Table 28.

Table 28 Mass Budget for MAV Communications Systems.

Item	Qty	Mass (kg)	Total
X-Band TWTA	2	2.5	5
X-Band Diplexer	2	0.6	1.2
X-Band Switching Network	2	1	2
X-Band Cables	1	5	5
X-Band High Gain Antenna	1	1	1
Ultrastable Oscillator	2	1.3	2.6
UHF Diplexer	2	0.2	0.4
UHF Cables	1	3	3
UHF Low Gain Antenna	1	0.4	0.4
BAE RAD 750	2	5	10
Total Mass			30.6

F.6. Attitude Determination and Control

The MAV's demands for stability and control during EDL, ascent, and docking phases require an ADCS system that implements robustness, reaction control speed, and precision. The approach to designing the ADCS configuration begins with the RFP derived requirements for the subsystem, specifically for the MAV. Table 29 contains such requirements.

Table 29 MAV ADCS Requirements

Req. ID	Requirement Description
TRTL-ADCS-01	The MAV shall be capable of fully autonomous attitude determination and control during Mars ascent with crew.
TRTL-ADCS-02	The MAV shall be capable of autonomous docking using the ISS standard with both the taxi vehicle and a passing DST vehicle.

Table 30 subdivides the MAV's mission into phases based on the attitude determination and control requirement imposed on the system in that phase of flight. This is an obligatory step of analysis to best encapsulate all components of the mission that contain demands for ADCS.

Table 30 Attitude pointing budget for MAV mission phases

Control Mode	Required Accuracy	Notes
Entry, Descent, and Landing/ Ascent/In-Space Travel	1° 0.1°/s	Thermal and aerodynamic load management
Contingency Ground Communications	0.001°	In case of primary comms failure – Earth antenna pointing requirement
Docking	1° 0.1°/s	Allowable misalignment for International Docking Adapter

The primary attitude determination driving requirement here is the contingency associated with the failure of the primary high-gain communications system on the OT. In this case, the MAV would need to handle communications from the surface of Mars back to ground stations on Earth; in order to properly point the high gain antenna on the MAV, the vehicle's attitude on the Martian surface must be determined to within 0.001°. This knowledge, combined with accurate mapping of the MAV's surface position knowledge of the location of Mars relative to Earth would allow critical communications even in the event of system-level failures on the orbital taxi. In addition to this, another driving requirement is the assurance of mission safety during Mars entry and on ascent. To do this, it was found that we needed to be able to sufficiently control attitude to within 1° of the commanded attitude.

To size these systems, we again needed to constrain the torque environment under which we were operating, which involved taking the worst-case internal and external torque values from entry or ascent.

Since the mission requirements for the MAV mandate a far shorter regime in which the ADCS must be active, the architectural choices are somewhat different. A primary concern for this vehicle was propellant slosh, particularly on ascent when all tanks were completely full. This is an inherently nonlinear problem, and accurate simulation of the fluid

Table 31 Analysis of internal and external torques on Mars Ascent Vehicle

Torque Type	Torque Source	Maximum Magnitude (Nm)
Internal	Slew (180°/hr)	0.057
External	Solar Radiation Pressure	0.029
External	Aerodynamic Drag (1deg AoA)	1.48
External	Gravity Gradient	2.2E-4
Internal	Slosh	51600

Table 32 Attitude determination and control hardware for Mars ascent vehicle

Hardware	Specification	Notes/Uses
4x Custom single-gimbal control moment gyros	200 Nms momentum storage 10 Nm torque	Fine attitude control and momentum storage
2x Ball HAST star trackers	0.5 arcsec accuracy	Low-frequency state estimation updates and fine attitude determination
2x Honeywell HG9900 RLG IMU	0.0006 deg/hr drift	Kalman filtered attitude propagation
16x NewSpace NFSS-411 sun sensors	0.1 deg accuracy	Coarse attitude acquisition/contingency
16x Safran-Ariane 200 N RCS thrusters	180-279N per thruster	Momentum dumping – 5x pods of 4 thrusters

dynamics at play would have been incredibly computationally expensive and well beyond the scope of this project, but as a first-order estimate, we made the assumption that 10% of the propellant mass shifted from the tanks' respective centers of mass to the same side of each tank as a worst case scenario. While this does generate a moment of 51600 Nm, orders of magnitude greater than any other internal or external torque on the vehicle, a similar first-order approximation found that roughly six degrees of gimbal range on the main propulsion system engine would be sufficient to counteract this moment. Thus, it was assumed that main engine gimballing would be sufficient to manage the bulk of the loads imposed on the vehicle by sloshing. The 200 N RCS thrusters offer very high specific impulse and fairly precise control, but their minimum firing time of 0.1s is not sufficient to achieve the attitude control requirements imposed on ascent and during Mars entry. Thus, we have chosen to include control moment gyros for fine attitude control, while these have packaging limitations and are less volume-efficient, as mentioned in the previous section, they are able to provide a significant amount more torque for far less power than a similarly-sized reaction wheel system. This will allow it to exert control authority even under the difficult flight regimes imposed by Mars EDL and ascent with humans.

F.7. Power

Design plan of attack for configuring the MAV power system was to produce an architecture that could safely and reliably allocate for all of the subsystem demands within the vehicle. Vehicular power consumption, storage methods, and generation methods are analyzed for best practice to equip the MAV with proper energy inventory. As the majority of the mission lifetime will be spent on Martian surface, where the MAV will be linked with the Lander, both the MAV and Lander power systems are elaborated on within this section. The two vehicles are configured together during mission entirety until the MAV detaches and launches separately from the Lander during ascent. Table 33 details all the aspects of the MAV power requirements derived from the RFP mission requirements.

Table 33 MAV Power Requirements

Req. ID	Requirement Description
TRTL-PW-01	The system shall utilize a 10kW Fission 5000kg power source.
TRTL-PW-02	Necessary power shall be supplied to all subsystems for vehicle operation.
TRTL-PW-03	The lander power system shall supply sufficient power to the ISRU propellant generation system.
TRTL-PW-04	All systems shall not exceed 10kw during peak usage without additional energy storage.

Satisfaction of such requirements necessitates further specifications of power consumption demands for each phase of the mission. Tables 34 35 encapsulate the vehicular power necessary to fulfill subsystem operations for overall mission execution.

Table 34 MAV Power Requirements

		Subsystem power demand (W)							
Phase	**Duration (hours)**	**Propulsion**	**Thermal**	**ECLSS**	**Comm.s**	**CDH**	**ISRU**	**Power**	**Total Power Required**
Transit	6600	1	0	0	25.1	20	0	0	46.1
Landing	1	1	0	0	25.1	20	0	0	46.1
Prop. Gen.	11700	1	0	0	25.1	20	0	0	46.1
Launch Prep.	12	1	67	1000	25.1	20	0	0	1113.1
Launch to Taxi	6	47	67	1000	25.1	20	0	0	1159.1
Taxi to DST	9	1	67	1000	25.1	20	0	0	1113.1

Table 35 Lander Power Requirements

		Subsystem power demand (W)							
Phase	**Duration (hours)**	**Propulsion**	**Thermal**	**ECLSS**	**Comm.s**	**CDH**	**ISRU**	**Power**	**Total Power Required**
Transit	6600	1	10	0	25.1	20	1	0	376860
Landing	1	1	250	0	25.1	20	1	320	617.1
Prop. Gen.	11700	1	250	0	25.1	20	12980	0	155330370
Launch Prep.	12	1	250	0	25.1	20	0	0	3553.2
Launch	1	40	250	0	25.1	20	0	0	335.1

After each of the main subsystems were designed and power requirements determined, a 30% margin was added to all power systems to account for any unexpected problems or inefficiencies.

F.7.1. Lander Power Configuration

Power storage system for the Lander was finalized to be Panasonic lithium-ion batteries. These batteries are relatively inexpensive, commonly utilized within industry, commercially available, high TRL, and high energy density 165 W-h/kg [45]. Then the power generation systems on the lander were sized for the most demanding phases of supplying enough energy for the ISRU process during Martian surface mission operation. Specifically, sizing the power generation for the maximum power required during LOX generation phase. This stage of the mission is guaranteed to last at least 14 months, in accordance with optimal ISRU propellant collection, but depending on surface conditions and harvesting performance, the process could could last up until MAV launch preparations. A total power generation of 17.258 kW is required to produce to LOX continuously. In compliance with the RFP-3 provided by the AIAA, the lander is equipped with the 5000 kg 10 kW nuclear fission reactor. This fission reactor is only able to supply 58% of the needed power to permit ISRU operation for MAV refueling. Limitations within the total landed mass of the Lander and MAV during EDL prevented the addition of a second reactor. Other lighter power generation options were investigated in order to give the ISRU is remaining power to complete the refueling process. A final option of solar arrays were chosen to supplement power for LOX generation because of its high power output per mass. The solar array selected are four scaled up gallium arsenide triple junction Ultraflex solar arrays with a diameter of 8 meters and an efficiency of 33-35%. The Ultraflex solar arrays are commercially available, compatible for storage, and a high TRL because it is being used on NASA's insight lander [46]. Two improvements will be added to increase the efficiency of the arrays: The first is a mechanism on the arm to allow the array to gimble during each sol and the second is is an Electromagnetic Dust Shield (EDS) to prevent the buildup of electrically charged dust Martian dust during dust storms [45]. On the surface 97% of generated solar power is devoted to ISRU generation. The total power delivered by the solar arrays, P_{sa}, was calculated from:

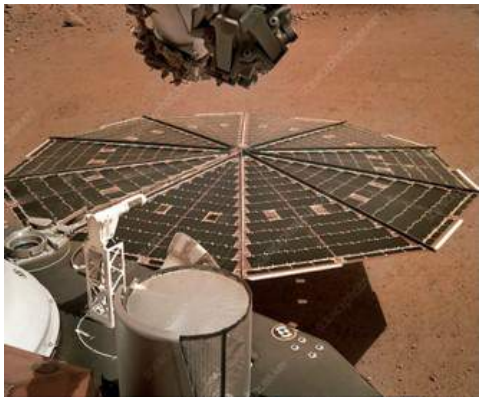

Fig. 22 NASA's Insight Ultra Flex Solar Arrays [44].

$$P_{\text{sa}} = A_{\text{sa}} \left[\eta_{\text{degradation}}\right] \left[\eta_{\text{pointing}}\right] \left[\left(\eta_{\text{cell}}\right) \left(\eta_{\text{array}}\right) S_{\text{Mars}}\right], \tag{18}$$

with A_{sa} as the total surface area of the arrays, η_{cell} as the loss factor due to the solar cell, η_{array} as the loss factor due to the array, and S_{Mars} as the solar constant at Mars, equivalent to 590 W/m^2 [37]. The degradation the arrays will experience throughout the mission, $\eta_{\text{degradation}}$, can be further modeled as $\eta_{\text{degradation}} = (1-\zeta)^{\tau}$, with ζ and τ as the solar array degradation per year and the duration in years respectively. Also, η_{pointing}, or the efficiency with respect to the

pointing angle of the arrays is a function of θ, or the normal viewing angle to the sun, as $\eta_{\text{pointing}} = \cos(\theta)$ [37]. These equations were also utilized to size the solar arrays for end of life mission phases for power security and redundancy, so that the arrays could provide sufficient power for every phase of the mission. Figure 23 depicts the solar power, along with the two other power suppliants, used for daily power consumption for ISRU production. The solar arrays will efficiently charge the batteries for 10 hours each sol. 53% of the output from the solar arrays go to the batteries each sol.

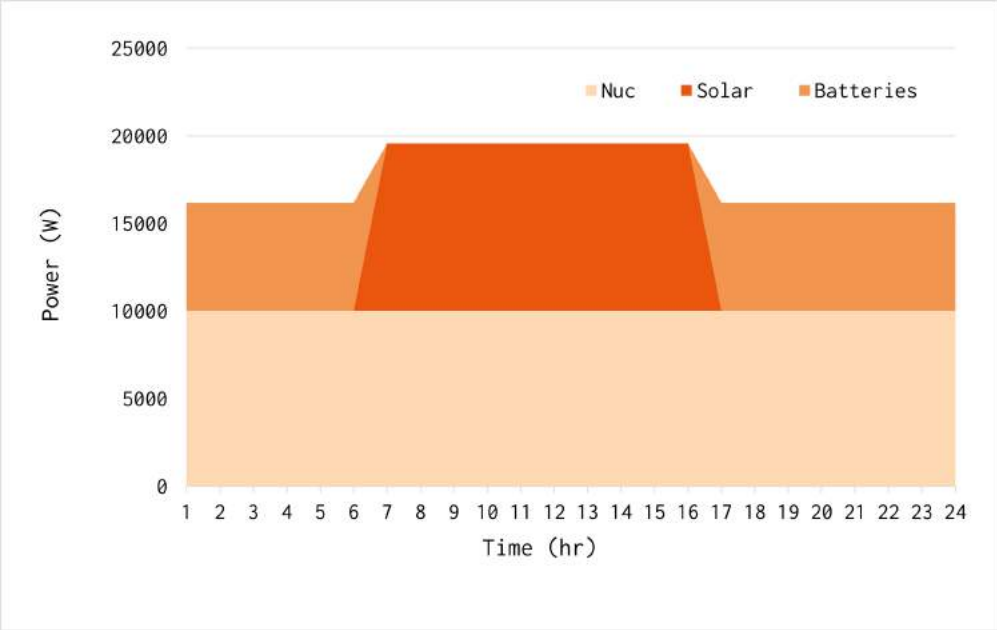

Fig. 23 Daily Power Used for ISRU Production

For journey to Mars, the Lander and MAV power requirement is minimal. All systems pertaining to the Lander and the MAV will operate by drawing power from the previously selected EDL HIAD systems's 784 kg batteries. Once the Lander with the MAV has successfully landed, and system checkouts are performed. The next step is power generation startup for Martian surface mission stage. This process of deploying the UltraFlex solar arrays is precarious and takes up to 500 W for operation. The safest procedure is to deploy one array using battery reserves and then use that array's power output to assist in deploying the remaining arrays. When all the arrays are deployed, start up of the reactor may commence and the power generation system is finally complete, allowing the ISRU process to begin and mission operations to continue.

F.7.2. MAV Power Configuration

The power supply for the MAV, while on Mars surface and connected to the Lander, is completely dependent on the energy generated by the solar arrays mounted on the Lander. Then, when ascent initiates, the MAV will need a separate power system to meet demands. For the power storage systems within the MAV, Panasonic lithium-ion batteries were also selected for reasons described in the previous Lander Power Configuration Section Åfter launch from Martian

surface and ascent phase towards Taxi rendezvous, all the systems on the MAV will draw power from its 267 kg battery pack. Battery pack sizing was determined with

$$E_{\text{stored}} = (T_{\text{day}})[(P_{\text{sa}})(\gamma_{\text{bat}})](\epsilon), \tag{19}$$

with T_{day} as the time in hours of the day, P_{sa} as the generated power, and γ_{bat} as the percent of solar power to the batteries. This equation calculates the required energy stored. The computed required energy stored also has an additional applied margin and accounts for charging efficiency, battery margin, charge time within each sol, and the percentage of solar power to the batteries. A charging efficiency of 80% was implemented in each charging cycle. For battery longevity, the best practice is to avoid charging batteries above 80% and discharging below 20% [37]. Including a battery margin of 50% accounts for each battery cell's unusable percentage. Then the mass of the battery pack, M_{battery} was determined by using Equation (20), or

$$M_{\text{battery}} = \frac{E_{\text{stored}}}{\rho}, \tag{20}$$

which E_{stored} and ρ denote the total energy stored and the energy density of the battery cells respectively. This battery pack was sized to sustain the MAV for the decided worst case scenario of 5 extra sols in orbit.

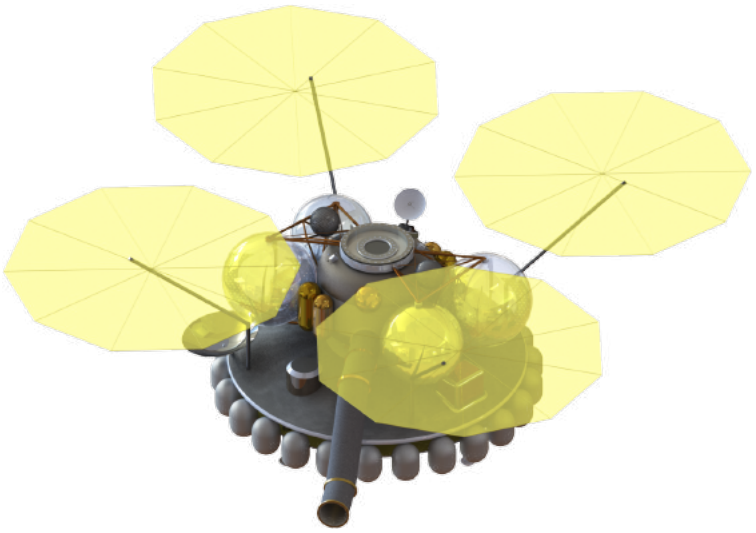

Fig. 24 Lander and MAV with deployed UltraFlex Solar Arrays.

F.8. Thermal Control Systems

Overall thermal control systems aims to preserve spacecraft integrity as well as maintain ideal temperature working ranges for the components within the vehicles. The selections in thermal management were intended for robustness and reliability to cultivate the needs of all other subsystem instruments for mission success. The fundamental design driver for the thermal control system relies on other subsystem demands for operational conditions and the temperature environment of each vehicle. Specifically, propulsion's need for fuel to remain in practical temperature ranges to persevere propellant integrity and reduce propellant boil-off, as well as ECLSS needs to maintain reasonable temperatures for the crew within the MAV capsule. Additionally, a baseline operational temperature range was established for the electronic components so that all hardware involved in communications, ADCS, and other subsystems may be accounted for.

Static single node analysis (SSNA) was the selected mathematical strategy, which was performed for each vehicle to assess whether the final thermal control system achieves desired temperature ranges and allows for the valuables within to be managed in good condition throughout the mission. Of all the assumptions SSNA incorporates to facilitate analytical computation, the most noteworthy for discussion is the steady-state model assumption. SNAA assumes a steady-state model, which eliminates the time derivatives within the heat transfer equation, and thus thermal capacitance opts out of the equation so that the mathematical model can be represented with the conservation of heat-energy ideology, or heat in is equal to heat out. We only consider sizing the vehicles for the absolute worst case scenarios: the hottest case, where the MAV spacecraft is in view of the Sun and withstanding Mars' hottest atmospheric temperature, receiving respective heat loads, and the coldest cases, in which the spacecraft is in eclipse, absent of any solar radiation and in Mars' coldest atmospheric temperatures. This was done for simplicity in the mathematical representation of the thermal modelling to determine the final respective temperature ranges.

F.8.1. MAV Thermal Design

The MAV has three temperature requirements for the three components of the MAV: the liquid oxygen cryogenic tanks, the methane cryogenic tanks, and the capsule. All requirements are indicated in Table 36 below and achieving such temperature ranges is critical to mission success.

Table 36 MAV Thermal Requirements

Req. ID	Requirement Description
TRTL-TCS-01	The MAV LOX cryogenic propellant tank temperatures shall be maintained at 70-90 K.
TRTL-TCS-02	The MAV Methane propellant tank temperatures shall be maintained at 100 - 120 K.
TRTL-TCS-03	The MAV capsule, which has the electronics bay and humans bay, shall be kept between temperatures of 263 K and 293 K.

The MAV design motivation approach stems from analysing the worst case climate situation for temperature. Sizing according to the worst case scenario would provide measures of protection from all other situations of the MAV's

mission journey. Considering all phases of operation for the MAV: the journey from Earth to Mars, the EDL stage, ISRU propellant generation on Martian surface, the ascent, and the passage to DST, the worst case scenario was determined to be ISRU propellant generation on Martian surface for 2 years. This judgement was made on the basis that, alongside the radiative heat loads from solar, albedo, and planetary infrared, there would be convective heat transfer to account for. No other phase of MAV operation timeline endures the effects of convection over such periods of time, and as such, the MAV design motive and calculations for sizing were solely based on conditions at Martian surface.

F.8.1.1 Heat Transfer Load Analysis

Before deciding between thermal control methodologies and in order to know what is required for thermal protection, we must first completely understand the total thermal loads that our vehicle undergoes during worst case circumstances. Mathematical approach to thermal analysis is modelled as heat in equal to heat out, or

$$Q_{\text{in}} = Q_{\text{out}}, \tag{21}$$

as the primary thermal equation [47]. Preliminary Heat transfer load analysis on the MAV begins by adjusting the original heat equation (21) to account for the absolute worst case climate situation, or while the MAV is resting on Martian surface. Radiative and convective heat forces are in full effect, along with conductive effects within the Titanium struts that bond all the MAV components to one another. A simple model representation of all the thermal effects the MAV cryogenic tanks and capsule experience on the Martian surface for the tanks and capsule are provided below in Figures 25a and 25b, with symbols R, K, and H representing heat transfers of radiation, conduction, and convection respectively.

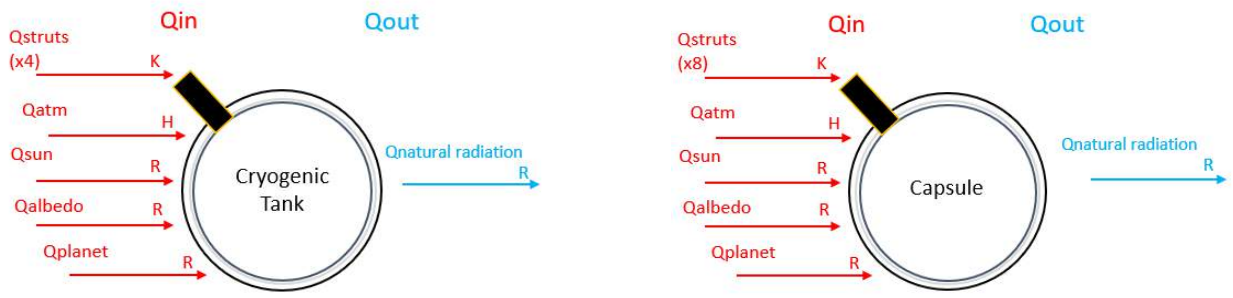

(a) Cryogenic Tank Model.

(b) Capsule Model.

Fig. 25 Thermal model representation of all heat transfer occurring within the MAV components.

The generalized heat transfer equation for the MAV is then represented as

$$Q_{\text{Sun}} + Q_{\text{Albedo}} + Q_{\text{IR}} + Q_{\text{Mars Convection}} + Q_{\text{Strut Conduction}} = Q_{\text{Natural Radiation}}, \tag{22}$$

with the conduction term as

$$Q_{\text{Strut Conduction}} = h\ A_{\text{total}}(T_{\text{sc}} - T_{\text{fluid}}), \tag{23}$$

including a k = 17 W/m-K as the conductivity of the Titanium strut material[48], and $A_{\text{cross section}}$ as the cross sectional area of the titanium struts supporting the components. Then also with the Martian convection term is further defined as

$$Q_{\text{Mars Convection}} = h\ A_{\text{total}}(T_{\text{sc}} - T_{\text{fluid}}), \tag{24}$$

and a h, or convection coefficient term introduced along with T_{fluid} as the temperature of the fluid surrounding our spacecraft. This convection coefficient value and the fluid temperature value is obtained from documentation and represents the hottest and coldest Martian temperatures: h = 17 W/m^2-K with T_{fluid} = 248 K and h = 3.4820 W/$m^2 - K$ with T_{fluid} = 163 K, respectively [49]. The rest of the radiative heat terms are defined as:

$$Q_{\text{Sun}} = \alpha_{\text{sc}} A_{\text{proj}} S_{\text{Mars}}, \tag{25}$$

$$Q_{\text{Albedo}} = a\ F_{\text{sc-planet}} \alpha_{\text{sc}} A_{\text{total}} S_{\text{Mars}}, \tag{26}$$

$$Q_{\text{IR}} = A_{\text{tot}} F_{\text{sc-planet}} \sigma \epsilon_{\text{sc}} (T_{\text{p}}^4 - T_{\text{sc}}^4), \tag{27}$$

$$Q_{\text{Natural Ratiation}} = \epsilon_{\text{sc}} \sigma F_{\text{sc-space}} A_{\text{tot}} * (T_{\text{sc}}^4), \tag{28}$$

with α_{sc} being the absorptance of the spacecraft, A_{proj} as the projected area of the spacecraft facing the Sun, S_{Mars} as the solar constant, equivalent to 590 W/m^2, $F_{\text{sc-planet}}$ as the view factor of the spacecraft towards the planet, a as the albedo factor of Mars, equal to 0.17, A_{total} as the total spacecraft external surface area, σ as the Stefan-Boltzmann constant, ϵ_{sc} as the emissivity of the spacecraft, T_{p} as the black body temperature of planet Mars, equivalent to 209.8 K, T_{sc} as the temperature of the spacecraft itself, and $F_{\text{sc-space}}$ as the view factor of the spacecraft towards space.

A static single node analysis of the raw MAV components shows that the solar radiation and convection effects are the main contributors in final temperature of the spacecraft, Tables 37 and 38below showcase such preliminary analysis.

F.8.1.2 Trades

The main driver of the MAV thermal control design is to combat against convective and radiative effects in order to keep the cryogenic LOX and methane fuel tanks in operation temperature ranges. The large amount of radiative and

Table 37 Unregulated MAV Cryo Tanks Quantitative Heat Load Data

Heat Source	Heat load (W)
Sun, radiation	4608.7
Albedo, radiation	391.74
Planetary Infrared, radiation	-526.7
Struts, Conduction	106.4
Mars Atmosphere, convection	-3063.31

Table 38 Unregulated MAV Capsule Quantitative Heat Load Data

Heat Source	Heat load (W)
Sun, radiation	19648
Albedo, radiation	1670
Planetary Infrared, radiation	-2254.71
Struts, Conduction	-196.26
Mars Atmosphere, convection	-12954

convective heat load requires that the use of active controls systems be employed. Passive strategies such as Cryogenic Thermal Control Coating were considered early on as it possesses very low absorptance values to protect against radiation [50]. However, while low absorption does aid in eliminating radiative solar load, this strategy does not assist in protecting against convective heat transfer and other strategies must be considered. Several Technology-Ready-Level (TRL) methods have been employed to keep such convection effects from penetrating the extreme low temperatures fuel tanks and achieve little to no boil off. The most prominent and traded strategies being the use of silica aerogel [51] the use of cryocooler and boil-off gas flow in Multi-Layer-Insulation (MLI) [52], and the use of thermodynamic vent system and vacuum jacketing for MLI [53]. The aerogel and vacuum jacket systems would prove most useful against convection, as it effectively creates a region of stagnant air, therefore convection cannot occur across the medium. The alternate strategy of cryocooler fluid loops within MLI takes a brute approach in maintaining cryogenic temperatures through direct refrigeration with coolant and does not incorporate any means to combat against convection directly. To operate this cryocooling flow system also demands higher power requirements compared to the other two power draw needs [52], since it will not only be cooling from the radiation, but also all of Martian convection occurring. All three components to the MAV require protection against convection in order to maintain cryogenic temperatures as well as keep the capsule within ideal "shirt-sleeved" temperatures for the crew. Therefore, the cryocooler fluid loops within MLI was no longer considered a viable option and the trade continued between aerogel and the vacuum MLI thermodynamic vent system. While the aerogel is extremely light and does perform well against convection and conduction, the delicate properties of installing aerogel as well as its ineffectiveness against solar radiation deems it an unfeasible option. Therefore, for the cryocooling, the thermodynamic venting system with vacuum jacket MLI and vapor cooling shields (VCS) was selected. For the capsule, the similar design was incorporated, but without use of vapor cooling shields and instead heaters are implemented within the interior volume. The choice in heaters was traded between commonly used Kapton Patch heaters or Cartridge heaters. Since the volume of the capsule will host the crew and electronics together, which all possess similar operational temperature ranges, a final configuration of Cartridge heaters with a copper belt to disperse the heat was selected.

F.8.1.3 Final Configuration

The final selected thermal control system for our MAV components includes the use of an active control system for convective protection measures and heating of the interior capsule volume, then the use of passive exterior control measures for manipulating absorptance and emissivity levels to combat radiation loads. For the cryogenic fuel tanks, the complete system comprised of: Aluminized Mylar MLI with fiberglass paper spacers, a thermodynamic vent system, a vacuum jacket system, and a vapor cooled shielding (VCS) system connected with a refrigerator was selected for thermal control. The very low conductivity properties of Aluminized Mylar MLI spaced with fiberglass paper, k = 0.000135 W/m-K, and the low absorptance values, makes it an ideal candidate as a choice in MLI [54]. The concern of heat loads reduces down to solely conductivity occurring within the MLI, since the ample amount of MLI layers will protect against radiation heat and since the MLI layers will be suctioned together with the vacuum jacket system to help eliminate convection heat load entirely. The vacuum jacket system is contains jacket plumbing, a vacuum pump, and insulation vent valving [53]. Then, to maintain desired low temperatures within the MLI and before the cryo-tanks, a vapor cooled shielding strategy is implemented. A coolant fluid, generated from the refrigerant system circulates through a section of the MLI to reduce overall heat load, Figure 26 shows the mechanism of the MLI layers with vacuum jacket and VCS [52].

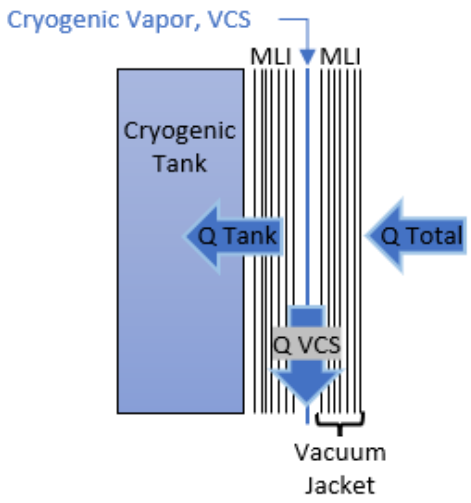

Fig. 26 Schematic visual of the MLI with vacuum jacket and VCS.

Then, finally, the Thermodynamic Vent System has several components for operation: a mixer, heat exchanger, Joule-Thompson Throttling device, and a Liquid Acquisition Device [53]. All components can be seen below on the MAV vehicle with Figure 27.

Redundancy measures for the MAV have been implemented to ensure the thermal control system can still acquire adequate operational temperatures for both the tanks and the capsule. The 10 cm MLI that surround the tanks and

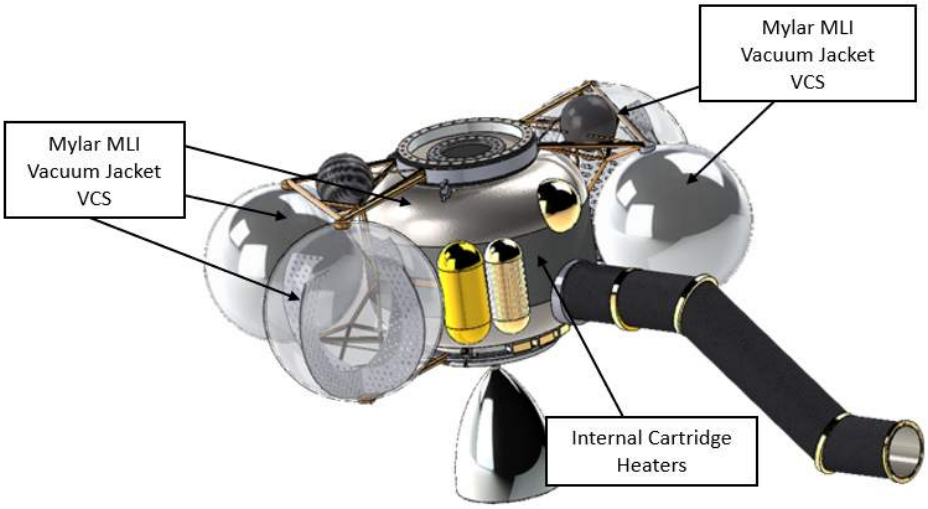

Fig. 27 MAV TCS component locations.

capsule contains 200 layers, specifically so that should debris penetrate some layers, the rest of the bulk sheet can perform its duties. Then, for the cryogenic tank TCS, there are 2 VCS divisions within the MLI, the Vacuum jacket has a backup vacuum pump in the event should one fail, and the thermodynamic vent system also has backup sized components. For the capsule, the vacuum jacket pump has a backup unit, then there are two independent cartridge heater copper band systems so that one may operate and achieve desired temperatures should the other fail.

A SSNA performed on both the tanks and capsule indicate that indeed the selected TCS can achieve desirable temperature ranges. Tables 39 and 40 includes the analysis and results from the SSNA.

Table 39 Final MAV Cryo Tanks Quantitative Heat Load Data

Heat Source	Heat load (W)
Sun, radiation	518.99
Albedo, radiation	44.11
Planetary Infrared, radiation	-17.9
Struts, Conduction	89.86
Mars Atmosphere, convection	-596.39

Table 40 Final MAV Capsule Quantitative Heat Load Data

Heat Source	Heat load (W)
Sun, radiation	255.4
Albedo, radiation	217.1
Planetary Infrared, radiation	-97.68
Struts, Conduction	-196.26
Mars Atmosphere, convection	-226.99

The reader should note that this SSNA was performed differently than typical methods of calculation in order to help size the chosen MAV thermal control architecture. Firstly, the exterior temperature that our MLI will experience in worst case scenarios was determined, then that data was used to determine the interior heat load that the tank will experience. This heat load is denoted as "waste heat" that needs to be removed by the cryocooling thermodynamic vent system, and such a number sizes the entirety of the configuration. As for the capsule, the experienced load by the interior was added to so desired temperatures were achieved. This added heat sizes our cartridge heaters and generates

final numbers. Thus, the final accomplished temperatures were between 84.28 K and 76.3 K for the LOX tank, between 113.32 K and 106.72 K for the methane fuel tanks, and between 286.5 K and 279.5 K for the capsule.

The Table 41 below contains the mass, power, and volume data determined from sizing the MAV TCS.

Table 41 Final MAV subsystem data for mass, volume, and power.

Componenet	Mass (kg)	Volume (m^3)	Power (W)
LOX Tanks	146.21	2.2	150
Fuel Tanks	102.15	2.2	100
Capsule	29.38	1.3	70

F.9. MAV Vehicle Overview

Table 42 MAV Mass and Power Budget with Margins.

	PRP	Propellant	STR	ECLSS	TCS	COMMS	ADCS	CDH	PWR	ISRU	Total
CBE Mass (kg)	968	2814	1440	925	278	31	105	105	7581	1784	16,031
Allocated Mass (kg) **% margin**	1210 25%	3517 25%	1800 25%	947 50%	347 25%	39 25%	131 25%	131 25%	9476 25%	2408 35%	20,006
Power (W) **30% margin**	2	0		756	325	10	370	120		13000	14,583

Fig. 28 Visualization of the MAV grounded configuration.

G. Orbital Taxi

G.1. Structures

Orbital Taxi structural design approach is very similar to the MAV design approach. Similar derived requirements, matching Table 10, were determined for the Taxi. The same requirement was imposed that all Taxi materials used must come from NASA's stress corrosion and cracking Tables I and II. The same FOS table previously used for the MAV, Table 11, was utilized again for Taxi structural design. X-ray and blue light scanning requirements were implemented for all welds and vehicle components to, again, account for cracking concerns from manufacturing deficits and thermal expansion. The Taxi's primary structural members also were required to undergo load and vibration testing [29].

G.1.1. Load Cases

All loads for the Taxi were examined for every mission phase. For preliminary analysis of the Orbital Taxi, the vehicle thrust acceleration load and the angular velocity radial loads were both the majorly influencing loads. Specifically, the driving Taxi load situation was the Taxi during MAV docking connection and boost to DST. Tables 43 44 are a depiction of the expected boost loads and vehicle geometry. The driving load case is the tank hoop stress due to pressurization, as the pressurized tank design is very strong and the taxi experiences minimal loading otherwise.

The moments of inertia (MOI) for attitude control system requirements were acquired from similar methods as the prior Section F.3.1, generated from CAD software and parallel axis theorem of simplified body shapes. The resulting

Table 43 Taxi Solar Panel Acceleration Analysis

Property	Value	Unit
Arm Length	2.5	m
Acceleration	16	m/s^2
Arm Mass	80	kg
Beam width	0.05	m
Thickness	0.01	m
Area MOI	4.53E-07	m^4
Moment	3200	Nm
Stress	176.47	MPa
7075 Yield	503	MPa

Table 44 Taxi Body Acceleration Analysis

Property	Value	Unit
Acceleration	16	m/s^2
Total Mass	2082	kg
Acceleration Loading	33312	N
Minimum Cross Section	0.0057	m^2
Maximum Axial Stress	5.83E+06	Pa
Yield	5.03E+08	Pa
Margin	85	
Tank Diameter	1.82	m
Tank Thickness	0.002	m
Tank Pressure	800000	Pa
Tank Hoop Stress	364	MPa
7075 Yield	503	MPa
Margin	0.38	

Taxi MOIs about the axes shown in Figure 29 are $I_x = 4273.44$ kg· m^2, $I_y = 65307.74$ kg· m^2, $I_z = 64950.15$ kg· m^2.

G.1.2. Structural Trades

G.1.2.1 Material Selection

Aluminum 2024-T3 was chosen for the OT for similar reasons of negligible thrust loads on the main vehicle body. This material allows for much more maneuverability and simplicity of welding manufacturing [31].

G.1.2.2 Orbital Taxi Packaging

The Taxi was chosen to have similar design to a typical rocket for simplicity in the packaging of the fuel. A common dome was placed inside the main tank to separate the fuel and oxidizer tanks while minimizing structural mass. The docking port and the engine were placed on the primary axis of the vehicle due to the dynamics of controlling the spacecraft.

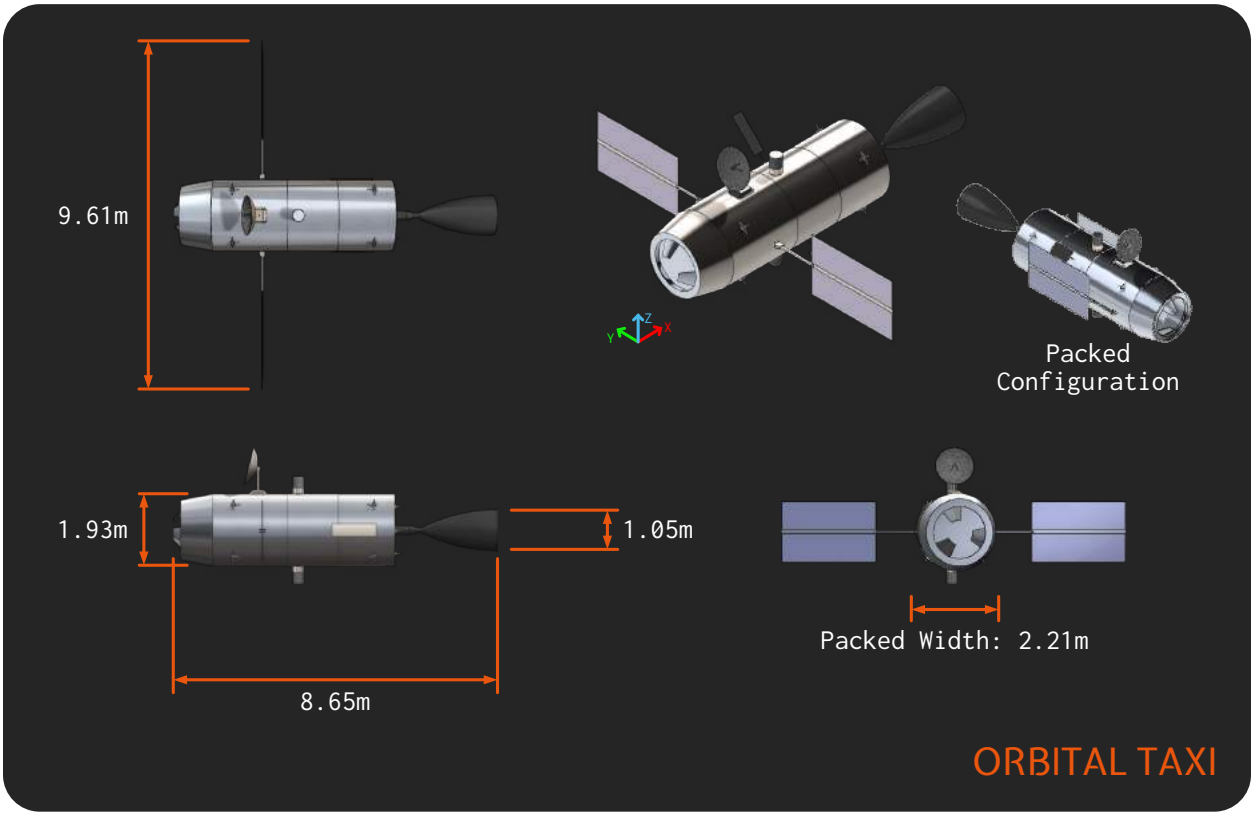

Fig. 29 Overall Taxi CAD and Dimensions.

G.1.3. Orbital Taxi Structure Driving Stress Analysis

The driving load case for the orbital taxi was the pressure equivalent bending load (PEQ) due to acceleration, tank pressure, and angular acceleration of the vehicle [30]. This PEQ equivalent load may cause local buckling on the thin walled pressure vessel under compression load from vehicle acceleration. Although a detailed large scale nonlinear finite element analysis model would be required to optimize the structure and predict this buckling failure, stiffening structure was placed inside the tank to avoid this failure mode pending a more detailed analysis [55].

G.1.4. Orbital Taxi Structural Mass Budget

Table 45 showcases the structural mass budget breakdown for the Orbital Taxi vehicle. Similar methods of acquisition, by determining required component size for loads and fabrication, as Section F.3.4 above, were performed to obtain a structural mass budget.

Table 45 Mass Breakdown for Orbital Taxi Structure (Dry Mass)

Component	Mass (kg)
Tanks	1300
Dock Fairing	75
RCS tanks	75
COPVS	27
Intertank 1 and Thrust Structure	200
Intertank 2 Walls	85
Docking System	320
Total Mass	2082

G.2. Propulsion

The design of the Orbital Taxi propulsion system was intended for robustness, reliability, and longevity, as the mission requires the Taxi to boost the crewed MAV to DST after sitting in orbit for 2 years.

The requirements associated with the Orbital Taxi are outlined in Table 46, which are derived from the original given RFP.

Table 46 Taxi Propulsion Requirements

Req. ID	Requirement Description
TRTL-PS-08	The Taxi engine shall be throttle-able to 50% of their nominal thrust.
TRTL-PS-09	The Taxi engine shall be capable of changing propellant mixture ratio between 3.5 and 3.7, as determined by the vehicle computer.
TRTL-PS-10	The Taxi engine shall communicate chamber pressure to the vehicle computer.
TRTL-PS-11	The Taxi engine shall provide 100 kN of thrust.
TRTL-PS-12	The Taxi MPS shall achieve a Delta V of 1360 m/s.

G.2.1. Taxi Main Propulsion System Trades

The Taxi is not limited by ISRU constraints since it spends the entire duration of the mission in space, so more propellants can be considered. Weighing the nature of the Taxi's mission, it is not logical to use cryogenic fuel since it spends 2 years in space which is a difficult environment to maintain cryogenic liquids due to leakage and thermal management constraints. Thus, the propellants considered were [33]:

- Nitrogen Tetroxide (NTO) / Monomethyl Hydrazine (MMH)
- 75% NTO 25% Nitric Oxide (MON25) / Monomethyl Hydrazine (MMH)
- Hydrogen Peroxide (H2O2) / RP-1

Most of these propellants have similar thermal properties and would need to be kept around the same temperature range. All of the options can go down to about 240 K, except NTO which cannot go below 280 K. They all have similar Isp (RP-1 would have higher if used with Liquid Oxygen) of around 300-330 s. The H2O2 brings a decomposition concern because it is not a particularly stable molecule as it decays easily and development would be needed in order to keep the fraction of H2O2 in the oxidizer high. The benefit of MON25 over solely NTO is the increase of operating temperature ranges, which makes it more similar to MMH. MON25 also eradicates tank oxidation concerns with NTO. The choice of a hypergolic propellant like MON25/MMH also improves robustness and simplicity since there is no separate ignition system required as there otherwise would be for H2O2/RP-1. With this information, MON25 and MMH were chosen as the propellants for the Taxi MPS.

The engine cycle was chosen to be the same as the MAV MPS, an ox-rich staged combustion cycle, for the same reasons discussed previously in Section F.4.1.

G.2.2. Taxi RCS/OMS

The Taxi propellant for the RCS/OMS system was chosen to be the same as the orbital taxi MPS, MON25/MMH for propulsion design simplicity. The RCS propellant will be located in separate tanks from the main propellant on the Taxi since the RCS system will need to be pressure-fed to, again, obtain the quickest possible response to commands (a necessity, for RCS thrusters, from ADCS subsystem). The tanks for the RCS were also selected to be titanium bladder tanks for microgravity region operation.

G.2.3. Taxi Propulsion System Sizing and Design

G.2.3.1 Taxi Main propulsion system sizing

The required ΔV for mission operation is 1360 m/s for the Taxi. The required propellant mass determination followed the same process from Section F.4.3.1, utilizing the Taxi ΔV, the dry mass from the total mass of all other subsystems, and the ideal rocket Equation (1). Then propellant mass tank volume is generated based on the density of

the propellant and incorporating the same previous ullage factor of 1.05 [33]. Again, since the structural mass takes the propellant tanks into account, the process of iteration, similar to within Section F.4.3.1, is performed to reach a desired tank mass, and thus a total vehicle mass. With this total Taxi vehicle mass, a thrust was calculated assuming the same vehicle thrust to weight ratio (TWR) of 4. This thrust, combined with the Taxi design parameters, can determine the exhaust throat and exit areas of the Taxi engines. The Taxi engine parameters are a mixture ratio of 2.3, a chamber pressure of 100 barA, a chamber temperature of 3300 K, a specific heat ratio of 1.23, and an expansion ratio of 150. The same contraction ratio of 5 was assumed to obtain the combustion chamber area. Therefore, the final exit diameter of 1.05 m was found, along with a Isp of 315 s, a $\dot{m}$ of 35.6 kg/s, and a thrust of 113 kN.

The Taxi RCS and OMS system also needs a supply of pressurant, for engine captivation prevention, so a common COPV was sized to supply Helium to both the RCS system and MPS. Steps taken within Section F.4.3.1 for sizing the COPV section were replicated, but for the Taxi to calculate a total COPV volume of 155 L. The COPV pressures are the same, 3.5 barA for MPS and 25 barA for RCS for a similar pressure fed system. Two entirely redundant COPVs of the same size and pressure were added for redundancy measures.

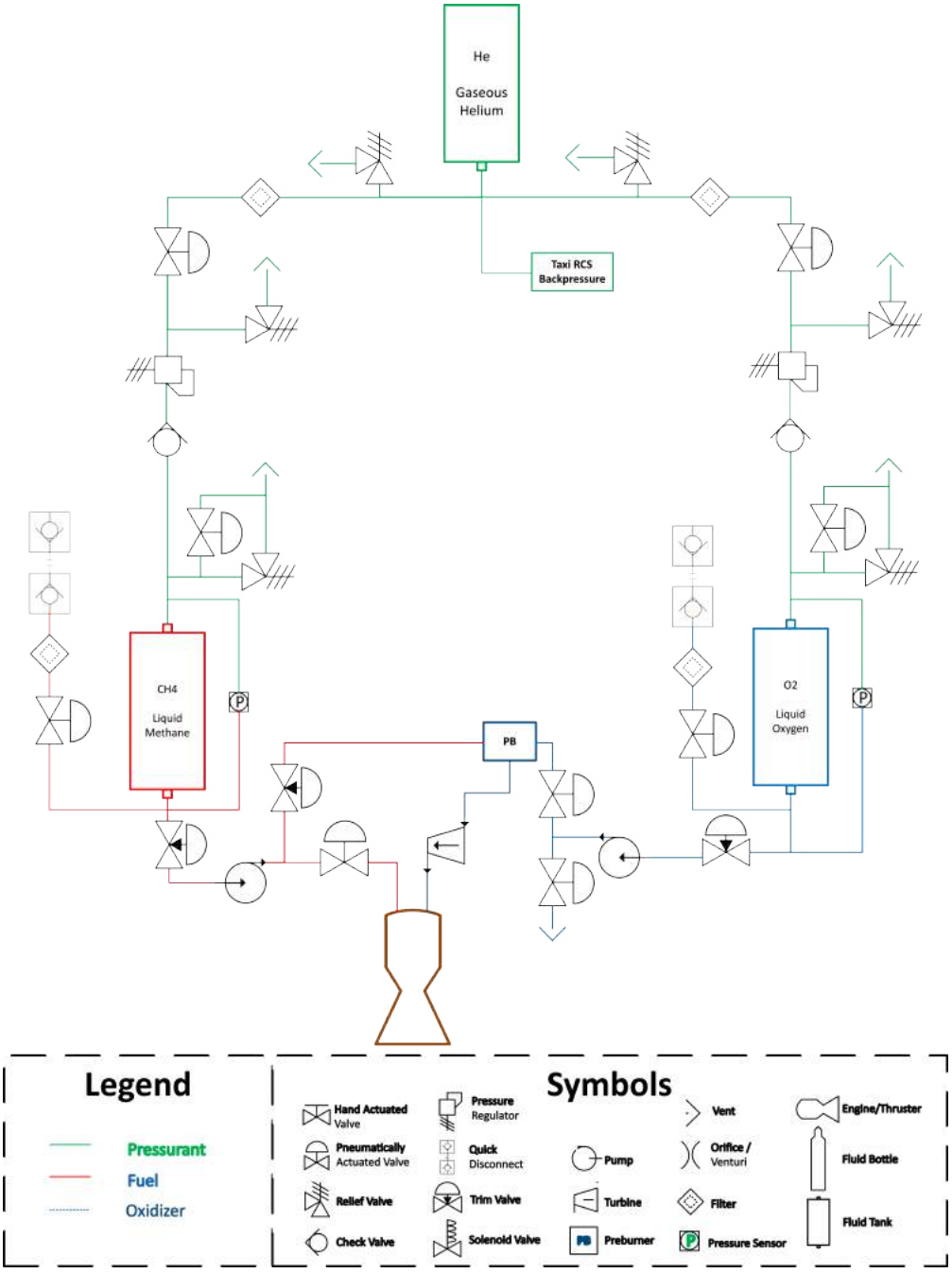

Fig. 30 Taxi MPS P&ID

Figure 30 is the Taxi MPS, which again is very similar to the MAV, however, each propellant only has one tank so there is only one pressurant flow path and one main propellant flow path.

G.2.3.2 Taxi RCS and OMS sizing

For sizing the Taxi RCS system 16 RCS thrusters in 4 pairs of 4 seems was also chosen for the Taxi based of previous legacy usage and historical reliability. The RCS system is comprised of the same 220 N thrusters that run off of MON and MMH [36]. The Taxi will also have 4 extra thrusters to act as ullage thrusters, to ensure that the main propellant is fully covering the MPS tank drains before starting the main engine. The Taxi P&ID can be seen within Figure 31.

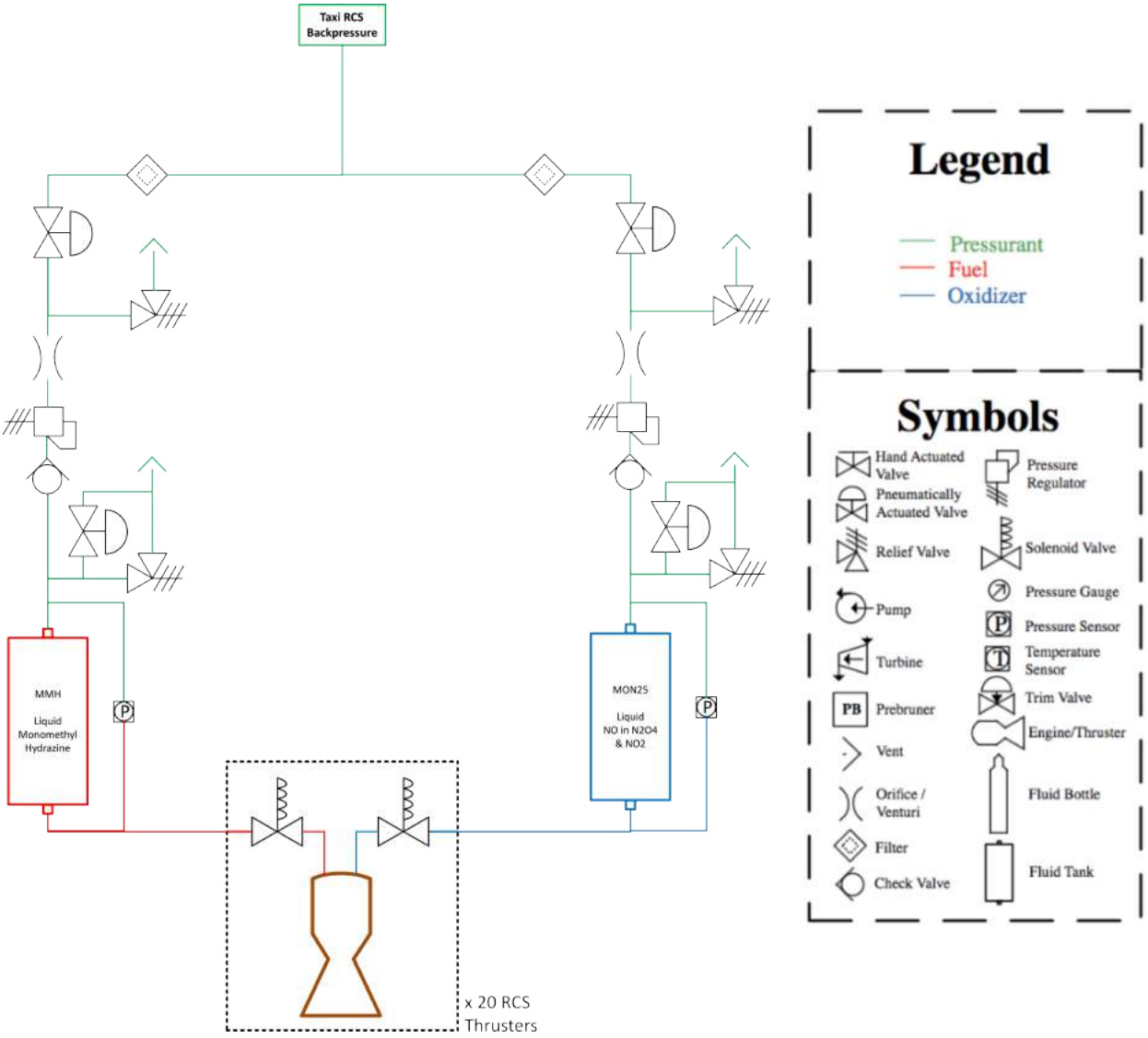

Fig. 31 Taxi RCS P&ID

Masses of the Taxi RCS system and Taxi common pressurant COPV were obtained with the same previous methods within the end of Section F.4.3.1. The resulting Taxi MPS mass is 319 kg, the pressurant gas mass is 13.3 kg, the COPV mass is 31.3 kg, and 98 kg for the RCS/OMS mass for a total propulsion system mass of 461.6 kg.

G.3. Communications

The communications subsystem is designed to facilitate the stated overarching mission goal of safely delivering two humans and 50 kg of samples from the surface of Mars to the DST. The requirements necessary for the communications subsystem to meet this goal are given in Table 47.

Table 47 Overall System Requirements

Req. ID	Requirement Description
TRTL-COM-3	The OT shall maintain uplink and downlink with ground control during the stated mission duration.
TRTL-COM-4	The OT communications shall support the full data budget of 132.47 kbps.

The complete methodology used for design trades and communications sizing is outlined in Section F.5. This section outlines the final configuration which was chosen for the OT based on this method.

G.3.0.1 Final Configuration

The Orbital Taxi will serve as a communications relay for the MAV. The primary link path will consist of data sent and received from the MAV via low gain half wave dipole antenna, and data sent and received to ground control via a one meter parabolic high gain antenna. This system has been sized to support the full data budget outlined in Section F.5.1. An additional low gain half wave dipole antenna has been placed on the OT and easily be configured for communications with any other spacecraft excepted to be operational during the mission. Command and data handling considerations are outlined in Section F.5.3.4.

G.3.0.2 Complete Link Budget and Sizing

The link budget outlines the relevant selected parameters for the final link configuration. Most notable for overall craft design are the transmit power requirements and the bandwidth.

Table 48 Key link budget parameters for link between OT and the DSN

Parameter	Taxi to DSN 70 m	DSN 70 m to Taxi
Max Distance (km)	3.74E+08	3.74E+08
Transmit Power (W)	600.00	20000.00
Max Pointing Error (deg)	0.01	0.01
Central Frequency (GHz)	8.45	8.45
Bandwidth (kHz)	132.47	14.00
DSN Channel	37	37
Transmitting Antenna Gain (dB)	36.34	74.40
Antenna Diameter (m)	1.00	70.00
Antenna Mass (kg)	3.93	
Receiving Antenna G/T (dB)	61.30	0.01
Design Signal to Noise Ratio (dB)	17.50	17.50
Available Signal to Noise Ratio (dB)	17.51	18.13

G.3.0.3 Mass Estimate

Mass estimates for the antennas are as described in Section F.5.3.3. Mass estimates for all other components are based on typical systems of similar design [37]. While the individual components of a finalized system may not be identical, these should provide a representative mass estimate. All electronic components except for the antennas have also been doubled for redundancy. The complete mass budget is given in Table 49.

Table 49 Mass Budget for Orbital Taxi Communications Systems.

Item	Qty	Mass (kg)	Total
X-Band TWTA	4	2.5	10
X-Band Diplexer	4	0.6	2.4
X-Band Switching Network	4	1	4
X-Band Cables	2	5	10
X-Band High Gain Antenna	1	4	4
Ultrastable Oscillator	2	1.3	2.6
UHF Diplexer	2	0.2	0.4
UHF Cables	1	3	3
UHF Low Gain Antenna	1	0.4	0.4
X-Band Low Gain Antenna	1	0.4	0.4
BAE RAD 750	2	5	10
Total Mass			47.2

G.4. Attitude Determination and Control

Since the orbital taxi will be remaining in orbit for the entire mission duration, up to 2 years, the driving requirements are a combinations of ADCS system accuracy and longevity. Table 50 provides RFP derived subsystem requirements for the Taxi attitude determination and control.

Table 50 Taxi ADCS Requirements

Req. ID	Requirement Description
TRTL-ADCS-03	The orbital vehicle shall be capable of reaching and maintaining a prescribed 250 km orbit until rendezvous with taxi vehicle

More specifically, we subdivide the taxi's mission into phases based on the attitude determination and control requirements driving that particular phase. This pointing budget is found in Table 51.

Table 51 Attitude pointing budget for orbital taxi mission phases

Control Mode	Required Accuracy	Notes
Acquisition/Slew	1° 0.01°/s	Initial acquisition of Mars-nadir attitude, slews, contingency operations
Station Keeping/ Lander Communication	1° 0.01°/s	Primary mission mode
High-gain Earth Communication	0.01° 0.001°/s	Required accuracy for communication antenna
Docking	2° 0.1°/s	Allowable misalignment for International Docking Adapter
Boost	1° 0.01°/s	Requires separate control law, as capsule will be docked to taxi

As would be expected, the driving requirement here is the high-gain Earth communication mode, where we must be able to determine the spacecraft's attitude to within 0.01° to allow the gimballed antenna to point accurately at the Earth ground station. This essentially limits the Taxi to a three-axis stabilized control scheme with a combination of inertial and non-inertial attitude control devices. To size these devices, it is then critical to consider the impacts of internal and external torques on the vehicle. We use the estimations found in Space Mission Engineering [37] to derive worst-case estimates for these torques and their corresponding momentum accumulation over the course of the mission, a tabulation of which can be found in Table 52 [37].

Solar radiation torque assumes a uniform reflectance and a simplified model of projected frontal area, aerodynamic drag simply uses the projected area of the spacecraft and the moment arm between the center of mass and center of pressure as calculated from CAD software, and the gravity gradient calculation is a simplified model assuming the minimum principal axis is in the Z direction.[37]

Table 52 Analysis of internal and external torques on orbital taxi in 250 km Mars orbit

Torque Type	Torque Source	Maximum Magnitude (Nm)
Internal	Slew (180°/hr)	0.057
External	Solar Radiation Pressure	0.029
External	Aerodynamic Drag	6.9E-12
External	Gravity Gradient	2.2E-4

Considering the requirements, as well as the desire to minimize cost and risk, we made the decision to utilize a combination of reaction wheels and hypergolic bipropellant RCS thrusters. The complete hardware selection for the orbital taxi is detailed in Table 53.

Table 53 Attitude determination and control hardware for orbital taxi

Hardware	Specification	Notes/Uses
4x Honeywell HR-16-150 reaction wheels	150 Nms momentum storage 0.4 Nm torque	Momentum storage and fine maneuvering
2x Ball CT-2020 star trackers	1.5 arcsec accuracy	Low-frequency state estimation updates
2x Honeywell HG9900 RLG IMU	0.0006 deg/hr drift	Kalman filtered attitude propagation
16x NewSpace NFSS-411 sun sensors	0.1 deg accuracy	Coarse attitude acquisition/contingency
16x Safran-Ariane 200N RCS thrusters	180-279N per thruster	Momentum dumping – 4x pods of 4 thrusters

One may note the selection of momentum exchange device, a set of 150 Nms reaction wheels, each providing 0.4 Nm of torque. Reaction wheels are more space and volume efficient mechanisms of momentum storage than the alternative control moment gyros, while still offering sufficient momentum storage so as to require momentum dumping burns from the RCS thrusters only a maximum of every 18 orbits, though these burns would be even less frequent should the described. Table 54 details the calculations associated with dumping the required momentum through burns of the RCS system.

Table 54 Quantification of required momentum dumping burns for orbital taxi

Momentum to be dumped	Thruster force	Moment Arm	Burn Time	No. of Burns	Propellant Mass
150 Nms	200 N	2 m	0.375 s	395	54.3 kg

The focus of this system for the Orbital Taxi, of course, was ensuring that the vehicle could survive in orbit while maintaining all desired communications with Earth and with the lander on Mars for the duration of the surface mission. Then, further mission demands were dependent on ensuring safe and accurate docking with the MAV followed by rendezvous with the Deep Space Transit vehicle. This requires accurate state estimation and attitude determination

as well as fine attitude control. Similar redundancy is built into all components of the system: there are four reaction wheels to service three roll axes, four sets of four RCS thrusters to ensure a similar level of fault tolerance - allowing full mission completion with the failure of any four individual thrusters, and finally, fully independent redundant sensor-IMU configurations to provide accurate attitude determination in the event of sensor failure. Despite all of this, the use of commercial off-the-shelf components offers an incredible degree of cost effectiveness while bringing a legacy of flight-proven hardware.

G.5. Power

The Taxi power subsystem breaks down into three components for analysis and sizing: storage, generation, and consumption. Table 55 details all the aspects of the Taxi power requirements derived from the RFP mission requirements.

Table 55 Taxi Power Requirements

Req. ID	Requirement Description
TRTL-PW-05	Necessary power shall be provided to all subsystems for vehicle operation.
TRTL-PW-06	The Taxi shall power supply during eclipse on orbit.
TRTL-PW-07	The Taxi shall supply power for 5-sol as margin for emergencies.

Analysis of power consumption within each mission phase is required to meet overall vehicle power demands. Within Table 56, the needed energy to satisfy subsystem operations for overall mission operation is depicted.

Table 56 Taxi Power Requirements

		Subsystem power demand (W)							
Phase	Duration (hours)	Propulsion	Thermal	ECLSS	Comm.s	CDH	ISRU	Power	Total Power Required
Transit	6600	2	0	0	505	20	0	0	527
On-Orbit	11700	2	200	0	505	20	0	0	727
Boost Prep	4	2	200	0	505	20	0	0	727
Boost	9	81	200	0	505	20	0	0	806

The same margin of 30% was applied to all Taxi final power configurations as well to assist in redundancy measures and ensure power supply reliability towards other subsystems.

G.5.1. Orbital Taxi Power Configuration

The orbital Taxi operates in a 250 km orbit around Mars for 2 years before attaching with the MAV and propelling towards the DST. Since of the long orbital mission duration, reliable power generation trades between small nuclear reactors and solar arrays were considered. In the end, solar arrays were selected over the small nuclear reactor in order to minimize bureaucratic logistics. The solar arrays selected were two gallium arsenide triple junction solar panels with an efficiency of 33 to 35%. The Taxi can deploy its solar arrays after boost phase in Mars orbit to begin generating power. The orbital taxi will store power within its 115 kg Panasonic lithium-ion battery pack. The battery type was chosen primarily for its high density capacity among other benefits, all of which are outlined within Section F.7.1. Battery sizing was determined from equations (F.7.2). The battery pack was sized to sustain all systems for 5 sols in the worst case that the solar arrays become non-functional after docking with the MAV. Therefore the battery pack is sufficient to run all systems during the 44 minute eclipse portion of the 250 km orbit.

G.6. Thermal Control Systems

The design approach for robustness and reliability was also implemented in choosing a thermal management system for the Orbital Taxi. Similar methods of analyzing a worst case thermal situations and trades incorporating the use of SSNA will be utilized to determine a final, satisfactory, thermal control system for the OT.

G.6.1. Orbital Taxi Thermal Design

The Taxi will host the hypergolic fuel as well as the electronics bay for communications and propulsion hardware. The required temperature range, as deemed necessary from the propulsion subsystem, for the hypergolic and electronics within the taxi are depicted below in Table 57.

Table 57 Taxi Thermal Requirements

Req. ID	Requirement Description
TRTL-TCS-04	Within the Taxi, the RCS hydrazine/MON propellant temperature shall be kept between 270 K and 300 K.
TRTL-TCS-05	The electronics bay within the Taxi shall be kept between 263K and 313K.

The OT is responsible for giving the MAV a boosts from the 250 km orbit to the DST near the end of the mission timeline, inability to maintain operational temperatures for the hypergolic fuel needed for the kick would result in mission failure. The Orbital Taxi's worst case thermal situation for analysis remains with its most predominant phase, during its routine orbit around Mars. During this stage, the OT experiences a large temperature fluctuation between eclipse shade to outlying in the Sun's exposure. Therefore, the design motivators were to protect the interior components from radiation thermal loads as well as to preserve heat during cold case eclipse cycles.

G.6.1.1 Heat Transfer Load Analysis

The heat load analysis procedure for the Taxi follows suit of the previous MAV section, and begins with modifying Equation (21) to incorporate the worst case thermal hot and cold situation. Of the three methods of heat transfer, the OT only experiences radiation heat. Convection does not occur in the vacuum of space, and conduction between the interior of the OT is assumed to be minimal because the thermal requirements for the Taxi are in similar enough ranges that the conductive processes may be neglected. A simple thermal model of the Taxi is provided below in Figure 32, the symbol, R, indicates a radiative heat transfer occurring.

Therefore, the final equations for the hot and cold temperatures can be developed:

$$Q_{\text{Sun}} + Q_{\text{Albedo}} + Q_{\text{IR}} = Q_{\text{Natural Radiation}}, \tag{29}$$

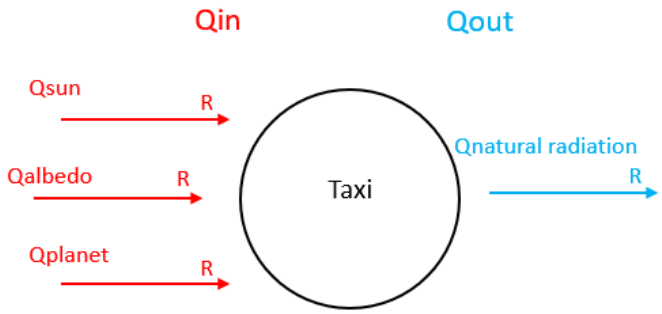

Fig. 32 Thermal model representation of all heat transfer occurring within the Taxi.

$$Q_{\text{IR}} = Q_{\text{Natural Radiation}}, \tag{30}$$

with (29) as the worst case hot situation equation and (30) as the worst case cold scenario equation.

Quick SSNA of the unregulated OT without a thermal control system indicates that the range of temperatures experienced will not suffice. Tabulated heat loads, below in Table 58, are far too immense and leave unsustainable conditions for the valuable components within the vehicle.

Table 58 Unregulated Taxi Quantitative Heat Load Data

Heat Source	Heat Load (W)
Solar, Radiation	700.84
Albedo, Radiation	757.8618
Planetary Infrared Radiation	-184.11

Resulting our Taxi without temperature control reaches temperatures of 282.68 K and 157.79 K, which an unacceptable lower boundary for the hypergolic fuel and electronics.

G.6.1.2 Trades

Discovering a method to manipulate the exposed thermal load of the naked Taxi is necessary for the final configuration, and establishing a passive way to achieve this is desired. Spacecraft coatings were considered for the sake of application simplicity and since there exists some coatings that may provide low enough apsorption levels to combat solar radiation. The lowest values of absorption and emmitance were found to be a silver vapor deposited glass substrate [56]. However, even with applying these new values to SSNA, the temperature values were not narrow enough for satisfaction. The alternative passive option considered is the use of MLI. General MLI will be able to effectively maintain low emmitance levels for heat preservation in the cold case, but do not successfully maintain ordinate temperatures for the hot case.

The final selection was a combination between MLI and spacecraft coating. Specific configured MLI will be able to maintain low emmitance levels, and a spacecraft coating can be applied to the underside to provide protection for solar and albedo radiation. Such a method is utilized in industry today and possesses high TRL [57]. The MLI and spacecraft layer coating method selected follows that of documentation [57]. However powerful the combination of MLI and spacecraft coating was, it still does not effectively rid of enough waste heat during worst case hot scenario. Therefore, an active cooling control system must be employed in order to maintain adequate temperatures for the Taxi. A Teflon 0.5 mil sized radiator to dump away the waste heat was deemed a fine decision, as it is heavily used in industry [47]. The radiator is an active systems that demands power, and such an option was decided to be a valid approach, as the solar panels and batteries on the Taxi would provide more than enough power to supply the taxi thermal control system.

G.6.1.3 Final Configuration

The final selected configuration for Taxi thermal management includes the use of passive MLI and spacecraft coating configuration as well as sized radiators for the worst case hot temperatures. Specifically, the combination of a Kapton exterior layer, followed by metal aluminium coating on plastic Mylar substrate, then 33 layers alternating between Dacron web spacer and aluminized Mylar was implemented for the entire surface area of the Orbital Taxi. Figure 33 portrays the MLI and spacecraft coating sequence that composes the exterior [57].

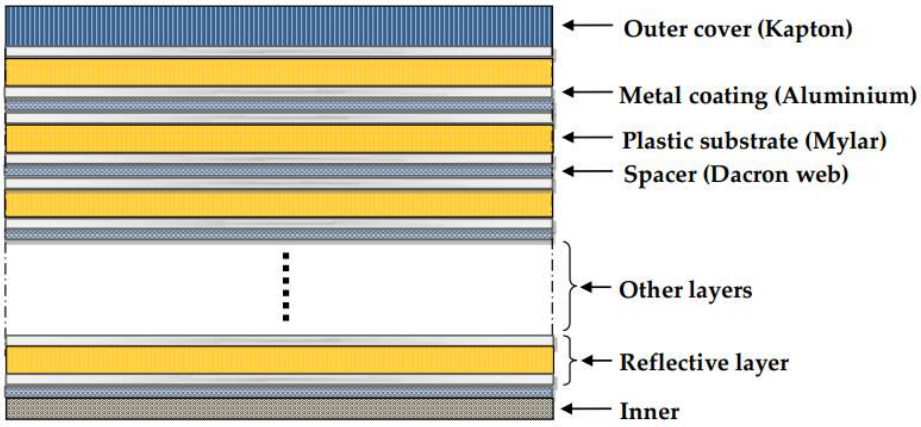

Fig. 33 MLI and spacecraft coating configuration.

Then two Teflon 0.5 mil radiators are installed. A heat pump loop system is coupled with the radiator to ensure that heat is being pulled from critical areas of the spacecraft.

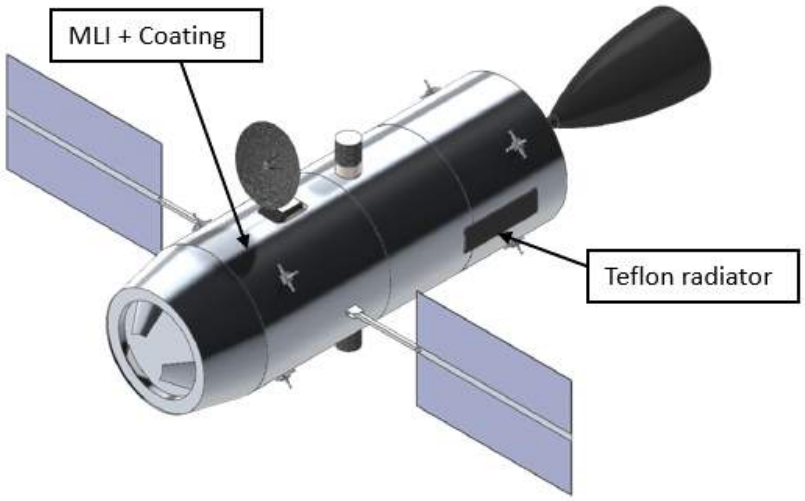

Fig. 34 Taxi TCS Component Locations

The location of the thermal control parts on the Taxi are shown within Figure 34. The radiator lays flush against opposite sides of the Taxi and the MLI spacecoating configuration is all along the exterior.

Redundancy measures have been implemented every step of the thermal control sizing in order to best create safeguards around maintaining the mission critical fuel for the MAV. The MLI layers contain the optimal amount of layering to prove most effective, however, should any debris impact the MLI and degrade some of the layers, the MLI will still operate at reasonable performance. There are two radiators placed on either side of the Taxi to ensure that while one radiator may be radiating inefficiently in the Sun-side, the other may radiate the necessary waste heat. Both radiators have been sized to account for the growth in spacecraft coating absorption levels that occurs over long mission lifespans [58].

SSNA shows that the final configuration for the Taxi control system is able to achieve operational temperature ranges for the hypergolic fuel and electronics 59. Mission success is reliant on the Taxi thermal control system operating correctly.

Table 59 Taxi Quantitative Heat Load Data

Heat Source	Heat Load (W)
Solar, Radiation	280.34
Albedo, Radiation	30.21
Planetary Infrared Radiation	-1.69

Therefore the final accomplished temperatures are lie between 303.96 K and 287.189 K, falling within the needed

range for thermal management on the Taxi.

All taxi masses, volumes, and power demands are outlined in Table 60. These quantities do not warrant further

Table 60 Final Taxi subsystem data for mass, volume, and power.

Componenet	Mass (kg)	Volume (m^2)	Power (W)
MLI + SC Coating	183.5	0.229	0
Radiators	25.75	0.061	200

concern for propulsion or power subsystems for overweight or large energy consuming issues.

G.7. Taxi Vehicle Overview

Table 61 Taxi Mass and Power Budget with Margins.

	PRP	Propellant	STR	ECLSS	TCS	COMMS	ADCS	CDH	PWR	ISRU	Total
CBE Mass (kg)	320	5557	955		216	47	138	100	141		7,474
Allocated Mass (kg)	400	6946	1194		270	59	173	125	176		9,343
% margin	25%	25%	25%		25%	25%	25%	25%	25%		
Power (W)	2	0			200	460	344	80			1,086
30% margin											

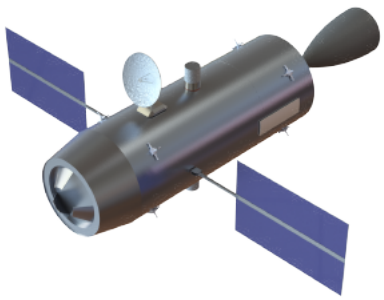

Fig. 35 Visualization of the Orbital Taxi.

H. Risk Analysis and Mitigation

Two mission risk matrices has been developed to account for all of the notable liabilities that may arise. Figures 36 37 showcases the risk and associated risk reduction path due to the corresponding mitigation strategy employed. Catastrophic risks include the L1, L2, HF1, S1, Pr1, and 5 other indicated risks. L1 is the danger of missing launch window to DST. Mitigation plans to size the ECLSS system to 11-sol to be able to miss up to two launch windows will reduce the consequence, therefore reducing concern level surrounding such threats to crew life. S1 are the dangers involved with the possibility of MAV structural failure on launch from Mars surface. The planned mitigation action of incorporating two sets of two titanium struts and FOS margin will assist with the likelihood of such hazards occurring, and therefore, the result is a shift of the risk towards regions outside of the catastrophic red region of the matrix. Similar implementation of contingency plans to minimize danger are performed for all other indicated risks. Descriptions of all risks, associated hazard categorizations, mitigation strategies, and resulting shifts can again be found within Figures 36 37.

Notation	Risk Classification
E	Environmental
Pr	Propulsion
S	Structures
Pw	Power
Th	Thermal
C	Comm.s
Att	Attitude
Op	Operations

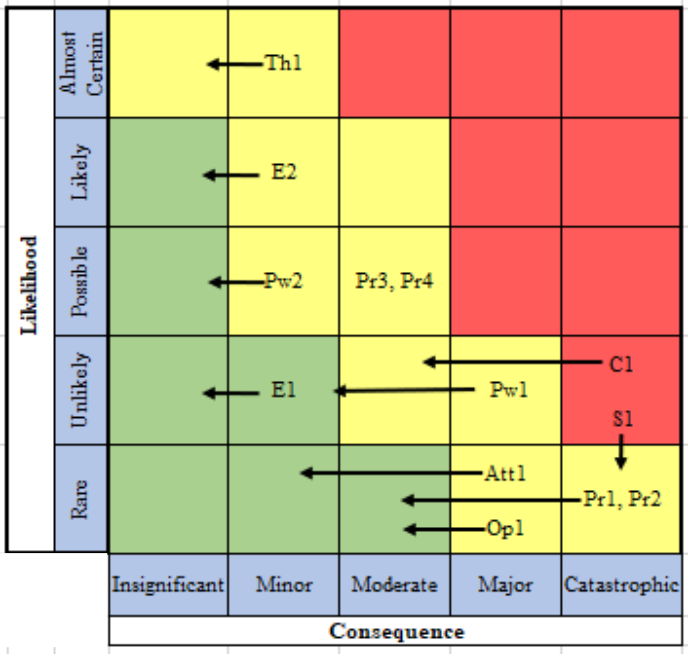

Index	Risk	Consequences	Mitigation Strategy
E1	Mars soil conditions not optimal for ISRU process.	MAV will not have enough fuel to launch from Mars surface; **Mission failure & crew safety maintained.**	2nd ISRU system added for redundancy and assistance if needed.
E2	Martian dust/duststorms blockading solar panels.	Lander solar panels cannot supply ISRU with power to generate LOX; **Mission failure evident & crew safety maintained.**	Electromagnetic Dust Shields installed on all Ultra Flex Solar Arrays on the Lander.
C1	MAV/Taxi Communications system failure.	MAV/Taxi will not be able to communicate with Mission Control/DST; **Mission Failure & Crew safety at risk**	Backup comm. systems for MAV/Taxi. 30% margin applied for pointing node accuracy.
Pr1	MAV engine failure.	Failure to launch from Mars surface; **Mission failure & crew endangered.**	Contengincy flowpaths implemented within MPS PI&D.
Pr2	Taxi Engine failure.	Failure to kick MAV out to DST; **Mission failure & crew endangered.**	Contengincy flowpaths implemented within MPS PI&D.
Pr3	HIAD failure to deploy.	Major strutural damage to MAV and Lander; **Mission status: potential failure, would need to be re-assessed.**	Redundancy implemented through dual inflation catalysts.
Pr4	EDL Lander engine failure to ignite for touchdown.	Major strutural damage to MAV and Lander; **Mission status: potential failure, would need to be re-assessed.**	3 engines added for redundancy measures. Parachute also added for final touchdown assist.
S1	MAV titanium Struts structural failure.	Severe structural damages to the MAV; **Mission and crew at large risk.**	Two sets of two titanium struts linked to each fuel tank, redundancy implemented through FOS margin.
Pw1	Taxi Solar Panel degradation over time.	Insufficient power to the comms and thermal demands onboard, potential threat of inability to dock with MAV or fuel integrity compromised; **Mission failure & potential crew endangerment.**	Solar panels sized for EOL performance according to hardware information. 20% margin implemented.
Pw2	Lander Solar Panel degradation over time.	Insufficient power to the ISRU, comms, and thermal demands onboard; major threat of inability to produce LOX; **Mission failure & crew safety maintained.**	Solar panels sized for EOL performance according to hardware information. Margin of 20% extra solar panel area implemented for redundancy.
Th1	Cryogenic fuel boil-off.	MAV will not have enough fuel to launch from Mars surface; **Mission failure & crew safety maintained.**	ISRU system continues harvesting so if needed extra fuel, it may be supplemented.
Att1	Taxi/MAV thuster malfunction.	EDL/ascent at risk, docking procedure at risk; **Potential crew endangerment & potential mission failure.**	Additional RCS thrusters implemented on both vehicles. RCS system independency established for functionality.
Op1	Docking latch mechanism failure.	Taxi unable to propel MAV & crew to DST; **Mission failure and crew endangerment evident.**	Increase in overall latch claw count implemented & contigency plan for alternate docking procedure.

Fig. 36 Mission Risk Matrix

Notation	Risk Classification
L	Life Support
HF	Human Factors

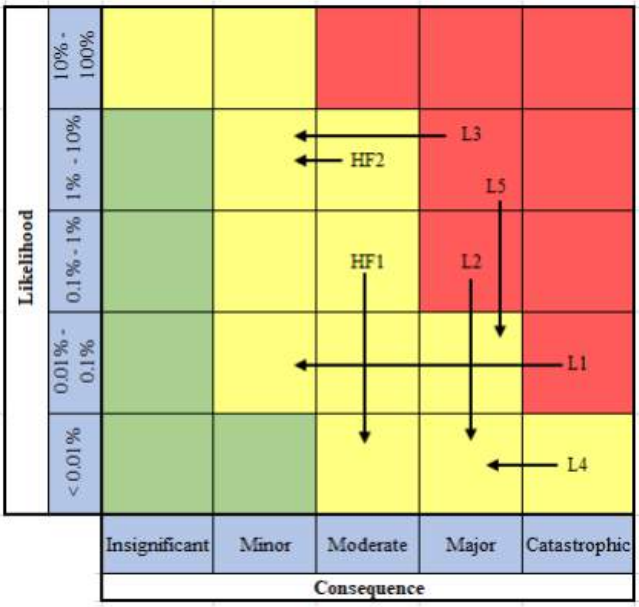

Index	Risk	Consequences	Mitigation Strategy
L1	Missed launch window with Taxi/ DST in 5 sol.	ECLSS may not have enough supply to support crew; **Mission at risk, Crew lives endangered.**	ECLSS sized for 11-sol to be able to miss up to two launch windows.
L2	Fission reactor power source radiation overexposure to the crew.	**Crew health/lives endangered, mission risk of failure imminent.**	Fission reactor system is shut off once ISRU propellant generation is complete; No later than a week before human arrival to Mars.
L3	Loss of MAV pressure.	Potential inhabitable capsule volume for crew; **Crew lives endangerd, Mission failure imminent.**	Separate system for oxygen supply to the crew IVA suits.
L4	Failed Docking with DST.	Human retrieval at risk; **Crew safety threatened and mission failure.**	Docking contingency plans with procedure of using extra long umbilical chords.
L5	ECLSS equipment failure.	**Crew lives at risk, potential failure.**	Redundant units & backup systems implemented.
HF1	Insufficient supply of consumables.	**Crew health and performance at risk, mission failure probable.**	50% safety margin applied to all consumables.
HF2	Medical emergency.	**Potential crew health at risk, potential mission failure.**	MAV will have a Med Unit to supply the crew with needed medical equipment.

Fig. 37 Crew Risk Matrix

I. Cost Estimate and Schedule

TRTL's cost in FY22 is determined using NASA's Project Cost Estimating Capability (PCEC) [59], which uses the data from previous NASA missions to estimate the cost of future ones. The mission is indicated as a multi-element robotic spacecraft one with two spacecraft elements: the MAV and orbital taxi. As this mission is purely a transportational one, no payload is specified; however, additional subsystems are added to both spacecraft to more accurately reflect expected costs. Solar arrays are added to both spacecraft, and to the MAV, thrust vector control, reaction control, a propulsive EDL system, and crew accommodations are added. To the orbital taxi, a reaction control system was added and EDL are removed. These changes align with the characteristics unique to these two spacecraft that were not included in the default mission profile.

For the PCEC global inputs, TRTL is specified as a directed, Class A Mars mission with phases divided into the schedule shown in Fig. 38.

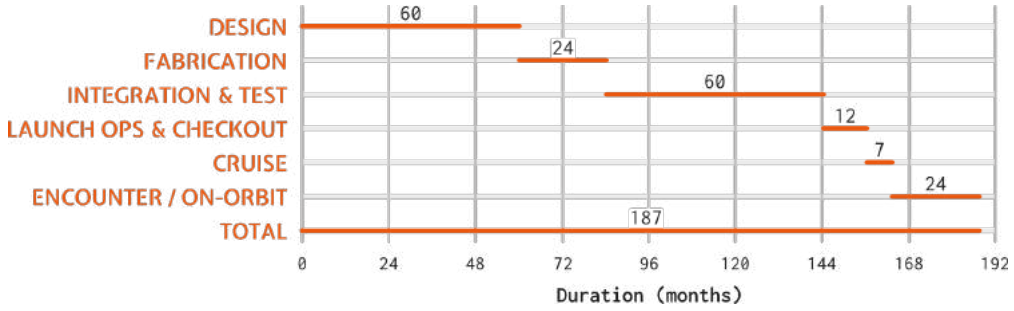

Fig. 38 Gantt chart showing TRTL's mission phase timing breakdown.

The total cost estimate for project TRTL is a net $3.942 billion USD based on the table on page 95, which meets the AIAA RFP requirement to not exceed a budget of $ 4 billion (RFP-17). First, note that the cost of the lander and HIAD within EDL systems were not included within this overall cost, as the RFP specifies that EDL is outside the scope of this mission. Second, ISRU is not mentioned as a subsystem, primarily because it does not exist as an option within PCEC. This cost is instead reflected through additional months allocated towards design and testing, where both durations are set to 60 months, around the maximum values of past missions. An additional 10% of reserves - amounting to roughly $358 million - is included in the overall cost to account for any unexpected items or delays. When looking at the cost of the two spacecraft, the MAV reaches almost $1 billion compared to $234 million for the orbital taxi. This is the result of the novelty of design for the MAV, which requires TVC to keep the vehicle stable, especially with the four liquid-filled tanks a distance away from the central axis. Meanwhile, the orbital taxi is extremely similar to other spacecraft already in use, resulting in a low cost.

WBS #	Level	Line Item Name/Description	Non-Recurring	Design & Development	System Test Hardware	Flight Unit	Recurring Production	Non-Allocated	Operations	TOTAL
0	1	TRTL - Transit, Rendezvous, & Taxi Launcher	$ 1,474.6	$ 331.8	$ 106.0	$ 81.5	$ 1,923.3	$ 92.6	$ 93.4	$ 3,584.0
1.0	2	Project Management	$ 66.5	$ -	$ -	$ -	$ 98.3	$ -	$ -	$ 164.8
2.0	2	Systems Engineering	$ 36.7	$ -	$ -	$ -	$ 61.8	$ -	$ -	$ 98.5
3.0	2	Safety and Mission Assurance	$ 40.0	$ -	$ -	$ -	$ 109.7	$ -	$ -	$ 149.7
4.0	2	Science/Technology	$ -	$ -	$ -	$ -	$ -	$ 92.6	$ -	$ 92.6
5.0	2	Flight System \ Spacecraft	$ 1,074.8	$ 331.8	$ 106.0	$ 81.5	$ 1,140.1	$ -	$ -	$ 2,214.8
5.01	3	Flight System Project Management	$ 54.4	$ -	$ -	$ -	$ 80.4	$ -	$ -	$ 134.8
5.02	3	Flight System Systems Engineering	$ 26.0	$ -	$ -	$ -	$ 43.8	$ -	$ -	$ 69.8
5.03	3	Flight System Product Assurance	$ 32.5	$ -	$ -	$ -	$ 89.3	$ -	$ -	$ 121.9
5.10	3	Mars Ascent Vehicle (MAV)	$ 615.2	$ 310.7	$ 93.0	$ 71.6	$ 361.2	$ -	$ -	$ 976.3
--	4	MAV - Management	$ -	$ -	$ -	$ -	$ -	$ -	$ -	$ -
--	4	MAV - Systems Engineering	$ -	$ -	$ -	$ -	$ -	$ -	$ -	$ -
--	4	MAV - Product Assurance	$ -	$ -	$ -	$ -	$ -	$ -	$ -	$ -
--	4	MAV - Structures & Mechanisms	$ 78.3	$ -	$ -	$ -	$ 70.6	$ -	$ -	$ 148.9
--	4	MAV - Thermal Control	$ 2.8	$ -	$ -	$ -	$ 25.8	$ -	$ -	$ 28.7
--	4	MAV - Electrical Power & Distribution	$ 49.9	$ -	$ -	$ -	$ 93.5	$ -	$ -	$ 143.4
--	4	MAV - Battery	$ 21.3	$ 3.1	$ 18.1	$ 13.9	$ 13.9	$ -	$ -	$ 35.2
--	4	MAV - Propulsion	$ 53.0	$ -	$ -	$ -	$ 54.8	$ -	$ -	$ 107.8
--	4	MAV - Tanks	$ 25.0	$ 18.2	$ 6.8	$ 5.2	$ 5.2	$ -	$ -	$ 30.2
--	4	MAV - Thrust Vector Control	$ 105.6	$ 99.4	$ 6.2	$ 4.8	$ 4.8	$ -	$ -	$ 110.3
--	4	MAV - Reaction Control System	$ 6.2	$ 5.1	$ 1.1	$ 0.8	$ 0.8	$ -	$ -	$ 7.0
--	4	MAV - Communications	$ 21.5	$ -	$ -	$ -	$ 37.5	$ -	$ -	$ 58.9
--	4	MAV - C&DH	$ 2.9	$ -	$ -	$ -	$ 7.5	$ -	$ -	$ 10.5
--	4	MAV - Entry, Descent, and Landing	$ -	$ -	$ -	$ -	$ -	$ -	$ -	$ -
--	5	MAV - Lander Propulsion	$ -	$ -	$ -	$ -	$ -	$ -	$ -	$ -
--	5	MAV - Thermal Protection System	$ -	$ -	$ -	$ -	$ -	$ -	$ -	$ -
--	4	MAV - Solar Array	$ 17.9	$ 5.9	$ 12.0	$ 9.2	$ 9.2	$ -	$ -	$ 27.1
--	4	MAV - Crew Accommodations	$ 163.5	$ 142.0	$ 21.6	$ 16.6	$ 16.6	$ -	$ -	$ 180.1
--	4	MAV - Crew Systems	$ 59.4	$ 32.2	$ 27.2	$ 20.9	$ 20.9	$ -	$ -	$ 80.3
5.20	3	Orbital Taxi (TAXI)	$ 111.3	$ 21.1	$ 12.9	$ 10.0	$ 122.2	$ -	$ -	$ 233.5
--	4	TAXI - Management	$ -	$ -	$ -	$ -	$ -	$ -	$ -	$ -
--	4	TAXI - Systems Engineering	$ -	$ -	$ -	$ -	$ -	$ -	$ -	$ -
--	4	TAXI - Product Assurance	$ -	$ -	$ -	$ -	$ -	$ -	$ -	$ -
--	4	TAXI - Structures & Mechanisms	$ 24.7	$ -	$ -	$ -	$ 25.2	$ -	$ -	$ 49.9
--	4	TAXI - Thermal Control	$ 2.0	$ -	$ -	$ -	$ 7.7	$ -	$ -	$ 9.7
--	4	TAXI - Electrical Power & Distribution	$ 0.5	$ -	$ -	$ -	$ 0.1	$ -	$ -	$ 0.6
--	4	TAXI - Propulsion	$ 29.2	$ -	$ -	$ -	$ 32.9	$ -	$ -	$ 62.1
--	4	TAXI - Reaction Control System	$ 19.9	$ 16.0	$ 3.9	$ 3.0	$ 3.0	$ -	$ -	$ 22.9
--	4	TAXI - Communications	$ 20.8	$ -	$ -	$ -	$ 38.9	$ -	$ -	$ 59.7
--	4	TAXI - C&DH	$ -	$ -	$ -	$ -	$ 7.5	$ -	$ -	$ 7.5
--	4	TAXI - Solar Array	$ 14.1	$ 5.1	$ 9.1	$ 7.0	$ 7.0	$ -	$ -	$ 21.1
5.x	3	Flight System I&T	$ 235.4	$ -	$ -	$ -	$ 443.2	$ -	$ -	$ 678.6
6.0	2	Mission Operations System (MOS)	$ 18.7	$ -	$ -	$ -	$ 65.4	$ -	$ 93.4	$ 177.6
--	3	MOS/GDS Development (Phase B-D)	$ 18.7	$ -	$ -	$ -	$ 65.4	$ -	$ -	$ 84.1
--	3	Mission Ops & Data Analysis (Phase E)	$ -	$ -	$ -	$ -	$ -	$ -	$ 93.4	$ 93.4
9.0	2	System Integration, Assembly, Test & Check Out	$ 237.9	$ -	$ -	$ -	$ 447.9	$ -	$ -	$ 685.9

FY2022, $M
Inflation Factor: 1.134

	Reserves %	Total w/Reserves
Reserves	10%	$ 3,942.36

J. Final Conclusions

Project TRTL has demonstrated its capability in providing a system that is able to carry out the AIAA RFP and successfully bring two crew members and 50 kg of samples to a DST rendezvous location. The mission architecture, comprising of a MAV utilizing ISRU propellant generation, and an Orbital Taxi provides an architecture that has a large field of development and historical backing. The largest risks associated with mission operation, aforementioned within Section H, have been accounted for with mitigation strategies. Overall danger level has, therefore, decreased in probability of occurrence and severity of the consequence, allowing for TRTL mission to maintain its mission safety and robustness.

Final mission costs result to $3.942 billion USD, falling within the $4 billion given budget. A final budget breakdown for subsystems has been provided. Tables 42 and 61 contain final mass and power estimates for both vehicles.

To ensure mission development adheres to the projected timeline, we recommend prioritizing research further developing ISRU techniques including MOXIE, which has been successfully tested. While this mission is highly dependent further ISRU development, it is a field which is likely to see much development regardless due to its utility for a many future Mars missions. Further development on long term cryogenic storage techniques would also be highly beneficial to TRTL, as boiloff of the cryogenic propellants used by TRTL is a concern using present day techniques. This is another field likely to see some development, as it will be necessary for any missions seeking to use cryogenic propellants on interplanetary missions.

The TRTL mission design provides the following benefits over the original design posed by the AO. TRTL allows for a landed mass reduction of 68% from the maximum of two 25 tonne landers, which allows for significantly reduced EDL requirements and increased probability of successful landing. The TRTL mission design also relies on procedures which have been thoroughly developed on and around Earth including ascent, rendezvous, and docking; a surface fuel transfer procedure would introduce many risks and unknowns that could endanger astronauts. Additionally, the implementation of ISRU on the lander provides a lasting platform for LOX generation, continuing to serve as a functional vessel and laying the groundwork for future implementations of various ISRU techniques. Finally, the OT will remain in orbit as a refuelable orbital tug and communications relay after TRTL concludes its mission. These characteristics are unique to the TRTL mission design and set it apart from other designs.

K. Compliance Matrix

ID	Requirement Description	Explanation	Complies?	Section
RFP-1	Each lander payload shall not exceed the payload capacity of 25,000kg per lander.	The lander payload is ~16,000kg. Shown in mass table.	Yes	F.9 (pg.73)
RFP-2	The lander shall not exceed an 8.4m diameter payload fairing.	The lander diameter is 8.4 m, including the EDL HIAD.	Yes	E.3 (pg.21)
RFP-3	One of the landers must carry a 5,000 kg 10kW Fission Surface Power unit.	The lander uses the 10kW fission unit.	Yes	F.7.1 (pg.63)
RFP-4	Design all necessary elements to support this concept of operation, and provide detailed description of the operation of the concept.	TRTL mission CONOPS is provided.	Yes	C.2 (pg.12)
RFP-5	The two landers shall depart Earth no later than the 2037 mission opportunity, with Mars arrival in no later than July of 2038. The MAV must be ready to support crew ascent by July 1, 2040.	TRTL meets departure, arrival, and support readiness deadlines.	Yes	E.4 (pg.22)
RFP-6	The landers shall have landing accuracy of 1 km, the team shall describe operation assuming the two landers are ~1km apart from each other.	Does not apply for TRTL, only one lander involved with this proposal.	N/A	N/A
RFP-7	Teams do not need to design or describe the transit from Earth to Mars, but must describe the overall operation of the concept starting with Mars landing and ending with the crew ascent to Mars 5-sol.	Overall CONOPS entails operations for mission scope. Subsystems also evaluated within mission scope.	Yes	C. 2(pg.12)
RFP-8	Teams must discuss packaging and integration with an EDL system from current options that are being considered for landing payloads on Mars.	HIAD EDL system architecture configured and described.	Yes	E.3 (pg.21)
RFP-9	The MAV must be able to support 2 crew members for the duration of the ascent from the surface to an awaiting DST vehicle in Mars 5-sol parking orbit.	MAV ECLSS is able to support crew for journey to DST. 11-sol sized for redundancy.	Yes	F.1 (pg.24)
RFP-10	The MAV shall have capacity to return 50kg of Mars samples from the surface to rendezvous with the DST in 5-sol.	MAV ECLSS includes a system to house the 50kg samples.	Yes	F.1 (pg.24)
RFP-11	An autonomous robotic system shall be designed to transfer propellant into the MAV.	TRTL only has one lander. MAV will generate propellant through ISRU.	N/A	N/A
RFP-12	Team must analyze and describe the power requirement of the various elements ,and detail the operation to address their power needs, and discuss options if the single 10kW power source is insufficient to address the element's power needs.	The 10kW fission reactor is insufficient to meet needs, solar panels used. Power table of all subsystems provided.	Yes	F.7 (pg.62)
RFP-13	Team must provide a concept of operation to describe the propellant transfer process and timeline associated with such operation.	No propellant transfer required with TRTL's one lander proposal.	N/A	N/A
RFP-14	Team must provide analysis on the communication delays between Earth and Mars and describe how the autonomous refueling operation would be impacted by the delays and any mitigation options for any communication blackouts.	No autonomous fuel transport within TRTL, all other communications risks (delays, blackouts) considered.	N/A	F.5.4 (pg.57)
RFP-15	Perform trade studies on vehicle system options at the system and subsystem level to demonstrate the fitness of the chosen vehicle design.	High level vehicle trade performed. All subsystems include trade studies as well.	Yes	D (pg.15) F (pg.24) G (pg.73)
RFP-16	Discuss selection of subsystem components and the values of each of the selection and how the design requirements drove the selection of the subsystem	Design drivers evaluated on within each subsystem section.	Yes	F (pg.24) G (pg.73)
RFP-17	The cost for the vehicle shall not exceed $4 Billion US Dollar (in FY22), including development, hardware, and operation cost of the elements. Cost of the landers and the launch vehicles are not included in this cost cap.	TRTL total cost: $3.942 billion USD.	Yes	J (pg.94)

References

[1] mars.nasa.gov, "Historical Log | Missions," , Apr. 2023. URL https://mars.nasa.gov/mars-exploration/missions/historical-log.

[2] NASA, "In Depth | Curiosity (MSL)," , Feb. 2021. URL https://solarsystem.nasa.gov/missions/curiosity-msl/in-depth.

[3] Granath, B., "Gemini's First Docking Turns to Wild Ride in Orbit," , Feb. 2016. URL http://www.nasa.gov/feature/geminis-first-docking-turns-to-wild-ride-in-orbit.

[4] Garcia, M., "Visiting Vehicle Launches, Arrivals and Departures," , Apr. 2015. URL http://www.nasa.gov/feature/visiting-vehicle-launches-arrivals-and-departures.

[5] Lindemann, R., Bickler, D., Harrington, B., Ortiz, G., and Voothees, C., "Mars exploration rover mobility development," *IEEE Robotics & Automation Magazine*, Vol. 13, No. 2, 2006. https://doi.org/10.1109/MRA.2006.1638012, conference Name: IEEE Robotics & Automation Magazine.

[6] NASA, "2022 NASA Strategic Plan," , Mar. 2022. URL https://www.nasa.gov/sites/default/files/atoms/files/2022_nasa_strategic_plan.pdf.

[7] Polsgrove, T. P., Percy, T. K., Rucker, M., and Thomas, H. D., "Update to Mars Ascent Vehicle Design for Human Exploration," *2019 IEEE Aerospace Conference*, 2019. https://doi.org/10.1109/AERO.2019.8741709, iSSN: 1095-323X.

[8] Space Dynamics Group Universidad Politecnica de Madrid, "Easy Porkchop," , 2019. URL http://sdg.aero.upm.es/index.php/online-apps/porkchop-plot.

[9] Georgevic, R. M., "The solar radiation pressure on the Mariner 9 Mars orbiter," Tech. Rep. NASA-CR-130724, Dec. 1972. URL https://ntrs.nasa.gov/citations/19730009104, nTRS Author Affiliations: Jet Propulsion Lab., California Inst. of Tech. NTRS Document ID: 19730009104 NTRS Research Center: Legacy CDMS (CDMS).

[10] Qu, M., Merill, R. G., Chai, P., and Komar, D. R., "Optimizing Parking Orbits for Roundtrip Mars Missions," Stevenson, WA, 2017. URL https://ntrs.nasa.gov/citations/20170008844, nTRS Author Affiliations: Analytical Mechanics Associates, Inc., NASA Langley Research Center NTRS Report/Patent Number: NF1676L-26982 NTRS Document ID: 20170008844 NTRS Research Center: Langley Research Center (LaRC).

[11] Polsgrove, T. P., Thomas, H. D., Stephens, W., Collins, T., Rucker, M., Gernhardt, M., Zwack, M. R., and Dees, P. D., "Human Mars Ascent Vehicle Configuration and Performance Sensitivities," Big Sky, MT, 2017. URL https://ntrs.nasa.gov/citations/20170003404, nTRS Author Affiliations: NASA Marshall Space Flight Center, NASA Langley Research Center, NASA Johnson Space Center, Jacobs Engineering and Science Services and Skills Augmentation Group (ESSSA) NTRS Report/Patent Number: M17-5806 NTRS Document ID: 20170003404 NTRS Research Center: Marshall Space Flight Center (MSFC).

[12] Williams, D., "Mars Fact Sheet," , Mar. 2023. URL https://nssdc.gsfc.nasa.gov/planetary/factsheet/marsfact.html.

[13] Polsgrove, T., Percy, T. K., Sutherlin, S., Dwyer-Cianciolo, A. M., Dillman, R., Brune, A., Cassell, A., and Johnston, C., "Human Mars Entry, Descent, and Landing Architecture Study: Deployable Decelerators," *2018 AIAA SPACE and Astronautics Forum and Exposition*, American Institute of Aeronautics and Astronautics, 2018. https://doi.org/10.2514/6.2018-5191.

[14] mars.nasa.gov, "NASA's InSight Lander Detects Stunning Meteoroid Impact on Mars," , Oct. 2022. URL https://mars.nasa.gov/news/9289/nasas-insight-lander-detects-stunning-meteoroid-impact-on-mars.

[15] mars.nasa.gov, "Landing Site Selection | Pre-Launch," , Dec. 2022. URL https://mars.nasa.gov/insight/timeline/prelaunch/landing-site-selection.

[16] mars.nasa.gov, "Seven Possible MSL Landing Sites | Landing Site Selection," , Aug. 2019. URL https://mars.nasa.gov/msl/timeline/prelaunch/landing-site-selection/seven-possible-msl-landing-sites.

[17] Abercromby, A. F. J., Conkin, J., and Gernhardt, M. L., "Modeling a 15-min extravehicular activity prebreathe protocol using NASAs exploration atmosphere (56.5kPa/34% O2)," *Acta Astronautica*, Vol. 109, 2015. https://doi.org/10.1016/j.actaastro.2014.11.039.

[18] Autrey, D., Kocher, J., Kaufman, C., and Fuller, J., "Development of the Universal Waste Management System," 2020. URL https://ttu-ir.tdl.org/handle/2346/86292, accepted: 2020-07-24T14:22:44Z Publisher: 2020 International Conference on Environmental Systems.

[19] Kaufman, C., Anderson, S., and Johnson, K., "Urine Removal from Suited Crew in Orion Vehicle Depressurization Scenario," 2019. URL https://ttu-ir.tdl.org/handle/2346/84497, accepted: 2019-06-20T18:23:33Z Publisher: 49th International Conference on Environmental Systems.

[20] Howard, R. L., "Recommended Crew Systems Functionality for a Mars Ascent Vehicle as a Function of Flight Duration," *ASCEND 2020*, American Institute of Aeronautics and Astronautics, 2020. https://doi.org/10.2514/6.2020-4088, URL https://arc.aiaa.org/doi/abs/10.2514/6.2020-4088, _eprint: https://arc.aiaa.org/doi/pdf/10.2514/6.2020-4088.

[21] Museum, N. A. a. S., "Collection Assembly, Fecal, Apollo | National Air and Space Museum," , 1975. URL https://airandspace.si.edu/collection-objects/collection-assembly-fecal-apollo/nasm_A19750739000.

[22] Cooper, M., Douglas, G., and Perchonok, M., "Developing the NASA Food System for Long-Duration Missions," *Journal of Food Science*, Vol. 76, No. 2, 2011, pp. R40–R48. https://doi.org/10.1111/j.1750-3841.2010.01982.x, URL https://onlinelibrary.wiley.com/doi/abs/10.1111/j.1750-3841.2010.01982.x, _eprint: https://onlinelibrary.wiley.com/doi/pdf/10.1111/j.1750-3841.2010.01982.x.

[23] Norcross, J., Norsk, P., Law, J., Arias, D., Conkin, J., Perchonok, M., Menon, A., Huff, J., Fogarty, J., Wessel, J. H., and Whitmire, S., "Effects of the 8 psia / 32% O2 Atmosphere on the Human in the Spaceflight Environment," 2013. URL https://ntrs.nasa.gov/citations/20130013505, number: S-1141.

[24] Rucker, M. A., Jefferies, S., Mary, N., Howe, A. S., Watson, J., Howard, R., and Lewis, R., "Mars surface tunnel element concept," *2016 IEEE Aerospace Conference*, 2016, pp. 1–12. https://doi.org/10.1109/AERO.2016.7500781.

[25] Abercromby, A. F. J., Bekdash, O., Cupples, J. S., Dunn, J. T., Dillon, E. L., Garbino, A., Hernandez, Y., Kanelakos, A. D., Kovich, C., Matula, E., Miller, M. J., Montalvo, J., Norcross, J., Pittman, C. W., Rajulu, S., Rhodes, R. A., and Vu, L., "Crew Health and Performance Extravehicular Activity Roadmap: 2020," 2020.

[26] Howe, A. S., and Merbitz, J., "Deployable Extravehicular Activity Platform (DEVAP) for Planetary Surfaces," *AIAA SPACE 2012 Conference & Exposition*, American Institute of Aeronautics and Astronautics, ???? https://doi.org/10.2514/6.2012-5312, URL https://arc.aiaa.org/doi/abs/10.2514/6.2012-5312, _eprint: https://arc.aiaa.org/doi/pdf/10.2514/6.2012-5312.

[27] Cohen, M., "Testing the Celentano Curve: An Empirical Survey of Predictions for Human Spacecraft Pressurized Volume," *SAE International Journal of Aerospace*, Vol. 1, 2008. https://doi.org/10.4271/2008-01-2027.

[28] Boyd, W. K., "Stress-corrosion cracking in metals," , Aug. 1971. URL https://ntrs.nasa.gov/citations/19720010278, nTRS Report/Patent Number: NASA-SP-8082 NTRS Document ID: 19720010278 NTRS Research Center: Legacy CDMS (CDMS).

[29] Wu, K., Antol, J., Watson, J., Saucillo, R., North, D., and Mazanek, D., "Lunar Lander Structural Design Studies at NASA Langley," 2007. https://doi.org/10.2514/6.2007-6137.

[30] Griggs, L., Swatzell, S., Decker, A., Allgood, J., Oliver, N., and Moseley, J., "Methodology and Development of SLS Ascent Loads," San Diego, CA, 2021. URL https://ntrs.nasa.gov/citations/20210025234, nTRS Author Affiliations: Dynamic Concepts (United States), Marshall Space Flight Center NTRS Document ID: 20210025234 NTRS Research Center: Marshall Space Flight Center (MSFC).

[31] Rice, R. C., Jackson, J. L., Bakuckas, J., and Thompson, S., "Metallic Materials Properties Development and Standardization (MMPDS)." Tech. Rep. PB2003106632, Battelle Memorial Inst., Columbus, OH.; William J. Hughes Technical Center, Atlantic City, NJ.; Federal Aviation Administration, Washington, DC. Office of Aviation, 2003. URL https://ntrl.ntis.gov/NTRL/dashboard/searchResults/titleDetail/PB2003106632.xhtml, num Pages: 1728.

[32] Tabakman, A., and England, W., "NASA Docking System (NDS) Interface Definitions Document (IDD)," , Nov. 2013. URL https://ntrs.nasa.gov/citations/20150014481, nTRS Author Affiliations: NASA Johnson Space Center, Boeing Co. NTRS Report/Patent Number: JSC-CN-31165 NTRS Document ID: 20150014481 NTRS Research Center: Johnson Space Center (JSC).

[33] Sutton, G. P., and Biblarz, O., *Rocket Propulsion Elements*, 9th ed., Wiley, Hoboken, New Jersey, 2016.

[34] Ursa Major, T., "Arroway | Ursa Major Technologies," , May 2022. URL https://www.ursamajor.com/engines/arroway.

[35] Rohrschneider, R. R., "Development of a Mass Estimating Relationship Database for Launch Vehicle Conceptual Design," 2002. URL https://www.ssdl.gatech.edu/sites/default/files/ssdl-files/papers/mastersProjects/RohrschneiderR-8900.pdf.

[36] European Space Agency, "ESA - Propulsion," , Feb. 2023. URL https://www.esa.int/Science_Exploration/Human_and_Robotic_Exploration/Orion/Propulsion.

[37] Everett, D. F., Puschell, J. J., and Wertz, J. R. (eds.), *Space Mission Engineering: The New SMAD*, first edition ed., Microcosm Press, Hawthorne, CA, 2011.

[38] Reid, M. S. (ed.), *Low-noise systems in the Deep Space Network*, Deep-space communications and navigation series, Wiley, Hoboken, N.J, 2008. OCLC: ocn230181178.

[39] Ho, C., Golshan, N., and Kliore, A., "Radio Wave Propagation Handbook for Communication on and Around Mars," , Mar. 2002.

[40] Flock, W. L., "Propagation effects on satellite systems at frequencies below 10 GHz, a handbook for satellite systems design, 1st edition," , Dec. 1983. URL https://ntrs.nasa.gov/citations/19840005329, nTRS Author Affiliations: NASA Headquarters NTRS Report/Patent Number: NASA-RP-1108 NTRS Document ID: 19840005329 NTRS Research Center: Legacy CDMS (CDMS).

[41] Farahani, S., "Chapter 5 - RF Propagation, Antennas, and Regulatory Requirements," *ZigBee Wireless Networks and Transceivers*, edited by S. Farahani, Newnes, Burlington, 2008. https://doi.org/10.1016/B978-0-7506-8393-7.00005-4, URL https://www.sciencedirect.com/science/article/pii/B9780750683937000054.

[42] Wu, D., Nekovee, M., and Wang, Y., "Deep Learning-Based Autoencoder for m-User Wireless Interference Channel Physical Layer Design," *IEEE Access*, Vol. 8, 2020. https://doi.org/10.1109/ACCESS.2020.3025597.

[43] Bowles, J. V., Huynh, L. C., Hawke, V. M., and Jiang, X. J., "Mars Sample Return: Mars Ascent Vehicle Mission and Technology Requirements," 2013. URL https://ntrs.nasa.gov/citations/20140011316, number: NASA/TM-2013-216620.

[44] mars.nasa.gov, "InSight Images a Solar Panel," , Dec. 2018. URL https://mars.nasa.gov/resources/22197/insight-images-a-solar-panel.

[45] Rucker, M. A., Oleson, S., George, P., Landis, G. A., Fincannon, J., Bogner, A., Jones, R. E., Turnbull, E., Martini, M. C., Gyekenyesi, J. Z., Colozza, A. J., Schmitz, P. C., and Packard, T. W., "Solar vs. Fission Surface Power for Mars," Pasadena, CA, 2016. URL https://ntrs.nasa.gov/citations/20160002628, nTRS Author Affiliations: NASA Johnson Space Center, NASA Glenn Research Center, Zin Technologies, Inc., Vantage Partners, LLC NTRS Report/Patent Number: JSC-CN-35576 NTRS Document ID: 20160002628 NTRS Research Center: Johnson Space Center (JSC).

[46] Lam, G. Q., Billets, S., Norick, T., and Warwick, R., "Solar Array Design For The Mars InSight Lander Mission," *14th International Energy Conversion Engineering Conference*, American Institute of Aeronautics and Astronautics, Salt Lake City, UT, 2016. https://doi.org/10.2514/6.2016-4520, URL https://arc.aiaa.org/doi/10.2514/6.2016-4520.

[47] Gilmore, D. G., *Spacecraft Thermal Control Handbook Volume I: Fundamental Technologies*, 2nd ed., 1, Vol. 1, The Aerospace Corporation, 2002.

[48] Bauccio, M., "MatWeb - The Online Materials Information Resource," , 1996. URL https://www.matweb.com/errorUser.aspx?msgid=2&ckck=nocheck.

[49] Soria-Salinas, , Zorzano, M.-P., and Martín-Torres, F. J., "Convective Heat Transfer Measurements at the Martian Surface," 2015.

[50] Youngquist, R. C., Nurge, M. A., Johnson, W. L., Gibson, T. L., and Surma, J. M., "Cryogenic Deep Space Thermal Control Coating," *Journal of Spacecraft and Rockets*, Vol. 55, No. 3, 2018. https://doi.org/10.2514/1.A34019.

[51] Larisa, M., and Croitoru, C., "Aerogel, a high performance material for thermal insulation - A brief overview of the building applications," *E3S Web of Conferences*, Vol. 111, 2019. https://doi.org/10.1051/e3sconf/201911106069.

[52] Kinefuchi, K., Miyakita, T., Umemura, Y., Nakajima, J., and Koga, M., "Cooling system optimization of cryogenic propellant storage on lunar surface," *Cryogenics*, Vol. 124, 2022. https://doi.org/10.1016/j.cryogenics.2022.103494.

[53] Plachta, D. W., Tucker, S., and Hoffman, D. J., "Cryogenic propellant thermal control system design considerations, analyses, and concepts applied to a Mars human exploration mission," Monterey, CA, 1993. URL https://ntrs.nasa.gov/citations/19930066129, nTRS Author Affiliations: NASA Lewis Research Center, NASA Marshall Space Flight Center NTRS Report/Patent Number: AIAA PAPER 93-2353 NTRS Document ID: 19930066129 NTRS Research Center: Legacy CDMS (CDMS).

[54] Deng, B., Yang, S., Xie, X., Wang, Y., Bian, X., Gong, L., and Li, Q., "Study of the thermal performance of multilayer insulation used in cryogenic transfer lines," *Cryogenics*, Vol. 100, 2019. https://doi.org/10.1016/j.cryogenics.2019.01.005.

[55] Becker, H., "Compressive buckling of barrel-shaped shells." *Journal of Spacecraft and Rockets*, Vol. 5, No. 6, 1968. https://doi.org/10.2514/3.29349, publisher: American Institute of Aeronautics and Astronautics.

[56] Kauder, L., "Spacecraft Thermal Control Coatings References," , Dec. 2005. URL https://ntrs.nasa.gov/citations/20070014757, nTRS Author Affiliations: NASA Goddard Space Flight Center NTRS Report/Patent Number: NASA/TP-2005-212792 NTRS Document ID: 20070014757 NTRS Research Center: Goddard Space Flight Center (GSFC).

[57] Finckenor, M. M., and Dooling, D., "Multilayer Insulation Material Guidelines," , Apr. 1999. URL https://ntrs.nasa.gov/citations/19990047691, nTRS Author Affiliations: NASA Marshall Space Flight Center, D2 Associates NTRS Report/Patent Number: M-925 NTRS Document ID: 19990047691 NTRS Research Center: Marshall Space Flight Center (MSFC).

[58] Liu, T., Sun, Q., Meng, J., Pan, Z., and Tang, Y., "Degradation modeling of satellite thermal control coatings in a low earth orbit environment," *Solar Energy*, Vol. 139, 2016. https://doi.org/10.1016/j.solener.2016.10.031.

[59] Keeter, B., "PCEC – Project Cost Estimating Capability," , May 2016. URL http://www.nasa.gov/offices/ocfo/functions/models_tools/PCEC.